



SOME PROPERTIES OF A LOW-ORDER MODEL  
OF ATMOSPHERIC CIRCULATION

by

John D. Stackpole

B.A., Amherst College, 1957

M.S., Massachusetts Institute of Technology, 1959

SUBMITTED IN PARTIAL FULFILLMENT OF THE REQUIREMENTS

FOR THE DEGREE OF DOCTOR OF PHILOSOPHY

at the

MASSACHUSETTS INSTITUTE OF TECHNOLOGY

June, 1964

Signature of Author .....  
Department of Meteorology, May 15, 1964

Certified by .....  
Thesis Supervisor

Accepted by .....  
Chairman, Departmental Committee on Graduate Students

✓

Some Properties of a Low-Order Model of Atmospheric  
Circulation

by

John D. Stackpole

Submitted to the Department of Meteorology on May 15, 1964  
in partial fulfillment of the requirement for the  
Degree of Doctor of Philosophy

ABSTRACT

Numerical experiments are performed with a highly simplified model of the general circulation of the atmosphere in an attempt to gain insight into the physical causes of the surface zonal wind distribution (and associated momentum convergences) observed in the atmosphere. With the zonal wind constrained to be of the form  $u = \sqrt{2} u_A \sin y + 3\sqrt{2} u_C \sin 3y$ , ( $0 \leq y \leq \pi$ ) capable of non-linear interactions with a single wave in the x (zonal) direction in a two layer quasi-geostrophic model, numerical integrations are performed for various magnitudes of the thermal forcing (of the form  $\sqrt{2} \tau_A^* \cos y$ ) and the rotation rate. Four broad categories of flow are observed in the results: a Hadley circulation for sufficiently low rotation or sufficiently high or low thermal forcing; a west to east motion of the wave without change of shape; a "vacillation" showing periodic changes in the shape of the wave; and an irregular flow. Further subdivision of the results is made on the basis of whether the surface frictionally influenced lower layer shows an "earthlike" character in the zonal wind i.e. mid-latitude westerlies flanked by easterly winds, or the reverse.

The introduction of the "Q effect" into the dynamics of the wave alters the pattern of the locations of the different flow types on the thermal forcing-rotation rate plane and alters the qualitative appearance of the flows moderately, mainly by inducing a greater concentration of zonally averaged momentum in the central regions of the flow. For those regions of the thermal forcing-rotation plane where the flow is not changed from one broad category to another the Q induced changes are not very great in magnitude, however.

The momentum convergence structure of those flows which do not exhibit severe violation of the quasi-geostrophic assumption, generally those for moderate and low thermal forcing and moderate and high rotation rates, are examined in some detail. It is found that many of the salient characteristics of the atmospheric mean state, i.e. eddy momentum transports into the central regions of the flow balanced by divergence due to a thermally indirect mean meridional cell there, a central maximum in the westerly flow in the upper layer and prevailing westerlies flanked by easterly flow in the frictionally influenced lower layer, are reproduced in the model flows but that no single case captures all of these characteristics at once. Some of the flows do show a majority of the characteristics and show the highly simplified model to be capable of a reasonably good representation of the general circulation within its self imposed limitations.

From these results certain conclusions are drawn on the nature of atmospheric flow; in particular a single baroclinic wave by its nature incorporates sufficient dynamics to induce the zonal wind structure seen in the atmosphere, or that the dynamic effect of the many waves of the atmosphere upon the large scale zonal structure may be considered as equivalent to the effect of a single wave.

Thesis Supervisor: Prof. Edward N. Lorenz

Title: Professor of Meteorology

## Acknowledgements

It is the author's pleasure to express his gratitude to Professor Edward Norton Lorenz for his continual interest advice and assistance gratefully received during the performance of the work reported upon herein.

Further heartfelt appreciation is due to Miss Marie Louise Guillot for typing this manuscript.

Thanks are also due to the M.I.T. computation center for making available their IBM computer without which this study would not have been possible.

Finally deep appreciation must be expressed to the author's wife, Laurie, without whose patience encouragement and support this work could not have been undertaken.

## TABLE OF CONTENTS

1. Introduction: The General Circulation .....	1
2. The Ultimate Simplification of the General Circulation	
I. The Quasi-Geostrophic Model in Two Layers .....	13
II. The Spectral Form of the Model .....	17
III. The Truncation of the Spectral Expansion.....	21
IV. Commentary: Momentum Convergence, Energetics and other Details .....	31
V. Summary: The Simplified Representation .....	41
3. Solutions to the Equations	
I. A Simple Analytic Solution: The Hadley Flow .....	44
II. Numerical Solutions and Their Salient Characteristics	
A. Method of Approach and Outline of Results.....	49
B. Momentum Convergences	
i. Motion Without Change of Shape .....	56
a. High Rotation Rates .....	57
b. Moderate Rotation Rates .....	66
c. Low Rotation Rates .....	71
ii. Vacillation .....	73
C. Energetics .....	80
D. Other Features .....	88
4. The Atmosphere and the Equations	
I. Meteorology or Merely Mathematics? .....	92
II. The Model Atmospheres	
A. Qualitative Comparisons .....	99
B. Quantitative Comparisons .....	105
III. Summary, Conclusions and Lines of Further Investigation	110
References .....	120
Biographical Note .....	123

**FIGURES**

	<b>PAGE</b>
1.	38
2.	52
3.	53
4.	58
5.	63
6.	63
7.	67
8.	70
9.	72
10.	72
11.	74
12.	76
13.	78
14.	79a
15.	86

**TABLES**

1.	64
2.	81
3.	83
4.	84
5.	101
6.	102
7.	106
8.	108
9.	109

## 1. Introduction: The General Circulation

The problem of offering a physical explanation of the observed distribution of mean surface winds over the globe, i.e. equatorial and polar easterlies with the band of middle latitude westerlies between, has long been a major preoccupation of meteorologists. And it is right and proper that this should be so in that this distribution is intimately related to the observed momentum balance and transport of the general circulation as a whole. Any explanation of the surface wind distribution will be equivalent to an explanation of the momentum transports and vice versa. As the extensive observations of Starr and White (1954) clearly indicate, such a surface distribution is required to be consistent with the northerly momentum transport through a latitude circle  $30^{\circ}\text{N}$  (in the northern hemisphere) and a similar transport southward of  $30^{\circ}\text{S}$  (Obasi, 1963). But the question immediately presents itself: why not the other way around? Why should there not be mean surface easterlies in middle latitudes with corresponding higher tropospheric southward momentum transports at  $30^{\circ}\text{N}$  and similarly in the southern hemisphere? Numerous investigators have attacked this problem from sundry view points; this essay attempts to do the same by methods of numerical experimentation.

A philosophical question arises right at the outset of "explaining" any observed physical phenomenon. Naturally if the equations that are appropriate to the phenomenon are known, as they would almost seem to be in the present case, one could argue that all that is necessary is to point to them and say that there is the explanation — a complete mathemat-

ical description is available, what more could one ask. Just integrate the equations on a sufficiently large computer and look at the resultant answers. And indeed they, the answers, look like the flow observed in the atmosphere or the laboratory. This is of course rather unsatisfactory; all that has been said is that the equations describing the flow describe the flow. This is not to disparage the achievement that such a description would be; its value in practical weather prediction would be obvious and considerable. Its value as an explanation however is another matter. In explaining the characteristics of the flow one would like to be able to argue from the mathematics to the qualitative physical cause and effect that the mathematics indeed describes quantitatively. The approach to such an explanation is, of course, to ignore certain physical phenomena incorporated in the original equations or to simplify preexisting complete ones. The progression from Richardson's attempt at numerical weather prediction with its unrealistic results to the simplifications inherent in the quasi-geostrophic equations, via the methods of Charney's scale analysis (Charney, 1948) and more recently that of Phillips (1956), is the example that comes most readily to mind. Although the practical aim of Charney's work was also weather prediction with relatively limited computational facilities, its fruitful by-product was a much increased understanding of the physical processes inherent in the atmospheric flows considered. Indeed the understanding engendered by these studies of just what distinct physical phenomena the primitive equations do describe and how in detail they do this, rather than the

general statement that the equations describe the atmosphere, has made it possible for Phillips and many others to return to the original equations for numerical prediction purposes.

Such methods of more or less drastic simplification with consequent neglect of some physical processes and spotlighting and clarification of the effects of others have of course been characteristic of all theoretical considerations of the general circulation, and similar laboratory circulations.

One set of simplifications that has been most suggestive has been that incorporated by Kuo (1951) in his studies of the stability of various zonal flows represented by the linearized quasi-geostrophic equations appropriate to a barotropic atmosphere and subjected to small perturbations. In these studies the mean flow is disturbed by a small perturbation of the form

$$A(y) \left[ \exp \{ i \mu (x - ct) \} \right]$$

where  $A(y)$  the amplitude and  $c$  the phase velocity may be complex and  $\mu$  proportional to the wave number is real; second and higher order terms are then ignored, and the eigenvalue equation for the phase velocity, subject to appropriate boundary conditions, determines the conditions which will result in amplifying, neutral or damped waves. Interpreting these waves in terms of their resultant momentum (and energy) transports, Kuo finds that for typical atmospheric conditions positive momentum (to the east) is transported into regions of preexisting positive mean flow momentum and conversely; i.e. the waves are damped, momentum is transferred

from regions of low to high momentum, and the energy of the waves is transferred to the mean flow.

The necessary conditions for the reverse process, amplifying waves gaining energy from the mean flow and transporting momentum away from momentum maxima, is that the absolute vorticity of the mean flow

$Z_0 = f + f_0$  , where  $f_0$  is the relative vorticity of the mean flow and  $f$  the coriolis parameter, somewhere has an extremum, i.e.

$\beta + \frac{\partial Z_0}{\partial y}$  somewhere ( $\beta = \frac{\partial f}{\partial y}$ ) -- this condition alone is sufficient for the momentum transport, and  $\frac{\partial Z_0}{\partial y} > 0$  in regions of large mean flow and  $\frac{\partial Z_0}{\partial y} < 0$  in regions of small mean flow.

These conditions would seem to occur only during times of strong jet stream flow and so are less common than the stable wave case. Indeed

a condition of  $\frac{\partial Z_0}{\partial y} > 0$  is typical of the upper troposphere at most times (except for jet situations) in that  $\beta$  dominates the relative vorticity gradient. This of course is why the damped wave is more common.

These results, suggestive as they are, are of necessity, just that. Reasonably simple zonal flows of the type hypothesized are, in actuality, mathematical fictions, highly useful ones but still fictions. Also, of course, the use of linearized equations for disturbances that are, by observation, distinctly finite and hence would have all sorts of nonlinear interactions with the ambient flow, as well as with each other if more than one disturbance was allowed at one time, limits the conclusions that can be safely drawn to the mere beginnings of what might actually happen.

For example, initially damped disturbances might well evolve into a state in which they still transfer energy into the mean flow but tend to spread rather than concentrate mean flow momentum. There is just no telling. These limitations were of course, recognized in the contemplation of the linear stability results and a different approach to the same general problem was attempted by Platzman (1952) and a little later by Kuo (1953) and by Lorenz (1953) also.

Platzman, considering inviscid incompressible planar flow, obtains an integral for the second derivative with respect to time of the space averaged kinetic energy of the flow with a finite single wave disturbance. In the simple flow considered, such an integral when positive implies a damped wave and conversely, hence it is a stability criterion. The single wave considered does not allow for any momentum transport, but the second time derivative of the latitudinal mean wind can be found for special cases of the mean flow. In the cases investigated momentum was transported in such a way as to strengthen preexisting jets for both damped and amplified disturbances. These conclusions are all reached even though  $\beta$  was set equal to zero. The flows and geometry are rather specialized and their connection with the atmosphere are somewhat tenuous.

Kuo, employing this same approach, that of assuming a specifiable mean flow with a finite disturbance or disturbances, and computing subsequent changes, considers the flow on a spherical earth in two parts: the interaction between the disturbances and the earth's rotation (the  $\beta$

effect), and the disturbance-mean flow interactions. Again, as in Kuo's previous work, the flow is considered nondivergent barotropic and horizontal. The effect of the earth's rotation is to cause a tendency for northward momentum transport over the whole northern hemisphere except for the possibility of southerly transport in the northern reaches and this is true for any number of arbitrary wave forms considered separately or in concert. The disturbance-mean flow interactions, disregarding the earth's rotation, are of such complexity as to require consideration of particular disturbances and particular mean flows. For a selection of these, chosen to resemble observational flows, the momentum transport tendencies are quite similar to actual momentum transports measured in the atmosphere, i.e. there is a large maximum of northward transport at  $30^{\circ}\text{N}$  and an order of magnitude smaller southerly transport maximum around  $60^{\circ}$  or  $70^{\circ}\text{N}$ .

Finally Lorenz, returning to a nonrotating coordinate system, while retaining the barotropic nondivergent flow restrictions, has obviated the necessity of considering particular mean and disturbance flows in studying the energy tendencies arising from their interactions, by dealing with the ensemble of all random disturbances with arbitrary mean flows. Rather than selecting particular flow patterns, one specifies the statistics of the ensemble of flows, which latter procedure allows of considerably more generality than the former. The conclusions drawn indicate that random disturbances are capable of maintaining the mean flow, at least in so far as the energy tendencies imply. Whether they actually

exist and do such maintenance work cannot be answered. Kuo's work would imply that nonrandom disturbances similar to observed patterns can account for the maintenance of the observed mean flows.

These two sets of simplifications, in the gross sense, the study of perturbation instabilities and nonlinear energy change and momentum transport tendencies, have both pointed at in the same direction — a most heartening result. Both have pointed up the importance of barotropic flow and its relation to the rotation of the earth, or more exactly to the variation with latitude of the vertical rotation component, in the transport of relative angular momentum into middle latitudes from the south and perhaps also from the north. The conservation of angular momentum for the whole earth atmosphere system will necessitate for consistency that the region of momentum convergence be characterized by a frictional loss to the earth by westerly surface winds, and a gain in the momentum divergent regions. In a study of baroclinic stability Kuo (1952) finds, among other things, that baroclinically unstable waves, bearing a resemblance to observed waves, do transport momentum downward from regions of high to low momentum, at somewhat less than the rate required by continuity. In a later study (Kuo, 1956) he finds, also, that there exists a forced mean meridional cell in the region of eddy momentum convergence which induces momentum divergence there due to the rotation of the earth. This divergence serves to partially balance the convergence and reduces the amount of momentum which must be transported downward ageostrophically by the baroclinic waves. This rounds out the momentum cycle as implied by the stability and tendency studies.

Another type of simplification of the most general problem, one that has and continues to bear much fruit, is that of modeling the vertical structure of the atmosphere by various layers, rather than maintaining a continuous structure. One of the simplest such models has already been discussed by implication — the barotropic model used by Kuo in the stability studies alluded to previously. A large number of such models exist, capable of varying degrees of resolution on the vertical, and designed for various purposes: day-to-day weather prediction, theoretical studies and general circulation studies of a numerical nature; the two latter uses are of the greatest present interest.

The theoretical study by Phillips (1954) using the Charney-Phillips "2½ dimensional" two layer  $\beta$  plane model (Charney and Phillips, 1952) initially considers exclusively baroclinic instability with initial zonal velocities independent of  $y$ . Phillips uses the wave with maximum amplification rate to evaluate terms in the nonlinear tendency equations analogously to the work of Platzman, Kuo, and Lorenz above. The initial assumption of no latitudinal wind variation (initially) eliminates any perturbation vorticity, or momentum, being advected by the perturbation wind field although thermal effects are observed. However the tendencies do indicate a modification of the lower layer wind field (exactly compensated for by one of opposite sign in the upper layer thereby eliminating the possibility of any net transport of momentum across latitude circles) such as to induce westerly winds in mid latitudes and easterlies at the northern and southern extremes.

Charney (1959) carried this same approach a step further using the same model with the addition of heating and frictional dissipation. He computed the steady state symmetric flow, the Hadley circulation, appropriate to the forcing assumed. For a small wave perturbation the conditions for instability are ascertained by finite difference approximations; and the most (and next most) initially unstable perturbation was allowed to grow until a steady state condition resulted in which the rate at which the perturbations gained energy was just equaled by the rate at which they lost energy by radiation and by Reynolds stresses to the surroundings and to the now modified mean flow, respectively. The form of the steady state mean flow is seen to bear a gross resemblance to the atmosphere with middle latitude westerlies and easterlies at the sides. This is similar to Phillips' results. However the upper level flow, in Charney's model, is not just a mirror of the lower but has a strong westerly maximum in mid-latitude of about ten times the surface wind at that latitude. The easterly flows at the northerly and southerly sides are about three times the associated surface flow. The flow for the next most unstable eigenmode with a time constant or amplifying factor only about 2% smaller than the most unstable mode, however is very definitely not reminiscent of the atmosphere. The surface winds have the same east-west character but the upper flow shows strong westerly winds at latitudes where easterlies were before and a weak easterly flow over the central latitude. Recent studies of barotropic flow stability (Haltner and Song, 1962) would indicate that these two flows characterized by single and double maxima tend to be unstable with respect to

small perturbations and the tendency of the perturbations is to induce the one from the other. This possibility was excluded from Charney's work by his steady state assumption for the fully developed perturbation.

The possibility however of such markedly dissimilar flows arising from such apparently similar initial perturbations tends to give one pause for there can really be no assurance that the initially most stable or even next most stable mode will be the dominating one at a later time.

The resolution of this problem can only come by experimental approaches. The first and most famous of these is that of Phillips (1956), in which the equations whose stabilities were considered in his earlier paper were integrated numerically. Initially Phillips allows a symmetric circulation to grow uninfluenced by any eddies, perturbs it randomly and allows the unsteady eddies to grow to finite amplitude. In the earlier stages the resultant "weather" map looks quite similar to the contour map appropriate to Charney's steady state solution resulting from the initially most unstable eigenmode. The computed lower level mean zonal wind also bears resemblance to Charney's wind. However it is not until a later stage of the computation, a stage at which the kinetic energy of the perturbations remains at an almost constant level, that the jet-like character including high and low latitude easterly winds, shows up in the upper winds. One would argue from this that the most unstable mode, the one presumably first to be seen in the computations, is indeed the one that remains established in quasi-steady fully developed flows. However in Phillips computations the finite difference computational instabilities became predominant

shortly after the quasi-steady state was reached and the experiment ceased, so this presumption cannot be verified.

Regardless of whether the particular eigensolution or more exactly the collection of solutions observed, would have been those of a true steady state solution, the results are of course most significant. In most general terms they say that the rather extreme simplifications inherent in the two level quasi-geostrophic prediction equations and the also highly simplified heating and friction effects used, still leave one with a model that can and does describe the large scale features of the observed atmosphere. The suggestion that such simplifications would bear fruit even in their extremity arose of course from the work that went before, partially outlined here, but the verifying of them, showing that such a set of abstractions from reality were or included the right abstractions was the major import of the paper.

The way would seem open for extensive studies of the details of the atmospheric circulation: bigger and better (but never quite big enough) computing machines will allow for more and greater detail. The direction in which these studies seem to be tending is one away from the simplicities incorporated in the prior general circulation work. Smagorinsky's (1963) integrations for example employed the primitive equations in a two layer model; projections for further work envision multilayered models with incorporation of condensation and evaporation as heat sources and sinks, more realistic details of turbulent energy transformations and transfers, interactions with the sea and land surface, both thermal and frictional,

and a host of other physical effects known or suspected to have a significant influence upon the general circulation. The rationale for this is obvious. When the computations can reproduce the atmosphere closely experiments within the computations will take the place of perhaps unfeasible and presumably undesirable physical manipulation of the environment.

This tendency to eliminate simplification, though valid for the ends envisioned, does seem to be tending away from the hope of a physical explanation for the large scale features of the atmospheric flow. The very fact that the equations of motion reproduce the flow is taken as sufficient explanation of the flow. The other direction remains open however, that of making further simplifications, going beyond those employed by Kuo and Phillips in an effort to further bracket the physical causes of the large scale features of the flow.

## 2. The Ultimate Simplification of the General Circulation

The method of the present study, as suggested above, is to extract from the equations appropriate to describe all characteristics of atmospheric flow that portion which is sufficient to describe the gross features of the general circulation of interest, i.e. the east-west-east alternation of the surface zonal wind and the associated momentum convergences. To this end a hierarchy of simplifications are introduced until such time as it becomes obvious that further ones will eliminate even the possibility of successfully representing the desired elements of the circulation.

### I. The Quasi-Geostrophic Model in Two Layers

The initial simplification represents a very large step but one which has been taken many times in the past and hence through familiarity holds few terrors. It is to represent the atmosphere by a two level quasi-geostrophic "numerical weather prediction" model. The model selected is one by Lorenz (1960b), a model that allows for variations in the static stability of the atmosphere, an effect which would seem important in the study of the development and character of large scale flow characteristics. In this model the stream function for the nondivergent part of the wind is taken as  $\Psi + \tau$  and  $\Psi - \tau$  in the upper and lower layers respectively, the potential temperature as  $\theta + \sigma$  and  $\theta - \sigma$  in those layers and the velocity potential for the divergent part of the wind as  $-\chi$  and  $\chi$ . With  $f$  the coriolis parameter,  $C_p$  the specific heat of air at constant

pressure, "J" indicating a Jacobian in any as yet unspecified coordinate system, the equations for the model become

$$\frac{\partial}{\partial t} \nabla^2 \psi = -J(\psi, \nabla^2 \psi + f) - J(\tau, \nabla^2 \tau) \quad (1)$$

$$\frac{\partial}{\partial t} \nabla^2 \tau = -J(\psi, \nabla^2 \tau) - J(\tau, \nabla^2 \psi + f) + \nabla \cdot f \nabla \chi \quad (2)$$

$$\frac{\partial}{\partial t} \theta = -J(\psi, \theta) - J(\tau, \sigma) + \nabla \cdot \sigma \nabla \chi \quad (3)$$

$$\frac{\partial}{\partial t} \sigma = -J(\psi, \sigma) - J(\tau, \theta) + \nabla \theta \cdot \nabla \chi \quad (4)$$

$$bc_p \nabla^2 \theta = \nabla \cdot f \nabla \tau \quad (5)$$

b is a factor arising from the pressure differencing in the model, and t is the time.

Equations (1) through (5) are respectively the vorticity, the "thermal" or "shear vorticity", adiabatic, static stability and thermal wind equations, and form a closed set. Lorenz shows that this set properly describes the energetical relationships between potential and kinetic energies, available potential energy and gross static stability, and would seem to be about the simplest numerical prediction scheme capable of so doing.

Obviously before equations (1) - (5) can be used in any simulation of long term atmospheric flows some form of heating and frictional dissipation must be appended. In this model they are expressed in about the simplest form possible. The heating and static stability forcing are taken as proportional to the differences between the actual values and

some constant preassigned values denoted by  $\theta^*$  and  $\sigma^*$  respectively. The dissipation is taken as proportional to the flow in the lower layer and there is also a frictional drag at the interface between the two layers proportional to the shear,  $\tau$ , at the interface. The constants of proportionality for the heating and static stability forcing are denoted by  $h''$  and the ground and interface frictional coefficients by  $l''$  and  $l'''$  respectively. Under this notation the frictional and thermodynamic terms to be appended to equations (1) to (4) are:

$$\frac{\partial}{\partial t} \nabla^2 \psi = -\frac{l''}{2} \nabla^2 (\psi - \tau) \quad (1')$$

$$\frac{\partial}{\partial t} \nabla^2 \tau = \frac{l''}{2} \nabla^2 (\psi - \tau) - l''' \nabla^2 \tau \quad (2')$$

$$\frac{\partial}{\partial t} \theta = h'' (\theta^* - \theta) \quad (3')$$

$$\frac{\partial}{\partial t} \sigma = h'' (\sigma^* - \sigma) \quad (4')$$

One further modification is introduced into the model: rather than keeping the detailed structure of the static stability at all times it is smoothed out by an appropriate horizontal average and this horizontal average static stability replaces  $\sigma$  in equations (3), (4) and (4'). The resulting set of equations is identical to that studied by Bryan (1959) and similar to that studied by Lorenz (1962).

A possibly significant dynamic effect has been ruled out by the approximations introduced to date. There can be no ageostrophic transport of momentum by any meridional cells. The latter can be inferred to exist,

in a nongeostrophic sense, by study of the field of  $\chi$ , or better  $\nabla^2 \chi$  proportional to the individual pressure derivative, but their contribution to the momentum balance of the atmosphere is not recognized by the model. Making a model which was capable of reproducing this effect would so greatly unsimplify the study as to obviate the main point of the work. In working with the quasi-geostrophic model as defined by equations (1) through (5) it is perfectly possible to force circulations, via (3'), in which this effect would be important if it were incorporated. The expressions which would describe this effect and, if appended to equations (1) - (5), would transform them into the so called "balance equations" are, for

$$\frac{\partial}{\partial t} \nabla^2 \psi : \nabla \cdot \{ \nabla^2 \tau \nabla \chi + \nabla^2 \chi \nabla \tau \} \quad (1'')$$

and for

$$\frac{\partial}{\partial t} \nabla^2 \tau : \nabla \cdot \{ \nabla^2 \psi \nabla \chi \} \quad (2'')$$

A term of similar complexity (not however involving  $\chi$ ) must be appended to (5) for energetic consistency, c.f. Lorenz (1960b). Since these balance terms are not included in the model forced flows in which any momentum transports (and energy transformations) by this mode are as important as other modes could not be modeled properly and any quasigeostrophic model flows in which the balance terms could be inferred to be important if they were included would be of questionable significance.

The choice of a coordinate system with appropriate boundary conditions and appropriate means of dealing with the coriolis parameter is deferred until after consideration of the next major step in the simplification procedure.

## II. The Spectral Form of the Model

This next step is to express each of the variables in equations (1) through (5) as a sum of a series of orthogonal functions of space as done by Lorenz (1963b) the form and number of which will be selected as appropriate to the coordinate system and degree of detail in the representation desired. General statements about the set of functions can be proffered however. Denoting the set by  $F_i$  the following requirements must be fulfilled:

$$L^2 \nabla^2 F_i = -a_i^2 F_i \quad i = 0, 1, \dots \quad (6)$$

where  $L$  is a constant with dimensions of length and the  $a_i$  are the eigenvalues. On any boundaries the tangential derivatives, denoted by  $\partial/\partial s$ ,

$$\frac{\partial F_i}{\partial s} = 0 \quad (7)$$

We also require  $F_0 = 1$  hence  $a_0 = 0$ . As a consequence of the orthogonality and normalization of the functions

$$\overline{F_i F_j} = \delta_{ij} = \begin{cases} 1, & i=j \\ 0, & i \neq j \end{cases} \quad (8)$$

where the bar represents a horizontal average.

The jacobian of two orthogonal functions can itself be expressed as a series thusly

$$L^2 J(F_j, F_k) = \sum_{i=0}^{\infty} c_{ijk} F_i \quad (9)$$

where

$$c_{ijk} = L^2 \overline{F_i J(F_j, F_k)} \quad (10)$$

$c_{ijk}$  can be interpreted as the coefficient measuring the effect upon  $F_i$  of the nonlinear interactions of  $F_j$  and  $F_k$ . Certain relations among the  $c_{ijk}$ 's follow directly. From (10)

$$c_{ijk} = -c_{ikj} \quad (11)$$

By integrating (10) by parts and taking note of (7)

$$c_{ijk} = c_{jki} = c_{kij} \quad (12)$$

The variables are then expressed thusly:

$$\Psi = L^2 f \sum_{i=1}^{\infty} \psi_i F_i \quad (13)$$

$$\tau = L^2 f \sum_{i=1}^{\infty} \tau_i F_i \quad (14)$$

$$\theta = L^2 f^2 c_p^{-1} b^{-1} \sum_{i=1}^{\infty} \theta_i F_i \quad (15)$$

$$\bar{\sigma} = L^2 f^2 c_p^{-1} b^{-1} \sigma_0 \quad (16)$$

The boundary condition, (7), which states that the flow of the nondivergent wind across any boundaries is zero is not correct for an expansion of  $\chi$  similar to these for  $\psi, \tau$  etc. Instead we shall employ

$$\nabla^2 \chi = f \sum_{i=1}^{\infty} W_i F_i \quad (17)$$

In this set of expansions  $f$  is a constant with dimensions of inverse time shortly to be related to a constant coriolis parameter and  $\bar{\sigma}$  is the horizontally averaged static stability. The coefficients  $\psi_i, \tau_i, \theta_i, \sigma_i$  and  $W_i$  are nondimensional where we have non-dimensionalized with respect to the length  $L$  and time  $f^{-1}$ .

Before the expansions can be substituted into the governing equations as they are now written some specification of the coordinate system must be made for purposes of specifying the constant "f" appearing in the expansions. Again with an aim of introducing as much simplicity as possible we will settle upon a horizontal coordinate system, as opposed to spherical for example, with constant  $f$  but reintroduce later the terms necessary to add the " $\beta$  effect" to the stream function equations if this seems desirable in the light of the later investigation.

Since the assumption of a horizontal average static stability causes the second jacobian term on the right hand side of equation (3) to drop out, the third term there to become  $\bar{\sigma} \cdot \nabla^2 \chi$ , while equation (4) becomes simply

$$\frac{\partial}{\partial t} \bar{\sigma} = - \overline{\theta \nabla^2 \chi} ,$$

substitution of the orthogonal expansions into the governing equations and setting equal coefficients of like orthogonal functions result in

$$\dot{\psi}_i = \frac{1}{2} \sum_{j,k=1}^{\infty} a_i^{-2} (a_j^2 - a_k^2) C_{ijk} (\psi_j \psi_k + \tau_j \tau_k) - \frac{l}{2} (\psi_i - \tau_i) \quad (18)$$

$$\dot{\tau}_i = \frac{1}{2} \sum_{j,k=1}^{\infty} a_i^{-2} (a_j^2 - a_k^2) C_{ijk} (\psi_j \tau_k + \psi_k \tau_j) - a_i^{-2} W_i + \frac{l}{2} (\psi_i - \tau_i) - l' \tau_i \quad (19)$$

$$\dot{\theta}_i = \frac{1}{2} \sum_{j,k=1}^{\infty} C_{ijk} (\psi_k \theta_j - \psi_j \theta_k) + \sigma_0 W_i + h (\theta_i^* - \theta_i) \quad (20)$$

$$\dot{\sigma}_0 = - \sum_{i=1}^{\infty} \theta_i W_i + h (\sigma_0^* - \sigma_0) \quad (21)$$

and

$$\theta_i = \tau_i \quad (22)$$

In equations (18) through (21) the dot indicates the derivative with respect to the dimensionless time  $ft$  and the friction and thermal forcing terms (1') through (4') have been included with the coefficients  $l''$ ,  $l'''$  and  $h'$  non-dimensionalized with respect to  $f$ ; i.e.

$$l = l''/f, \quad l' = l'''/f, \quad h = h'/f$$

The forcing terms  $\theta^*$  and  $\sigma^*$  have been expanded in a series exactly corresponding to  $\theta$  and  $\bar{\sigma}$ , the expansion for the latter consisting of but one term. These equations (18) - (21) with the identity (22) are the spectral form of the two layer model.

### III. The Truncation of the Spectral Expansion

The last major step in the series of simplifications is to truncate severely the expansions for the variables, following the method introduced by Lorenz (1960a) keeping only the minimum number of terms needed to represent the large scale flow in at least an analogous way. Since the ability to at least characterize the general circulation's largest scale flows is desired consideration must also be given to the details of the coordinate system and the eigenfunctions,  $F_i$ , for that system. From the point of view of the spectral equations (18) - (21) however, the actual form of the  $F_i$ 's is of no direct concern. The functions enter in these equations via the eigenvalues  $a_i$  and interaction coefficients  $C_{ijk}$  only. Hence if different coordinate systems with their associated eigenfunctions give rise to the same  $a_i$ 's and  $C_{ijk}$ 's the spectral equations would apply equally in either coordinate system. On the other hand if the use of one coordinate system resulted in a whole class of interaction coefficients being equal to zero while another did not do so one would be tempted to prefer the latter on the basis of physical consistency. Maximum physical simplification is the aim of the present method of study but it would seem inconsistent to achieve such simplicity solely on the basis of the selection of a particular coordinate system. One would hope to have physical processes that are in a sense invariant under coordinate transformations. This should be a criterion in the selection of a coordinate system.

Two choices of coordinate systems seem to present themselves in the light of the previous assumption about the constancy of the Coriolis para-

meter, still allowing for the  $\beta$  effect if desired. The one would be a cylindrical system, analogous to the rotating dishpan experiments (Fultz et. al, 1959) and used by Lorenz (1962), for which the  $F_i$  would be Fourier-Bessel functions, and the other a simple cartesian system in which a double Fourier expansion would be appropriate (Lorenz, 1963b). In either case the truncated expansion should be capable of representing the two predominant modes of zonally averaged surface flow observed upon the earth. One of these is a flow of westerly (or easterly) winds throughout the region and the other is easterlies in low latitudes, westerlies in mid-latitudes and perhaps easterlies in northern latitudes as well. In any given case the observed flow would be a combination of these two modes together allowing, for example, the westerlies to be stronger than the associated easterlies. The simplest possible disturbance of the zonal average would be a single wave capable of interacting with either or both of the two zonal modes of flow. The existence of two zonal modes allows for barotropic instabilities and horizontal momentum transport by the wave which can assume an asymmetric shape about longitude lines. This would not be possible if only one zonal mode were allowed as was specified by Lorenz (1962) in his study of baroclinic instability with equations appropriate to the rotating dishpan.

If we settled upon a cylindrical coordinate system the simplest set of normalized orthogonal functions appropriate would be (cf. Lorenz, 1962)

$$\begin{aligned}
 F_1 &= J_0^{-1}(j_{11}) J_0(j_{11}r) \\
 F_2 &= \sqrt{2} J_0^{-1}(j_{11}) J_1(j_{11}r) \cos \phi \\
 F_3 &= \sqrt{2} J_0^{-1}(j_{11}) J_1(j_{11}r) \sin \phi \\
 F_4 &= J_0^{-1}(j_{1m}) J_0(j_{1m}r) \\
 F_5 &= \sqrt{2} J_0^{-1}(j_{1m}) J_1(j_{1m}r) \cos \phi \\
 F_6 &= \sqrt{2} J_0^{-1}(j_{1m}) J_1(j_{1m}r) \sin \phi
 \end{aligned}
 \left. \vphantom{\begin{aligned} F_1 \\ F_2 \\ F_3 \\ F_4 \\ F_5 \\ F_6 \end{aligned}} \right\} \begin{array}{l} \\ \\ \\ m > 1 \\ \\ \end{array} \quad (23)$$

where  $J_n$  is the Bessel Function of order  $n$ ,  $j_{nm}$  is the  $m^{\text{th}}$  root of the equation  $J_n = 0$  and  $r$  ( $0 \leq r \leq 1$ ) is the normalized radius of the nondimensional dishpan..

On the other hand the appropriate functions for a cartesian infinite strip are

$$\begin{aligned}
 F_1 &= \sqrt{2} \cos y \\
 F_2 &= 2 \sin y \cos kx \\
 F_3 &= 2 \sin y \sin kx \\
 F_4 &= \sqrt{2} \cos my \\
 F_5 &= 2 \sin my \cos kx \\
 F_6 &= 2 \sin my \sin kx
 \end{aligned}
 \left. \vphantom{\begin{aligned} F_1 \\ F_2 \\ F_3 \\ F_4 \\ F_5 \\ F_6 \end{aligned}} \right\} \begin{array}{l} \\ \\ \\ m > 1 \\ \\ \end{array} \quad (24)$$

In (24)  $x$  and  $y$  (nondimensional) vary from 0 to  $\pi$ , hence  $L = \frac{w}{\pi}$  with  $w$  the length of a side of the (square) region;  $k$  represents the wave number of the single allowed  $x$ -direction wave. In both (23) and (24) the coefficients of the transcendental variables have been chosen so that the average value of  $F_i^2$  equals unity.  $F_1$  and  $F_4$ , hereinafter refer-

red to, along with their respective  $\Psi_i$ ,  $\Theta_i$ ,  $\tau_i$ , and  $W_i$  expansion terms, as  $F_A$  and  $F_C$ , represent the zonal flow whose structure is determined by  $m$  while  $F_2 (= F_K)$  and  $F_3 (= F_L)$  represent one mode of the superposed wave and  $F_5 (= F_M)$  and  $F_6 (= F_N)$  is the other mode of the wave.

The specification of the zonal flow structure via "m" is, as it turns out, not unrelated to the choice between these two orthogonal sets (23) and (24), however a few preliminary remarks can be offered here. It would seem apparent that the choice of  $m$  would be between the values 2 or 3, higher harmonics would be superfluous.  $m = 2$  would describe a simple alternation of flow in the north south direction with westerlies in the northern half of the region, easterlies in the southern half or conversely.  $m = 3$  would represent the easterly-westerly-easterly alternation that is familiar from observations of surface and lower tropospheric winds. The use of  $m = 2$  would not necessarily be an unrepresentative choice however; it would be equivalent to representing the wind flow from the equator to  $60^\circ\text{N}$  or so, rather than the whole hemisphere. Delaying further consideration of which  $m$  is more appropriate we shall turn to the coordinate system choice.

The selection of one or the other of the two orthogonal sets depends upon their respective  $C_{ijk}$ . Consideration of (10) indicates that if any of the  $i$   $j$  or  $k$  are equal  $C_{ijk} = 0$ . (12) states that circular permutations of  $C_{ijk}$  are equal. Since we have six functions to select from, the number of  $C_{ijk}$  possible is the number of circular permutations of 6

taken 3 at a time, which is 40. Because of (11) half of these are but negatives of the other. Hence we have 20  $C_{ijk}$  to evaluate and consider. This reduction from 40 to 20 is equivalent to requiring the double summations of equations (18) - (20) be made only for  $k > j$  and dropping the " $\frac{1}{2}$ 's" from those equations.

It is easy to show either by inspection or actual evaluation that, regardless of which coordinate system is selected, 12 interactions coefficients will be identically zero, either because they measure the "interaction" of  $F_A$  and  $F_C$ , the two zonal components, or because they fall out during the zonal averaging over  $\lambda$  ( $\text{or } \phi$ ). The eight remaining coefficients are, using the new AKLCMN subscript notations,

$$C_{AKL}, C_{AMN}, C_{CKN}, C_{CLM}$$

$$C_{CKL}, C_{CMN}, C_{AKN}, C_{ALM}$$

Also irrespective of the coordinate system, the eigenvalues

$$a_K^2 = a_L^2, \quad a_M^2 = a_N^2.$$

Further reduction of the number of coefficients, however, can occur depending upon the selection of  $m$  and the orthogonal expansion set. Consider first the case  $m = 2$ . If the Fourier-Bessel expansion is selected then all eight coefficients remain as written. However if the Double Fourier expansion is employed the second row of  $C_{ijk}$  above  $C_{CKL}, C_{CMN}, C_{AKN}$  and  $C_{ALM}$  all equal zero, a fortuitous result of the  $y$  averaging. A number of rather undesirable, for present purposes, results accrue. For one, as a consequence of the equality of the  $a_K^2$

and  $a_L^2$  eigenvalues, all the nonlinear contributions to  $\Psi_A^*$  are washed out. This elimination of a physical processes occurs only because of the coordinate system choice and therefore violates the suggested criterion of physical invariance under coordinate transformations. Also, of course, the other physical processes represented by the various permutations of the subscripts of the eliminated  $C_{ijk}$  are likewise removed from the equations. Most important, however, is that in the full set of equations (see Lorenz, 1963b) certain symmetries occur such that (numerical) solutions with all variables with subscripts C, M and N replaced by those of opposite sign will be identical to the solutions with the original CMN variables except for the sign of those variables. Thus the equations allow of two equally probable solutions identical in all respects but for the rather large difference that the "climate", in particular the zonally averaged winds for an observer at a particular latitude, will be radically different in the two cases. In that this particular aspect of the climate is of primary interest in this work it would seem advisable to avoid this particular mode of representation in which the wind direction can be arbitrarily specified by a simple manipulation of the initial conditions.

On the other hand setting  $m = 3$  and using either the Fourier-Bessel or Double Fourier expansions leaves all eight  $C_{ijk}$  intact and eliminates the symmetries that give rise to the equal probability two climate solutions. This does not imply however that more than one solution, dependent upon various initial conditions, is not possible

either with  $m = 2$  or  $3$ . Such multiple solutions would not necessarily be equally probable in the sense that the  $m = 2$  two climate solutions are equally probable. By this it is meant that a wide range of initial conditions would lead to or be a part of one numerical solution while another distinct solution could only be achieved by specifying initial conditions in a relatively restricted range, if such a second solution existed at all.

On the basis of the physical consistency and representativeness arguments above we would seem to be left with a choice of three possibilities: the Fourier-Bessel expansion with  $m = 2$  or  $3$  or the Double Fourier  $m = 3$  options. The choice of one of the  $m = 3$  options has the additional attractions that it can suggest a structure of the wind field with a distinct maximum in the center of the region as well as leading to a representation of the whole hemisphere. Also a three cell meridional flow pattern will be representable. Since the physical effects represented by the equations are essentially the same in either case we shall settle upon the somewhat more representative  $m = 3$  case. As between using the Fourier or Fourier-Bessel expansions there seems little to indicate a preference of one over another; we will settle for the Double Fourier expansion (24) principally on the basis of the resultant ease in computing the  $C_{ijk}$ .

The selection of  $m = 3$  for the Double Fourier expansion marks the principal departure of the present study, as far as the formulation of the model goes, from the study by Lorenz (1963b) of the mechanics of

vacillation in which  $m = 2$ . In that study the symmetries in the equations which lead to the "two climate" solutions were of no consequence while here such a possibility had to be avoided. Furthermore although the formulation of the models in both the vacillation and present studies are along similar lines one should not anticipate that the numerical solutions will bear any but the grossest similarities to one another as the details of the final equations are quite different.

For the Double Fourier expansion with  $m = 3$

$$\left. \begin{aligned} C_{AKL} = C_{CMN} = -5 C_{AKN} = 5 C_{ALM} = -k \frac{\sqrt{2}}{\pi} \frac{8}{3} \\ C_{CKL} = -C_{AMN} = -\frac{27}{7} C_{CKN} = \frac{27}{7} C_{CLM} = k \frac{\sqrt{2}}{\pi} \frac{8}{5} \end{aligned} \right\} \quad (25)$$

while the eigenvalues  $a_i$  are

$$a_A^2 = 1, a_K^2 = a_L^2 = k^2 + 1, a_C^2 = 9, a_M^2 = a_N^2 = k^2 + 9. \quad (26)$$

Defining  $C = C_{AKL}$ ,  $C' = C_{CKL}$ ,

$$\left. \begin{aligned} \alpha &= a_N^2 - a_K^2 = a_M^2 - a_L^2 = 8, \\ \gamma &= \frac{a_L^2 - a_A^2}{a_K^2} = \frac{a_K^2 - a_A^2}{a_L^2} = \frac{a_N^2 - a_C^2}{a_K^2} = \frac{a_M^2 - a_C^2}{a_L^2} = \frac{k^2}{k^2 + 1}, \\ \gamma' &= \frac{a_N^2 - a_A^2}{a_K^2} = \frac{a_M^2 - a_A^2}{a_L^2} = \frac{k^2 + 8}{k^2 + 1}, \\ \gamma'' &= \frac{a_L^2 - a_C^2}{a_K^2} = \frac{a_K^2 - a_C^2}{a_L^2} = \frac{k^2 - 8}{k^2 + 1}, \\ \delta &= \frac{k^2 + 1}{k^2 + 9} \gamma, \quad \delta' = \frac{k^2 + 1}{k^2 + 9} \gamma', \quad \delta'' = \frac{k^2 + 1}{k^2 + 9} \gamma'', \end{aligned} \right\} \quad (27)$$

the equations of the model, (18 - 21) with  $\tau_i$  replacing  $\theta_i$ , become

$$\psi_A^\circ = -\frac{\alpha C}{5} (\psi_L \psi_M + \tau_L \tau_M - \psi_K \psi_N - \tau_K \tau_N) - \frac{\ell}{2} (\psi_A - \tau_A) \quad (28)$$

$$\psi_K^\circ = \delta C (\psi_A \psi_L + \tau_A \tau_L) - \frac{\delta' C}{5} (\psi_A \psi_N + \tau_A \tau_N) + \delta'' C' (\psi_C \psi_L + \tau_C \tau_L) - \frac{27}{7} \delta C' (\psi_C \psi_N + \tau_C \tau_N) + \frac{\delta}{K} \beta \psi_L - \frac{\ell}{2} (\psi_K - \tau_K) \quad (29)$$

$$\psi_L^\circ = -\delta C (\psi_A \psi_K + \tau_A \tau_K) + \frac{\delta' C}{5} (\psi_A \psi_M + \tau_A \tau_M) - \delta'' C' (\psi_C \psi_K + \tau_C \tau_K) + \frac{27}{7} \delta C' (\psi_C \psi_M + \tau_C \tau_M) - \frac{\delta}{K} \beta \psi_K - \frac{\ell}{2} (\psi_L - \tau_L) \quad (30)$$

$$\psi_C^\circ = -\frac{3}{7} \alpha C' (\psi_L \psi_M + \tau_L \tau_M - \psi_K \psi_N - \tau_K \tau_N) - \frac{\ell}{2} (\psi_C - \tau_C) \quad (31)$$

$$\psi_M^\circ = -\frac{\delta C}{5} (\psi_A \psi_L + \tau_A \tau_L) - \frac{9}{7} \delta' C' (\psi_A \psi_N + \tau_A \tau_N) - \frac{27}{7} \delta'' C' (\psi_C \psi_L + \tau_C \tau_L) + \delta C (\psi_C \psi_N + \tau_C \tau_N) + \frac{\delta}{K} \beta \psi_N - \frac{\ell}{2} (\psi_M - \tau_M) \quad (32)$$

$$\psi_N^\circ = \frac{\delta C}{5} (\psi_A \psi_K + \tau_A \tau_K) + \frac{9}{7} \delta' C' (\psi_A \psi_M + \tau_A \tau_M) + \frac{27}{7} \delta'' C' (\psi_C \psi_K + \tau_C \tau_K) - \delta C (\psi_C \psi_M + \tau_C \tau_M) - \frac{\delta}{K} \beta \psi_M - \frac{\ell}{2} (\psi_N - \tau_N) \quad (33)$$

$$\tau_A^\circ = -\frac{\alpha C}{5} (\psi_L \tau_M + \psi_M \tau_L - \psi_K \tau_N - \psi_N \tau_K) - W_A + \frac{\ell}{2} (\psi_A - \tau_A) - \ell' \tau_A \quad (34)$$

$$\tau_K^\circ = \delta C (\psi_A \tau_L + \psi_L \tau_A) - \frac{\delta' C}{5} (\psi_A \tau_N + \psi_N \tau_A) + \delta'' C' (\psi_C \tau_L + \psi_L \tau_C) - \frac{27}{7} \delta C' (\psi_C \tau_N + \psi_N \tau_C) + \frac{\delta}{K} \beta \tau_L - (1-\delta) W_K + \frac{\ell}{2} (\psi_K - \tau_K) - \ell' \tau_K \quad (35)$$

$$\tau_L^\circ = -\delta C (\psi_A \tau_K + \psi_K \tau_A) + \frac{\delta' C}{5} (\psi_A \tau_M + \psi_M \tau_A) - \delta'' C' (\psi_C \tau_K + \psi_K \tau_C) + \frac{27}{7} \delta C' (\psi_C \tau_M + \psi_M \tau_C) - \frac{\delta}{K} \beta \tau_K - (1-\delta) W_L + \frac{\ell}{2} (\psi_L - \tau_L) - \ell' \tau_L \quad (36)$$

$$\tau_c^\circ = -\frac{3}{7}\alpha c'(\psi_L \tau_M + \psi_M \tau_L - \psi_K \tau_N - \psi_N \tau_K) - \frac{1}{9}W_c + \frac{l}{2}(\psi_c - \tau_c) - l' \tau_c \quad (37)$$

$$\begin{aligned} \tau_M^\circ = & -\frac{\delta c}{5}(\psi_A \tau_L + \psi_L \tau_A) - \frac{9}{7}\delta' c'(\psi_A \tau_N + \psi_N \tau_A) - \frac{27}{7}\delta'' c'(\psi_c \tau_L + \psi_L \tau_c) + \\ & + \delta c(\psi_c \tau_N + \psi_N \tau_c) + \frac{\delta}{R}\beta \tau_N - \frac{1}{9}(1-\delta)W_M + \frac{l}{2}(\psi_M - \tau_M) - l' \tau_M \end{aligned} \quad (38)$$

$$\begin{aligned} \tau_N^\circ = & \frac{\delta c}{5}(\psi_A \tau_K + \psi_K \tau_A) + \frac{9}{7}\delta' c'(\psi_A \tau_M + \psi_M \tau_A) + \frac{27}{7}\delta'' c'(\psi_c \tau_K + \psi_K \tau_c) - \\ & - \delta c(\psi_c \tau_M + \psi_M \tau_c) - \frac{\delta}{R}\beta \tau_M - \frac{1}{9}(1-\delta)W_N + \frac{l}{2}(\psi_N - \tau_N) - l' \tau_N \end{aligned} \quad (39)$$

$$\begin{aligned} \tau_A^\circ = & c(\psi_L \tau_K - \psi_K \tau_L) - \frac{c}{5}(\psi_N \tau_K - \psi_K \tau_N) + \frac{27}{7}c'(\psi_L \tau_M - \psi_M \tau_L) - \\ & - c'(\psi_N \tau_M - \psi_M \tau_N) + \sigma_0 W_A + h(\tau_A^* - \tau_A) \end{aligned} \quad (40)$$

$$\begin{aligned} \tau_K^\circ = & -c(\psi_L \tau_A - \psi_A \tau_L) + \frac{c}{5}(\psi_N \tau_A - \psi_A \tau_N) - c'(\psi_L \tau_c - \psi_c \tau_L) + \\ & + \frac{27}{7}c'(\psi_N \tau_c - \psi_c \tau_N) + \sigma_0 W_K + h(\tau_K^* - \tau_K) \end{aligned} \quad (41)$$

$$\begin{aligned} \tau_L^\circ = & c(\psi_K \tau_A - \psi_A \tau_K) - \frac{c}{5}(\psi_M \tau_A - \psi_A \tau_M) + c'(\psi_K \tau_c - \psi_c \tau_K) - \\ & - \frac{27}{7}c'(\psi_M \tau_c - \psi_c \tau_M) + \sigma_0 W_L + h(\tau_L^* - \tau_L) \end{aligned} \quad (42)$$

$$\begin{aligned} \tau_c^\circ = & c'(\psi_L \tau_K - \psi_K \tau_L) - \frac{27}{7}c'(\psi_N \tau_K - \psi_K \tau_N) + \frac{c'}{5}(\psi_L \tau_M - \psi_M \tau_L) + \\ & + c(\psi_N \tau_M - \psi_M \tau_N) + \sigma_0 W_c + h(\tau_c^* - \tau_c) \end{aligned} \quad (43)$$

$$\begin{aligned} \tau_M^\circ = & \frac{c}{5}(\psi_L \tau_A - \psi_A \tau_L) - c'(\psi_N \tau_A - \psi_A \tau_N) - \frac{27}{7}c'(\psi_L \tau_c - \psi_c \tau_L) - \\ & - c(\psi_N \tau_c - \psi_c \tau_N) + \sigma_0 W_M + h(\tau_M^* - \tau_M) \end{aligned} \quad (44)$$

$$\begin{aligned} \tau_N^\circ = & -\frac{c}{5}(\psi_K \tau_A - \psi_A \tau_K) + c'(\psi_M \tau_A - \psi_A \tau_M) + \frac{27}{7}c'(\psi_K \tau_c - \psi_c \tau_K) + \\ & + c(\psi_M \tau_c - \psi_c \tau_M) + \sigma_0 W_N + h(\tau_N^* - \tau_N) \end{aligned} \quad (45)$$

$$\sigma_0^\circ = -\tau_A W_A - \tau_K W_K - \tau_L W_L - \tau_c W_c - \tau_M W_M - \tau_N W_N + h(\sigma_0^* - \sigma_0) \quad (46)$$

In these equations the  $\beta$  effect has been readmitted to the  $\psi$  and  $\tau$  equations, in effect making the  $\beta$  plane approximation.  $\beta$  is here nondimensionalized by the factor  $f/l$ .

The nineteen equations (28) - (46) can easily be reduced to thirteen equations by the elimination of the  $W_A, W_K, \dots$  terms. These thirteen equations and their performance in representing the gross features of the general circulation will be our concern henceforth.

#### IV. Commentary: Momentum Convergence, Energetics and other Details.

A number of auxiliary formula, representing certain familiar atmospheric processes, should be noted. One of obvious importance to the present study expresses the change of zonally averaged momentum due to various forms of momentum convergence. We shall, for later comparison, include the convergence terms arising from the implied meridional circulations, given by the balance equation terms, (1'') and (2''), and enclose them in curly brackets. If square brackets are taken to indicate the zonal average of a quantity over one or more wavelengths, a prime the deviation therefrom and a subscript a partial derivative, it is a straightforward operation to show that the equation for the change in zonal momentum per unit mass for the upper layer is

$$\begin{aligned} \frac{\partial}{\partial t} [\psi + \tau]_{yy} = & - [(\psi'_x + \tau'_x)(\psi'_y + \tau'_y)]_{yy} + f [\chi]_{yy} - l''' [\tau]_{yy} \\ & + \left\{ ([\psi + \tau]_{yy} [\chi]_y + [\tau]_y [\chi]_{yy})_y + \right. \\ & + [(\psi' + \tau')_{yy} \chi'_y + \tau'_y \chi'_{yy}]_y + \\ & \left. + [(\psi' + \tau')_{xx} \chi'_y + \tau'_y \chi'_{xx}]_y \right\} \end{aligned} \quad (47)$$

and for the lower layer

$$\begin{aligned} \frac{\partial}{\partial t} [\psi - \tau]_{yy} = & - [(\psi'_x - \tau'_x)(\psi'_y - \tau'_y)]_{yy} - f[\chi]_{yy} + \ell'''[\tau]_{yy} - \ell''[\psi - \tau]_{yy} \\ & - \left\{ ([\psi - \tau]_{yy} [\chi]_y - [\tau]_y [\chi]_{yy})_y \right. \\ & + [(\psi' - \tau')_{yy} \chi'_y - \tau'_y \chi'_{yy}]_y \\ & \left. + [(\psi' - \tau')_{xx} \chi'_y - \tau'_y \chi'_{xx}]_y \right\} \end{aligned} \quad (48)$$

These expressions can be cast into a more familiar form by integrating from  $y = 0$  to  $y$  and noting from the definition of the stream function

$$u_3 = -\frac{\partial}{\partial y} (\psi + \tau) \quad (49)$$

in the upper layer and

$$u_1 = -\frac{\partial}{\partial y} (\psi - \tau) \quad (50)$$

in the lower. Also  $u = -\frac{\partial \psi}{\partial y}$  and  $u_s = -\frac{\partial \tau}{\partial y}$  . (51)

Before the integration can be carried out we must give some consideration to the boundary conditions at  $y = 0$ . Anticipating the substitution of the expansion formulae (24) into the ultimate mean momentum equations we see that all but the following two integrated terms will be identically zero at  $y = 0$ :

$$f[\chi]_y, \quad [\psi - \tau]_{yy} [\chi]_y$$

The difficulty with these terms arises because  $[\chi]_y$  is defined in the expansions only in terms of  $\nabla^2 \chi$ , hence there can be no assurance that it is zero at  $y = 0$ . However since  $[\chi]_y$  is a measure of the northward component of the divergent part of the wind it would seem consistent with the previously specified boundary conditions relating to the nondivergent wind field, i.e.  $\Psi_x = 0$  at  $y = 0$ , to set it equal to zero at  $y = 0$  as well. This assumption does not enter into the dynamics of the quasi-geostrophic model in any way as only  $\nabla^2 \chi$  appears in those equations.

Performing the integrations, substituting from (49) - (51) and rearranging the terms somewhat results in

$$\begin{aligned} \frac{\partial}{\partial t} [u_3] = & - [u'_3 v'_3]_y + f [\chi]_y - l''' [u_3] \\ & + \left\{ ([u_3][\chi]_y)_y - [u][\chi]_{yy} \right. \\ & \left. + [\nabla^2(\psi' + \tau')\chi'_y + \nabla^2\chi'\tau'_y] \right\} \end{aligned} \quad (52)$$

and

$$\begin{aligned} \frac{\partial}{\partial t} [u_1] = & - [u'_1 v'_1]_y - f [\chi]_y + l''' [u_3] - l'' [u_1] \\ & - \left\{ ([u_1][\chi]_y)_y - [u][\chi]_{yy} \right. \\ & \left. + [\nabla^2(\psi' - \tau')\chi'_y - \nabla^2\chi'\tau'_y] \right\} \end{aligned} \quad (53)$$

The interpretation of these terms is straightforward. In both (52) and (53) the first terms on the right represent the momentum convergence by horizontal eddy transports, the second the transport of the earth's angular momentum by the mean meridional cell, the third the vertical interchange of momentum by friction and the fourth term in (53) the frictional momentum transfer to or from the surface. Within the curly brackets the first two terms express the ageostrophic momentum convergence arising from the implied mean meridional circulation, the first being the horizontal transport within each layer and the second the vertical transport of the vertically averaged mean zonal wind. The second two terms represent essentially the same effects except the eddy meridional circulation and eddy momentum are involved.

Substitution of the expansions (13), (14), (17), (24) ( $m = 3$ ) and performing the  $x$  averaging is straightforward. In the expression for  $-[u_3' v_3']_y$  the  $y$  dependence is of the form  $(\cos 2y - \cos 4y)$ ,  $0 \leq y \leq \pi$ . To afford direct comparison with the dynamic equations this expression is expanded in a sine series and the first two terms only are retained. The final form of the terms for the upper layer are

$$-[u_3' v_3']_y / Lf^2 = \frac{8K}{\pi} \left\{ (\psi_K + \tau_K)(\psi_N + \tau_N) - (\psi_L + \tau_L)(\psi_M + \tau_M) \right\} \left\{ \frac{144}{35} \sin 3y - \frac{16}{15} \sin y \right\} \quad (54)$$

$$f [\chi]_y / Lf^2 = -\sqrt{2} \left\{ W_A \sin y + \frac{W_C}{3} \sin 3y \right\} \quad (55)$$

$$-L''' [u_s] / Lf^2 = -L' \sqrt{2} \left\{ \tau_A \sin y + 3 \tau_C \sin 3y \right\} \quad (56)$$

$$([u_3][\chi]_y)_y / L^2 = -2 \left\{ (\psi_A + \tau_A) W_A \sin 2y + \left( \frac{(\psi_A + \tau_A) W_c}{3} + 3(\psi_c + \tau_c) W_A \right) \times \right. \\ \left. \times (2 \sin 4y - \sin 2y) + 3(\psi_c + \tau_c) W_c \sin 6y \right\} \quad (57)$$

$$-[u][\chi]_{yy} / L^2 = \psi_A W_A \sin 2y + \psi_A W_c (\sin 4y - \sin 2y) + \\ + 3\psi_c W_A (\sin 4y + \sin 2y) + 3\psi_c W_c \sin 6y \quad (58)$$

The terms for the lower layer can be deduced by inspection of the upper layer terms without difficulty.

The truncation of the spectral expansion causes something of a distortion of reality in connection with the momentum balance of the model. In a steady state or time averaged flow, by definition, the rate of loss of momentum to the "ground" by friction in one latitude band is exactly compensated by a gain in some other band such that the net momentum flux averaged over  $x$  and  $y$  (and time) is zero. In that the zonally averaged velocity in the lower layer where ground friction acts is a combination of the orthogonal components

$u_{Ag} = \sqrt{2} (\psi_A - \tau_A) \sin y$  and  $u_{cg} = 3\sqrt{2} (\psi_c - \tau_c) \sin 3y$  one might anticipate that the condition for no net flux of momentum to the ground would be that the  $y$  averages of  $u_{Ag}$  and  $u_{cg}$  be equal and of opposite sign, or that  $(\psi_A - \tau_A) = -(\psi_c - \tau_c)$ . However the severity of the truncation prevents this from happening. The dynamic consequence of no

net flux of momentum is that the zonally averaged wind averaged in the vertical is constant in time i.e.

$$\psi_A^\circ = \psi_c^\circ = 0 \quad (59)$$

Incorporating (59) into equations (28) and (31) and eliminating the  $\psi_L \psi_M, \dots$ , etc., terms we obtain

$$\psi_A - \tau_A = \frac{7}{15} \frac{c}{c'} (\psi_c - \tau_c) = -\frac{7}{9} (\psi_c - \tau_c) \quad (60)$$

as the condition upon the "surface" (frictionally influenced) winds corresponding to no net momentum flux. Equation (60) besides being important for its own sake is also useful in specifying whether a steady state has been reached in any given numerical computation, or whether a time average of a varying zonal flow is representative of the true mean flow.

Another set of physical quantities that are modeled are the various forms of energy familiar from atmospheric studies and their modes of interchange by various dynamic processes. In the truncated model the appropriate forms of the zonal average kinetic energy  $\bar{K}$  per unit mass and the kinetic energy of the wave disturbances  $K'$  per unit mass are respectively in nondimensional form

$$\bar{K}/L^2 f^2 = \frac{1}{2} (\psi_A^2 + \tau_A^2 + 9[\psi_c^2 + \tau_c^2]) \quad (61)$$

$$K'/L^2 f^2 = \frac{1}{2} \left( a_{1K}^2 [\psi_{1K}^2 + \psi_{1L}^2 + \tau_{1K}^2 + \tau_{1L}^2] + a_M^2 [\psi_M^2 + \psi_N^2 + \tau_M^2 + \tau_N^2] \right) \quad (62)$$

while the spectral forms of the mean available potential energy  $\bar{A}$  per unit mass and eddy available potential energy  $A'$  per unit mass are, nondimensionally

$$\bar{A}/L^2f^2 = \frac{1}{2\sigma_0} (\tau_A^2 + \tau_c^2) \quad (63)$$

$$A'/L^2f^2 = \frac{1}{2\sigma_0} (\tau_K^2 + \tau_L^2 + \tau_M^2 + \tau_N^2) \quad (64)$$

It is easy to show, by substitution of equations (28) - (39) that

$$\frac{\partial}{\partial t} (\bar{K} + K' + \bar{A} + A') = 0 \quad (65)$$

if the friction and heating coefficients are temporarily set to zero. Expression (65) shows the equations of the model to have a proper energy integral conserving total energy in the absence of friction and heating.

By looking at the detailed form of (65) with the dynamic equations (28) - (39) substituted (and the friction and heating not set equal to zero) one can identify the terms which appear, say, in  $\frac{\partial}{\partial t} \bar{K}$  and  $\frac{\partial}{\partial t} K'$  with opposite sign and specify them as the energy interchange terms appropriate to the spectral model. Also the rate of energy gain, or loss, from the heating and friction will be expressed in appropriate terms. Employing the notation employed by Phillips (1956), where  $\{A \cdot B\}$  stands for the time rate of energy conversion from form A to form B (all nondimensionalized), we have

$$\{Q \cdot \bar{A}\}/L^2f^3 = \frac{h}{\sigma_0} (\tau_A^* \tau_A - \tau_A^2 - \tau_c^2) \quad (66)$$

$$\{A' \cdot Q\}/L^2f^3 = \frac{h}{\sigma_0} (\tau_K^2 + \tau_L^2 + \tau_M^2 + \tau_N^2) \quad (67)$$

$$\{\bar{A} \cdot A'\} / L^2 f^3 = \frac{1}{\sigma_0} \left\{ (c \tau_A + c' \tau_c) (\psi_k \tau_L - \psi_L \tau_k) + \left( \frac{9}{7} c' \tau_A - c \tau_c \right) (\psi_N \tau_M - \psi_M \tau_N) + \left( \frac{c}{5} \tau_A + \frac{27}{7} c' \tau_c \right) (\psi_N \tau_k - \psi_k \tau_N + \psi_L \tau_M - \psi_M \tau_L) \right\} \quad (68)$$

$$\{\bar{A} \cdot \bar{R}\} / L^2 f^3 = -\tau_A W_A - \tau_c W_c \quad (69)$$

$$\{A' \cdot K'\} / L^2 f^3 = -\tau_k W_k - \tau_L W_L - \tau_M W_M - \tau_N W_N \quad (70)$$

$$\{K' \cdot \bar{R}\} / L^2 f^3 = \alpha \left\{ \left( \frac{c}{5} \psi_A + \frac{27}{7} c' \psi_c \right) (\psi_k \psi_N - \psi_L \psi_M + \tau_k \tau_N - \tau_L \tau_M) + \left( \frac{c}{5} \tau_A + \frac{27}{7} c' \tau_c \right) (\psi_k \tau_N - \psi_L \tau_M + \psi_N \tau_k - \psi_M \tau_L) \right\} \quad (71)$$

$$\{\bar{R} \cdot F\} / L^2 f^3 = \frac{\rho}{2} (\psi_A - \tau_A)^2 + \rho' \tau_A^2 + a_c^2 \left[ \frac{\rho}{2} (\psi_c - \tau_c)^2 + \rho' \tau_c^2 \right] \quad (72)$$

$$\{K' \cdot F\} / L^2 f^3 = a_k^2 \left[ \frac{\rho}{2} \{ (\psi_k - \tau_k)^2 + (\psi_L - \tau_L)^2 \} + \rho' (\tau_k^2 + \tau_L^2) \right] + a_M^2 \left[ \frac{\rho}{2} \{ (\psi_M - \tau_M)^2 + (\psi_N - \tau_N)^2 \} + \rho' (\tau_M^2 + \tau_N^2) \right] \quad (73)$$

In these expressions  $Q$  represents the thermal source (or sink) of available potential energy restricted to  $\tau_A^*$  only and  $F$  the frictional sink of kinetic energy. Figure 1 summarizes equations (60) - (73) in an energy flow diagram. In Fig. 1 the boxes represent the dynamic and thermodynamic energy forms and the arrows are drawn as though all the energy interchanges were (arbitrarily) positive.

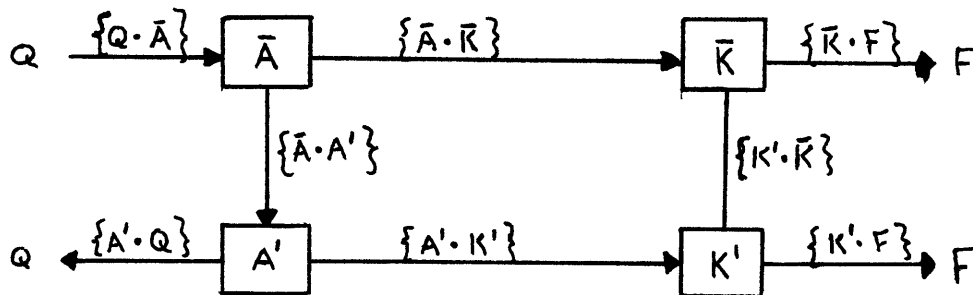


Fig. 1. Energy Interchange Diagram

As with the momentum equations these energy formulae will be of obvious use in the analysis of the behaviour of particular numerical solutions of the dynamic equations.

In investigating the numerical solutions it turns out to be convenient to make a change of the coordinate system. As written in equation set (24) the waves are viewed with respect to a fixed coordinate system. For present purposes a more useful system is one that moves with the first mode wave, the  $F_K, F_L$  wave. The variables in the new coordinates, indicated by primes, are defined by the following equations

$$\left. \begin{aligned}
 \psi_A' &= \psi_A & \psi_K' &= \sqrt{\psi_K^2 + \psi_L^2} & \psi_L' &= 0 \\
 \psi_C' &= \psi_C & \psi_M' &= \frac{\psi_N \psi_L + \psi_K \psi_M}{\psi_K'} & \psi_N' &= \frac{\psi_K \psi_N - \psi_L \psi_M}{\psi_K'} \\
 \tau_A' &= \tau_A & \tau_K' &= \frac{\psi_L \tau_L + \psi_K \tau_K}{\psi_K'} & \tau_L' &= \frac{\psi_K \tau_L - \psi_L \tau_K}{\psi_K'} \\
 \tau_C' &= \tau_C & \tau_M' &= \frac{\psi_L \tau_M + \psi_K \tau_M}{\psi_K'} & \tau_N' &= \frac{\psi_K \tau_N - \psi_L \tau_M}{\psi_K'}
 \end{aligned} \right\} (74)$$

The principal reasons for the introduction of this new coordinate system are for ease of recognition (in the computed results) of particular regimes of flow and to make averages of time varying flows meaningful. In the fixed system a time average of a steadily progressing wave would be equivalent to a zonal average and hence zero. This complete elimination of the wave in the averaging is avoided by presenting the computed results in the moving coordinates.

The method of numerical integration employed is the same as that used by Lorenz (1963a), and Bryan (1959), a double forward differencing

scheme. Letting  $X_n$  stand for the set of variables at time  $n\Delta t$ ,  $\Delta t$  the time increment, the equations to be integrated can be summarized by

$$\dot{X}_n = F(X_n) \quad (75)$$

Introducing the auxiliary definitions

$$\left. \begin{aligned} x_{n+1} &= X_n + F(X_n)\Delta t \\ x_{n+2} &= x_{n+1} + F(x_{n+1})\Delta t \end{aligned} \right\} \quad (76)$$

the double forward differencing is defined as

$$X_{n+1} = X_n + \frac{1}{2} (F(x_{n+1}) + F(X_n)) \Delta t$$

or by substitution of (76)

$$X_{n+1} = \frac{1}{2} (X_n + x_{n+2}) \quad (77)$$

Lorenz (1963a) has shown for equations similar to the ones considered here, that this scheme is not computationally stable but that the degree of instability is strongly dependent upon  $\Delta t$ . A solution to the conservative ( $h = \mathcal{L} = \mathcal{L}' = 0$ ) equations will eventually blow up. However if the nonconservative equation set is employed and  $\Delta t$  is sufficiently small the effects of the instability (an increase of the kinetic and potential energies in the system) will be equivalent to a reduced dissipation rate and no damage will be done. The selection

of an appropriate value of  $\Delta t$  is made essentially by a cut and try method; too large a value is immediately detectable in the numeric results (generally the numbers get, rapidly, too large for the machine to handle), too small a value, although not causing any instability will result in the necessity of inordinately long computations. As a practical matter a  $\Delta t$  which results in a period of at least twenty time steps or more, in the shortest of any periodic or quasiperiodic computational result, seems adequate to the task.

#### V. Summary: The Simplified Representation

For purposes of review and summary we shall consider how this highly simplified characterization of the atmosphere is capable of representing, in gross qualitative form, many of the more prominent features of the general circulation of present interest.

Starting at the "ground", the surface friction influenced lower layer, we have noted in some detail how the zonally averaged lower layer winds, described by  $\psi_{Ag} = \psi_A - \tau_A$  and  $\psi_{cg} = \psi_c - \tau_c$  in concert, can represent the familiar easterly-westerly-easterly variation with latitude ( $\psi_{Ag} > 0, \psi_{cg} < 0$ ) or the reverse. The former we shall call an "earthlike" regime, the latter "non-earthlike". Also, as noted, in a steady state or the time average of a varying state of flow the ratio of  $\psi_{Ag}$  to  $-\psi_{cg}$  would equal 7/9; this would be true whether the flow was earthlike or non-earthlike.

Another prominent feature representable in the model is the increase of westerly winds with height, the thermal wind, and in particular the formation of a mid-latitude maximum in the zonal mean, analogous to a climatological jet with its maximum intensity near the tropopause. The existence of an increase of westerlies with height is more or less required in the model by the quasi-geostrophic approximation and the thermal forcing upon the temperature, but the concentration of the flow into a central maximum is not inherent in the initial simplifications. For example given, in a steady or average state,

$\Psi_A > 0$ ,  $\Psi_C < 0$ , then  $\tau_A > 0$ ,  $\tau_C < 0$  would represent an increase of westerlies with height and also a tendency for the increase to be concentrated in mid-latitudes. However if  $\tau_C > 0$ , and the other terms unchanged, the tendency would be for the westerlies to be spread latitudinally in the upper reaches of the model atmosphere, an effect not characteristic of the real atmosphere. Further a configuration such as  $\tau_C > \Psi_C > 0$  would represent not only a spreading of the westerlies with height but an actual tendency for a double maximum with strong westerlies in the polar and tropical regions, a distinctly non-earthlike regime of flow.

Of major interest in this study is the structure of the momentum convergences in various regimes of flow because of their interrelation with the pattern of the lower layer zonal flow and the upper layer flow as well.

Finally, as detailed in the previous section, the energetics of the atmosphere are modeled by the various energy interchange terms summarized by Fig. 1. Of particular interest, among other things, will be the sign of the term  $\{ \bar{A} \cdot \bar{K} \}$ , the energy conversion brought about by the mean meridional cells. Interest has centered upon this term for some time in meteorological research as opinions of its importance in the energy cycle have waxed and waned. Consideration of its importance in the model energy cycle is obviously in order. Also of interest will be the relative magnitude of all the energy terms in selected cases as a qualitative description of how the model works, in a quite literal sense.

### 3. Solutions to the Equations

#### I. A Simple Analytic Solution: The Hadley Flow

Owing to the extreme simplifications introduced, the steady symmetric or Hadley flow, familiar from the rotating dishpan experiments, may be attained analytically for any numerical values of the forcing conditions when the thermal forcing is restricted to only the  $\tau_A^*$  ( $=\theta_A^*$ ) term. For this flow we require that all the wave coefficients  $\psi_k$ ,  $\psi_L$  etc. and all the time derivatives be zero in equations (28) - (46). The wave coefficients will then at all times remain zero and equation set (78) remains:

$$\left. \begin{aligned} -\frac{l}{2} \psi_A + \frac{l}{2} \tau_A &= 0 \\ \frac{l}{2} \psi_A - \left(\frac{l}{2} + l'\right) \tau_A - W_A &= 0 \\ -h \tau_A + \sigma_0 W_A &= -h \tau_A^* \\ -\tau_A W_A - h \sigma_0 &= -h \sigma_0^* \end{aligned} \right\} (78)$$

Solving in terms of  $\tau_A$  :

$$\left. \begin{aligned} \psi_A &= \tau_A (= \theta_A) \\ W_A &= -l' \tau_A \\ \sigma_0 &= \frac{h}{l'} \frac{\tau_A^* - \tau_A}{\tau_A} \end{aligned} \right\} (79)$$

and  $\tau_A$  is the single positive real root of the equation

$$\tau_A^3 + \left[ \left(\frac{h}{l'}\right)^2 + \left(\frac{h}{l'}\right) \sigma_0^* \right] \tau_A = \left(\frac{h}{l'}\right)^2 \tau_A^*$$

The Hadley flow solution of (79) is essentially the same as that obtained by Lorenz (1962, 1963b); the differences originate in a slightly different formulation of the temperature and temperature forcing fields which do not alter the physics of the solution. That the solution is the same as those obtained previously even though the complete sets of equations from which the Hadley solutions are drawn are quite different is not too surprising; the main reason is the restriction of the thermal forcing to the  $\tau_A^*$  term alone.

As Lorenz (1962) pointed out when discussing the Hadley flow perhaps the most striking feature of this solution is the ease with which it was attained while it still contains features reminiscent of much more general solutions. The surface flow  $\psi_A - \tau_A$  is identically zero reflecting the requirement that there be no net frictional accelerations in the steady state flow.

The momentum convergences are easily written down for the Hadley flow: from (52) and (55 - 58) the upper level convergence equation is

$$\frac{\partial}{\partial t} [u_3] / Lf^2 = -\sqrt{2} W_A \sin y - \sqrt{2} l' \tau_A \sin y + \left\{ -2(\psi_A + \tau_A) W_A \sin 2y + \psi_A W_A \sin 2y \right\} \quad (80)$$

where again the bracketed terms are the balance equation momentum terms. Incorporation of (79) shows that the geostrophic convergence terms balance exactly while the balance terms do not. A measure of the relative importance of the balance terms may be made by forming the ratio of the sum of the balance terms to either of the geostrophic terms. This ratio is of the

order of  $\Psi_A$ , hence the magnitude of  $\Psi_A$  determines the validity of the geostrophic assumption made in neglecting the balance terms in the dynamic equations.

This observation can be cast into more familiar terms by noting that for the Hadley circulation the maximum vertically averaged zonal velocity is given by

$$u = Lf \sqrt{2} \Psi_A$$

and recalling that the Rossby number  $R_o$  is customarily defined as the ratio of a characteristic velocity of the fluid to the absolute rate of rotation. Hence

$$R_o = \sqrt{2} \Psi_A \tag{81}$$

and the previous observation that  $\Psi_A$  be small for quasi-geostrophic validity is equivalent to the familiar requirement that the Rossby number be small.

The energetics of the Hadley flow are also easy to describe. It is simple to show that  $\{Q \cdot \bar{A}\} = \{\bar{A} \cdot \bar{K}\} = \{\bar{K} \cdot \bar{F}\} = \rho' \tau_A^2 (L^2 f^3)$ . In effect the single thermally direct meridional cell converts available potential energy to kinetic energy which in turn is lost from the system by friction.

In addition to the Rossby number a number of other nondimensional quantities familiar from studies of thermally forced rotating flows can be related to the nondimensional variables so far introduced. As  $\tau_A$  is

the coefficient appropriate to the vertical wind shear or thermal wind, it may be taken as proportional to the thermal Rossby number and  $\tau_A^*$  is similarly proportional to the forced thermal Rossby number. A caveat: these relations are precisely true only when  $\psi_c$  and  $\tau_c = 0$  e.g. in the Hadley flow. In more complex flows neither the zonal wind nor the vertical shear are uniquely determined by  $\psi_A$  or  $\tau_A$  but by a linear combination of respectively  $\psi_A$  and  $\psi_c$  and  $\tau_A$  and  $\tau_c$ . Provided however that the thermal forcing is restricted to  $\tau_A^*$  only, the proportionality of  $\tau_A^*$  to the forced thermal Rossby number for the whole regime of flow is maintained. Furthermore in the more complex flows the requirement that  $\psi_A$  be small for geostrophicity may not be sufficient. For greater assurance the complete zonal momentum convergence due to mean cell advection of the zonal wind, equations (57) - (58), may be computed on an auxiliary basis from time to time.

The heating and frictional coefficients  $h$ ,  $\mathcal{L}$  and  $\mathcal{L}'$  have been nondimensionalized, as noted above, by dividing the dimensional coefficients by  $f$ , the Coriolis parameter. In any investigation in which these coefficients are given a range of values, it would seem more logical to interpret these values as representing changes in the rotation rate rather than variations in the physical characteristics of the fluid modeled. Hence  $\mathcal{L}^{-1}$  may be taken as a measure of the rate of rotation, and  $\mathcal{L}^{-2}$  as the Taylor number. The ratio  $\mathcal{L}/h$  may be considered as a sort of large scale Prandtl number appropriate to the flow as a whole.

In the remainder of this discussion we shall arbitrarily set  $h = \mathcal{L} = 4\mathcal{L}'$  resulting in a gross Prandtl number of one. This relation is the same as that employed by Bryan.

A study of the stability of the Hadley circulation for small perturbations of the flow could be undertaken by the standard methods of perturbation analysis cf. Lorenz (1962). In such a study the  $\mathcal{W}$  terms would be eliminated from the original equations (28) - (46); the reduced set of equations would then be solved for  $\psi_k'$ ,  $\psi_L'$ ,  $\psi_m'$  and  $\psi_N'$  and the corresponding  $\tau'$  terms as functions of the equivalent undifferentiated terms. In a symbolic notation the equations in matrix form would be

$$\Psi' = M\Psi$$

where  $\Psi$  represents the  $8 \times 1$  matrix of  $\psi$ 's and  $\tau$ 's and  $M$  the  $8 \times 8$  matrix of coefficients. The  $M$  matrix contains terms depending upon the Hadley circulation and the forcing and as such determines the stability of the Hadley circulation. No attempt will be made to determine analytically the conditions under which  $M$  has eigenvalues with positive real parts, partially because of the considerable algebraic (or numeric) complexity involved and mainly because such an attempt doesn't seem germane to our present purposes. Also as will be seen shortly, the conditions for instabilities will be obtained implicitly by the experimental procedure followed.

## II. Numerical Solutions and Their Salient Characteristics

### A. Method of Approach and Outline of Results

The thirteen equations in the thirteen variables,  $6\psi$ 's,  $6\tau$ 's and  $\sigma_0$ , were programmed for solution on the MIT Computation Center IBM 7090 and stepwise time integrations carried out by the forward differencing method described above. In the computations the thermal forcing was restricted to  $\tau_A^*$  only, the forced static stability  $\sigma_0^*$  was set at zero and the wave number  $k$  was set at 2. In the majority of cases the initial conditions were specified as  $\psi_A = \tau_A = \tau_A^*$ ,  $\psi_K \neq 0$  and the other terms set equal to zero. These initial conditions represent an approximation to the Hadley flow with a perturbation in the first mode streamfunction wave. This perturbation was on the order of 15% or less of the zonal flow. The integrations were allowed to continue until such time as a discernable pattern was revealed in the printed output of the thirteen variables.

The two remaining controllable parameters,  $\tau_A^*$  and  $\ell$ , ranged over values of approximately 0.03 to 1.2. If we take the nondimensionalizing length  $\mathcal{W}$  as the pole to equator distance on the earth and the Coriolis parameter as that appropriate to  $40^\circ\text{N}$  latitude the equivalent dimensional temperature range corresponding to  $0.03 \leq \tau_A^* \leq 1.2$  is about  $42^\circ\text{C} \leq 2\tau^* \leq 1675^\circ\text{C}$  as the range of pole to equator forced temperature differences. The range of  $\tau^*$  considered was dictated by the results of the computations and not on any a priori considerations of the actual

temperature forcing on the earth. Needless to say the range of  $\tau^*$  is sufficiently great to include any reasonable guess of its correct magnitude.

The "correct" dimensional value for the ground friction coefficient  $\mathcal{L}$  is even more obscure than that of  $\tau^*$ . Bryan uses approximately  $1.8 \times 10^{-5} \text{ sec}^{-1}$  which when nondimensionalized by  $f$  at  $40^\circ\text{N}$  gives 0.19, a value approximately midway (logarithmically) between the extremes of  $\mathcal{L}$  considered. Again it would seem that anybody's reasonable guess for the ground friction can be accommodated.

In the basis of previous work both experimental (Fultz et al., 1959) and numerical (Lorenz 1963b) it was anticipated that at least four distinct types of flow would appear in the numerical results. For sufficiently low rotation rates and sufficiently high or sufficiently low heating the  $\psi_K$  perturbation upon the approximate Hadley flow should die out after a while leaving only the Hadley flow appropriate to the analytic solutions of the previous section. Such flows when they occur are denoted by a "0" on any pictorial representation of the computed results. The other three main types of flow were expected to occur at increased rotation rates and at heating values intermediate between the high or low values that resulted in the Hadley circulation. In the first of these the perturbation spreads to the other variables and they adjust themselves into a state of motion of the single wave without change of shape. As a result in the constancy of the wave shape the zonal variables  $\psi_A, \psi_c, \tau_A$  and  $\tau_c$  remain constant in time. This state of motion without change of shape, often referred to as the "Rossby mode", will be denoted by a "1".

The second wave regime, denoted by a "II", is the one known as vacillation: a periodic change in the shape of the progressing waves so as, for example, to add and subtract momentum alternately to the zonal flow. The periodicity may not be simple but it will be apparent nonetheless. Directly associated with the changing wave form will be a periodic variation in the intensity of the zonal flow.

The expectation of flows of type I and II was the principal reason for the introduction of the coordinate system moving with the wave of the first  $(\psi_r, \psi_e)$  mode (equation (74)). In this moving system type I flows will appear motionless, the printed results will show all thirteen variables as constant. Type II flows will also appear motionless but with periodic variations in the variables indicating the vacillations.

The third wave regime, "III", is essentially none of the previous ones: it appears as an aperiodic or random variation in the thirteen variables, although the irregularity does diminish somewhat under close scrutiny.

The results of an extensive series of computations all with the initial conditions outlined above are presented in Figs. 2 and 3. For the computations of Fig. 2  $\beta$  was set equal to zero, while those of Fig. 3 are for a (nondimensional)  $\beta$  value appropriate to approximately  $40^\circ\text{N}$  latitude. In these computations  $\beta = 0.6065$ . On both figures the ordinate is  $\tau_A^*$ , the thermal forcing or imposed thermal Rossby number, and the abscissa is  $\ell^{-1}$  proportional to the rotation rate. Both coordinates

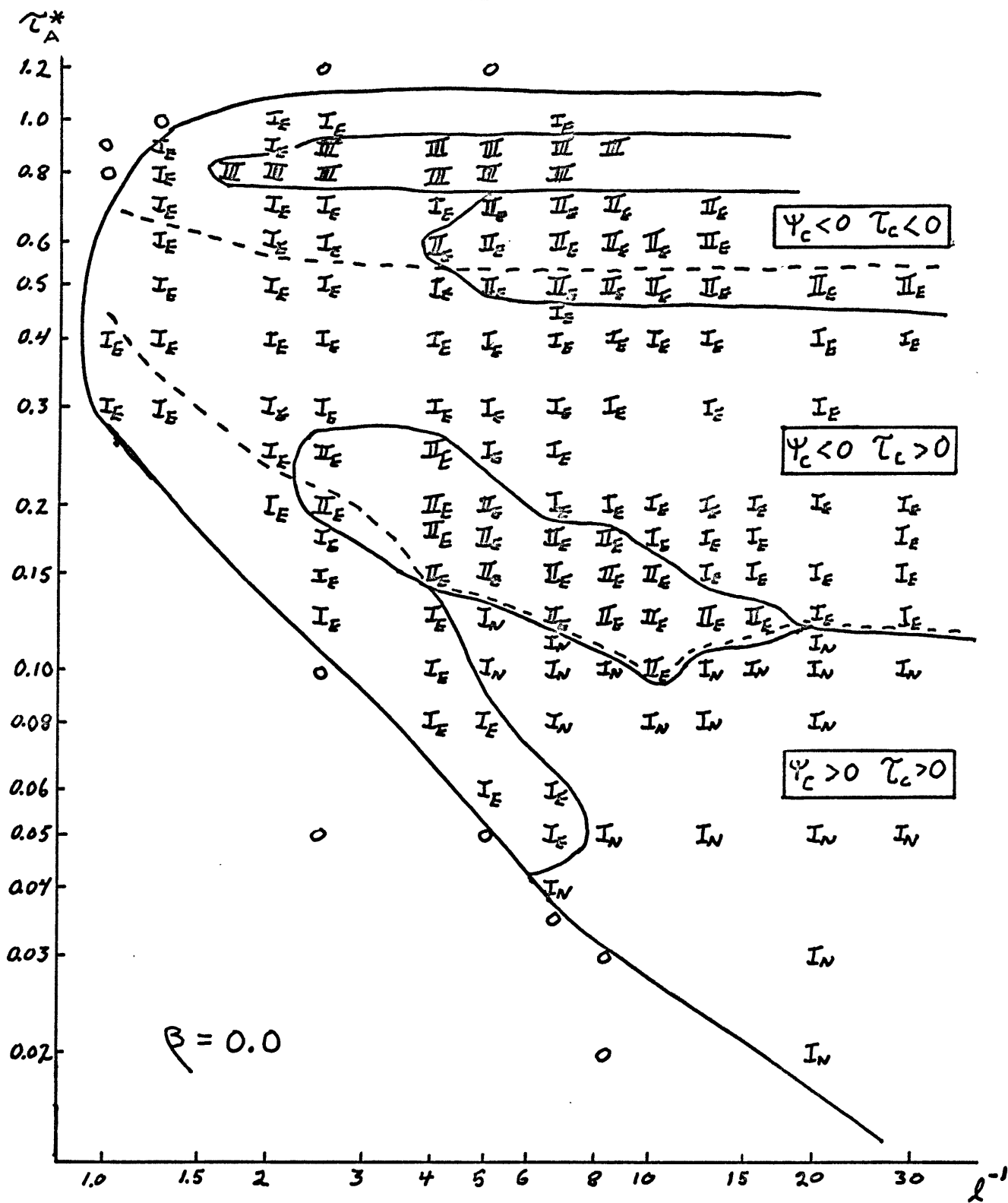


Fig. 2. Results of Computations without  $\beta$  effect. Ordinate: nondimensional forced temperature; abscissa: nondimensional rotation. Solid lines separate categories of evolved flow. O: Hadley; I: Rossby flow; II: vacillation; III: irregular. Subscripts indicate Earthlike or Non-earthlike surface zonal flow. Dashed lines separate certain characteristics of zonal flow structure.

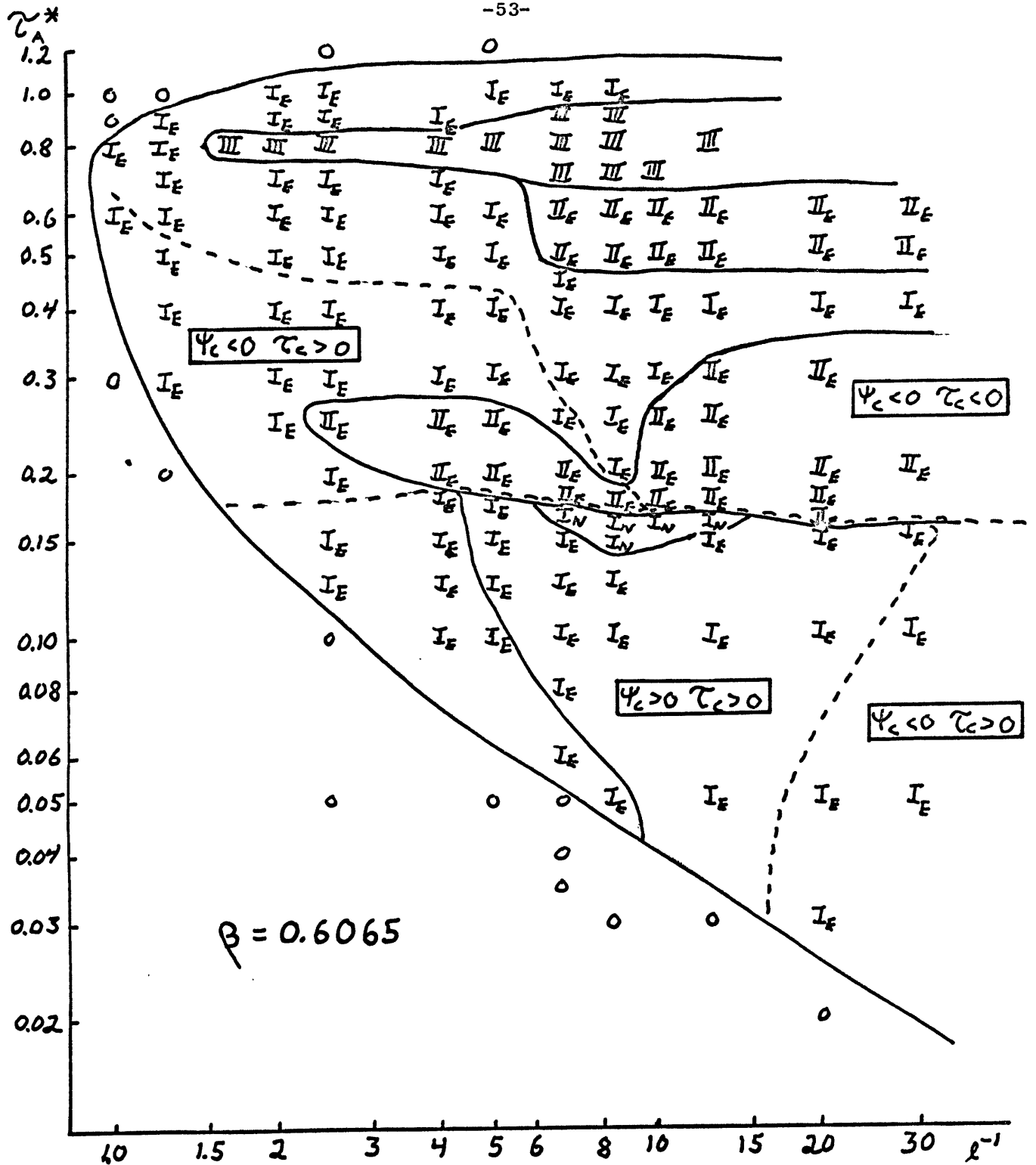


Fig. 3. Same as Fig. 2 but with  $\beta$  effect included.

are plotted logarithmically. In the body of the diagrams an "E" subscripted to the roman numeral indicating the evolved flow type designates an earthlike surface flow i.e.  $\Psi_{Ag} > 0$  ,  $\Psi_{cg} < 0$  ; if a subscript N appears the flow was non-earthlike. In the case of the type II vacillating flows, this determination was made on the basis of the surface flow averaged over one or more vacillation cycles. The solid lines indicate the approximate divisions between regimes of flow, while the dotted lines separate various categories of zonal maximum structure, in particular whether a single maximum exists at the 500 mb level of the model,  $\Psi_c < 0$  , or a double maximum exists there,  $\Psi_c > 0$  and whether the single maximum if it exists is increasing in intensity with height ( $\tau_c < 0$ ) or decreasing ( $\tau_c > 0$ ) . Again these distinctions are made on the basis of averages for the II flows.

Differences between the  $\beta = 0$  and  $\beta \neq 0$  flows are apparent but the overall similarities are quite marked also. As to the similarities most prominent among them is the division between the Hadley (0) and the Rossby (I) Regimes. Together they bear a close qualitative resemblance to both the experimental discoveries of Fultz et al. (1959) and the theoretical results of Lorenz (1962). Such was not unexpected as the same thermodynamic effects were incorporated into the equations as those used by Lorenz which in turn were designed to be appropriate to study the experimental results. Lorenz's work showed that the Hadley-Rossby transition could be explained in terms of the baroclinic instability alone of the Hadley flow. The present transition line presumably arises from

similar causes, at any rate the presence of the possibility of barotropic stability does not seem to inhibit the development of the Rossby flow in any apparent manner. Presumably the O-I transition lines in the two figures could have been arrived at theoretically by means of the perturbation eigenvalue method alluded to previously.

In both figures the type III irregular flow is confined to a relatively small area at relatively high thermal forcing and within roughly similar bounds. The same is true of the upper (higher  $\tau_A^*$ ) region of II flows in the two diagrams.

But there the major similarities end. The lower II regimes are quite different in shape; the I regime below this lower II regime is to a large extent earthlike as far as the surface winds go for  $\beta = 0.6065$  while the reverse is true for the  $\beta = 0$  computations; the area for which there exists a "500 mb" wind maximum, i.e.  $\psi_c < 0$ , which increases upward,  $\tau_c < 0$ , is considerably enlarged when the  $\beta$  effect is incorporated into the equations; other differences (and similarities) will be noted as the various regimes are studied in detail. The latter difference is, it may be noted, in a sort of qualitative agreement with the barotropic flow study of Kuo (1951) cited previously. In this study it was noted that the effect of  $\beta$  was to tend to concentrate momentum either into preexisting maxima of momentum or into the central portions of the zonal flows; in the present study the inclusion of  $\beta$  seems to have a similar effect, markedly increasing the area in which there is a 500 mb maximum that increases upward and somewhat enhancing the area in which the 500 mb wind has a single maximum at all.

## B. Momentum Convergences

Both for their intrinsic interest and relevancy to the present problem and as they are a convenient means of characterizing the various types of flow encountered, the momentum convergences or mean flow tendencies (eqs. 52 and 53) will be described and discussed in some detail. In addition the relative magnitudes of the geostrophic and ageostrophic momentum convergences will give a more reliable indication of the validity of the geostrophic assumption than the requirement that the Rossby number or  $\Psi_A$  be small.

### i. Motion Without Change of Shape

A few general remarks may be made at the outset. For one the net momentum convergence at any latitude in either level will be zero for the type I flows. This of course does not include any of the momentum convergences expressed by the balance equation terms as these are not recognized by the dynamic equations. Consideration both of the numerical results that went into the composition of Figs. 2 and 3 and a selected number of convergence figures indicate that within any region set off by solid lines on Figs. 2 and 3 the qualitative character of the flow and the associated convergences do not change greatly with a variation of the forcing parameters  $\tau_A^*$  or  $l^{-1}$ . The magnitudes of the convergence figures do change with important consequences but the changes appear more or less continuous within a given region. Discontinuous changes in the character of the numerical results and momentum convergences are observed across the boundaries

separating the various regimes of flow. There seems one exception to this: the small  $I_N$  region around  $\tau_A^* = 0.15$   $\ell^{-1} = 8.25$  on Fig. 3 ( $\beta = 0.6065$ ) is continuous with the  $I_E$  regime below it.

a. High Rotation Rates

Considering first the  $\beta = 0$  results we look first at the momentum convergence structure for the higher rotation rates and the associated mean flows. In particular Fig. 4 presents the structures for  $\ell^{-1} = 20$ , for  $\tau_A^* = 0.05, 0.1, 0.125$  and  $0.3$ . On the figures the ordinate is the geographic latitude, the abscissa, the nondimensional value of the convergence or mean velocity. The solid lines as indicated, are the eddy momentum convergence (eq. 54) for the upper and lower layers, the convergence of the earth's angular momentum due to the mean meridional cell in the upper layer (eq. 55) and on a separate abscissa the mean zonal velocity in the two layers, the subscript 3 designating the upper layer, 1 the lower layer. All the various quantities plotted are nondimensional although they are designated and referred to by dimensional symbols for simplicity and clarity. The mean cell earth's momentum convergence in the lower layer is simply the negative of the upper layer value and is not included in the figures; this is also true of the frictional convergence (or divergence) of upper layer momentum (eg. 56) which in the steady state I regimes just equals the negative of the sum of  $-[u_3' v_3']_y$  and  $f[\chi]_y$ ; also not included is the loss or gain of momentum by the lower layer through surface friction, it simply equals  $-\ell[u_1]$

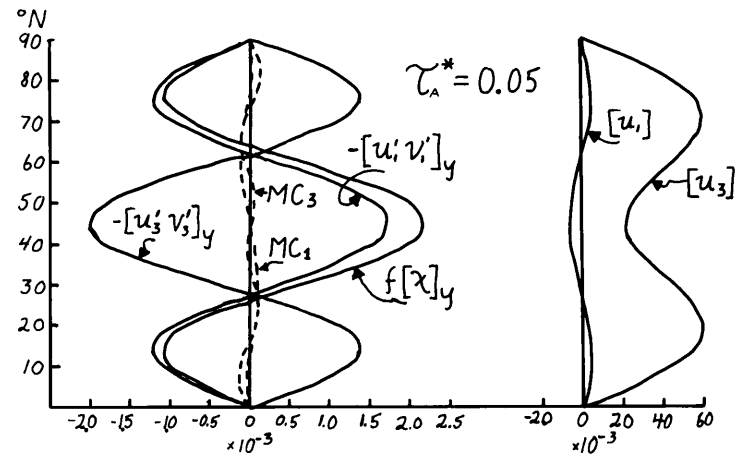
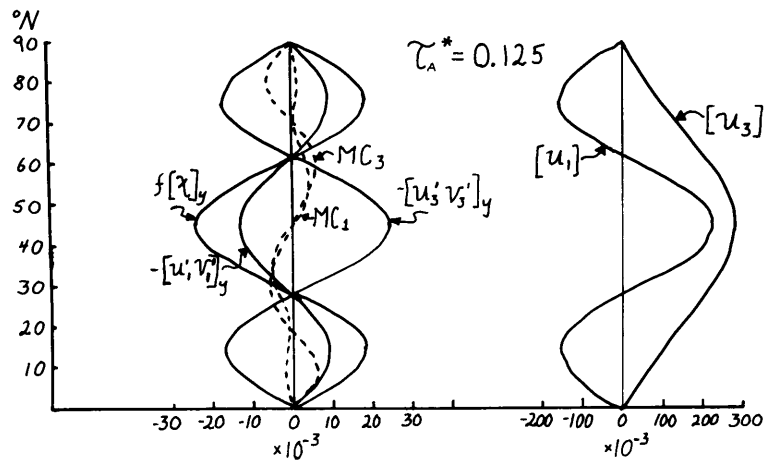
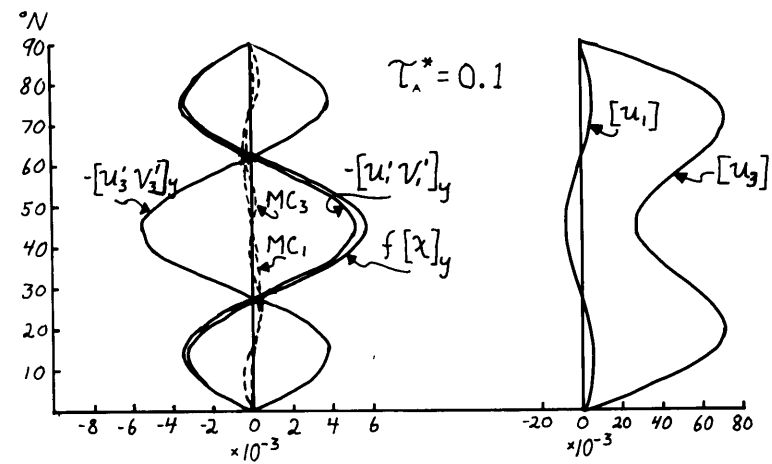
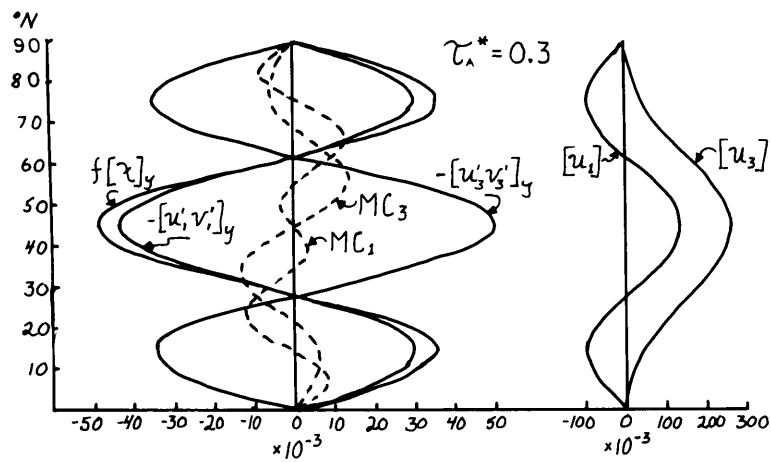


Fig. 4. Nondimensional Momentum Convergences and Zonal Velocities in the two Layers as Functions of Geographic Latitude.  $l^{-1} = 20.0$   $\beta = 0$   $\tau_A^*$  indicated in figures.

and its form can be inferred by consideration of the  $[u_1]$  figure. Also as a consequence of the steady state of the flow its value is given by a linear combination of the plotted convergences, namely

$$l[u_1] = -[u'_1 v'_1]_y - [u'_3 v'_3]_y \quad (82)$$

Included in the figures and represented by dashed lines is the net ageostrophic convergence of zonal mean momentum by the mean meridional cell, the sum of equations (57) and (58) for the upper and lower layer, indicated by  $MC_3$  and  $MC_1$ , respectively. The corresponding convergence arising from the eddy meridional cell (the last term of equations 52 and 53) has not been calculated as the principal reason for computing the ageostrophic convergence was to afford a check of the geostrophicity of the flow and not to study in any detail the ageostrophic "dynamics" of the flow. The mean cell convergences seem adequate to the task.

Reference to Fig. 2 shows that the  $\tau_A^* = 0.05$  and  $0.10$  cases belong to the lower  $I_N$  regime while the  $\tau_A^* = 0.125$  and  $0.3$  flows are characteristic of the upper  $I_E$  regimes. Inspection of Fig. 4 indicates the similarity of the flows except for the magnitudes within the same region and the dissimilarity of the pairs in different regimes. In the lower regime we have, of course, the non-earthlike surface flow with a very distinct double jet ( $\psi_c > \tau_c > 0$ ) in the upper layer. The eddy convergence, in the upper layer, is negative at mid-latitudes indicating a transport of momentum out of the center and into the regions of maximum flow. This term is slightly more than balanced at mid-latitudes, and

slightly less than balanced at the high and low latitudes by the  $f[\chi]_y$  term, resulting in a slight convergence everywhere in the upper region, balanced by friction. In the lower level the eddy convergence is positive at mid-latitudes as is the frictional transfer from the ground and the frictional transfer from above. The eddy convergence is by far the larger. This convergence is totally balanced by the  $f[\chi]_y$  term. The ageostrophic convergence is seen to be small, generally an order of magnitude or more less than the geostrophic terms indicating that the flow is certainly quasi-geostrophic.

The  $I_E$  regime characterized by the  $\tau_A^* = 0.125$  and  $0.3$  cases presents quite a different physical picture beyond the obvious one that the lower level flow is now earthlike in character, however there are physical similarities also. The upper flow no longer shows any double jet character; however  $\tau_c > 0$  indicating that there is a tendency for the increase of wind with height to be spread rather than concentrated into a single strong maximum. The upper level eddy convergence is now positive in mid-latitudes in contrast to the lower  $\tau_A^*$  cases, but like them the transport is still into the region of maximum zonal wind. As previously this convergence is nearly balanced by the negative (at  $45^\circ N$ )  $f[\chi]_y$  and exceeded by this term away from the center resulting in a net convergence throughout, compensated for by frictional transfer to the lower layer. In the lower layer the differences and parallels with the lower  $\tau_A^*$  case continue. The eddy

term is now divergent in mid-latitude as is the ground friction, where they were both convergent previously, and this divergence of momentum is principally balanced by the convergent  $-\{[\chi]\}_y$  term and to a lesser extent by the frictional convergence from above. At the extremes of latitude things are somewhat reversed with the convergent eddy ground friction and vertical friction terms balanced by the divergent  $-\{[\chi]\}_y$  term.

Consideration of the ageostrophic convergence terms for these flows characteristic of the  $I_E$  regime suggests the beginnings of some difficulties. The magnitudes of these terms are clearly an appreciable fraction of the geostrophic terms indicating a breakdown of the quasi-geostrophic assumption. Also they indicate the importance of considering the ageostrophic transport and not just looking at the Rossby number as defined by (81). For the  $\tau_A^* = 0.3$  case  $R_o = 0.116$  which might be considered to be satisfactorily geostrophic. Perhaps a better indicator of geostrophies in the model would be to take the Rossby number as the maximum  $[u_3]$ . Consideration of Fig. 4 shows that the maximum of  $[u_3]$  is clearly greater than 0.1 for the ageostrophic cases and conversely. We shall defer until later further consideration of the significance of this departure from geostrophicity, returning to the problem in the context of the discussion of the relevancy of the overall results to actual hydrodynamic flows.

Figure 5, the momentum terms for  $\ell^{-1} = 28.6$   $\tau_A^* = 0.15$ , is included to show the close resemblance between neighboring flows as alluded to

previously. Except for small differences in magnitudes the patterns are identical to the two  $I_E$  flows in Fig. 4.

The effect of including  $\beta$  in the dynamic equations is illustrated in Fig. 6, which presents the momentum results for  $\ell' = 20.0$  and  $\tau_A^* = 0.05, 0.10$  and  $0.15$ , all (see Fig. 3) within the lower  $I_E$  regime. The effects are most marked in the mean zonal wind structure, particularly in the lower layer but scarcely discernable in the momentum convergence variations, which seems quite remarkable. The lower level flow is now earthlike and the double maxima of the upper level are considerably reduced relative to the  $\beta = 0$  case. For  $\tau_A^* = 0.05$ , indeed, there is but a single broad maximum — however  $\tau_c$  is still positive indicating the tendency for spread rather than concentration of wind with height. This tendency toward, if not actual achievement of, a single maximum in the flow is again reminiscent of the result of Kuo cited previously. The upper level eddy momentum convergence is again negative in the center, nearly balanced throughout by the  $f[\chi]_y$  term with the small convergent residue balanced by vertical friction. The lower layer flow is, in overall appearance, similar to the  $I_N$  flows without  $\beta$  with, in mid latitudes, the convergent eddy and vertical exchange terms balanced principally by the divergent  $-f[\chi]_y$  term and to a lesser extent the now divergent surface friction term. The ageostrophic flow remains sufficiently small to assure quasi-geostrophicity as the maximum of  $[u_3]$  remain less than or at most equal to 0.1.

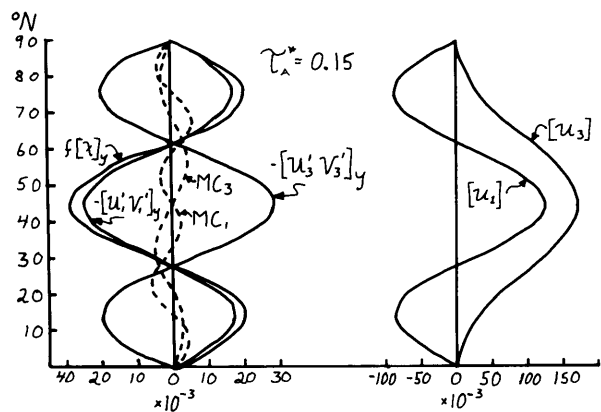


Fig. 5. Same as Fig. 4.  $l^{-1} = 28.6$   $\beta = 0$

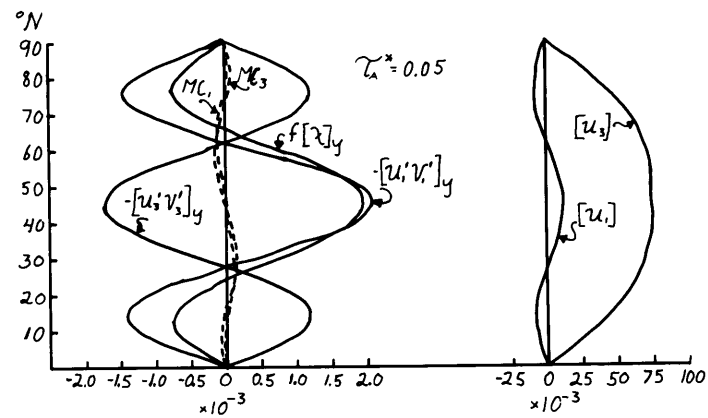
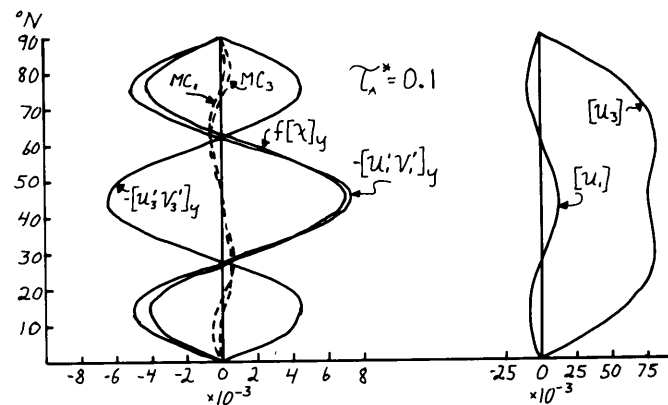


Fig. 6. Same as Fig. 4  $l^{-1} = 20.0$   $\beta = 0.6065$ .

A close look at the convergence terms at  $45^{\circ}\text{N}$  and actual computational results for the flow  $\tau_A^* = 0.1$ , for example, shows how the inclusion of  $\beta$  can profoundly alter the lower layer flow without making any major differences in the momentum convergence structure. Table 1 gives the nondimensional  $\psi$  and  $\tau$  values (multiplied by  $10^4$ ) for  $\ell^{-1} = 20$   $\tau_A^* = 0.1$ ,  $\beta = 0.0$  and  $0.6065$  for the steady states.

Table 1. Steady State Results  $\times 10^4$ .  $\ell^{-1} = 20$ ,  $\tau_A^* = 0.1$ .

$\beta$	Flow Type	$\psi_A$	$\psi_K$	$\psi_L$	$\psi_C$	$\psi_M$	$\psi_N$	$\tau_A$	$\tau_K$	$\tau_L$	$\tau_C$	$\tau_M$	$\tau_N$
0.0	$I_N$	215	152	0	48	-599	136	226	-57	-33	35	-59	315
0.6065	$I_E$	330	253	0	7	-798	-41	314	90	-20	28	-350	181

$\beta$  induces mainly three small changes to alter the surface flow. For one  $\tau_A$  is increased,  $\tau_C$  decreased causing an increase in the vertical shear at  $45^{\circ}$  and thus a larger frictional transfer of momentum to the lower layer. Secondly the relative magnitudes of  $-f[\chi]_y$  and  $-[u_1'v_1']_y$  are interchanged so that the net of these two terms alone in the lower layer becomes convergent with  $\beta$  where it was divergent previously. And finally the net of  $-[u_3'v_3']_y$  and  $-[u_1'v_1']_y$  shifts to convergent satisfying equation: (82). These effects are of course not independent of one another in that they are but different ways of looking at the fundamental results of table 1.

A further comment should be made on the physics of the  $\beta$  effect in the model. As introduced  $\beta$  has an influence only upon the waves and only indirectly, via the nonlinear coupling, on the zonal mean flows where

its effect is most noticeable. The nature of the direct influence upon the waves can be suggested by the familiar perturbation analysis of harmonic waves in a barotropic flow with finite lateral extent. The results of such analysis (see for example Haurwitz (1940)) states as the formula for the phase speed  $C$  of the wave

$$C = U - \frac{\beta L^2}{4\pi^2} \frac{D^2}{D^2 + L^2}$$

where  $D$  measures the lateral extent of the wave and  $L$  the wavelength, while  $U$  is the, constant, basic current speed. Thus, in this simple analysis, one may see that a wave with a smaller lateral extent will have a larger phase speed than a wave with a larger  $D$ . Hence one may infer that the inclusion of  $\beta$  into the system of finite amplitude waves here considered will alter the phase speeds of the KL wave differently from the MN wave. This in turn will influence their relative phase which alters the momentum convergence brought about by these two modes of the wave. Finally the changes in convergence will induce the changes in the mean flow structure described above.

The change induced by  $\beta$  for  $\tau_A^* = 0.15$  and above is of course quite substantial as can be seen from Figs. 2 and 3 involving obvious changes in the structure of the flow. But for the lower forcing and the higher rotation rates the effect of  $\beta$  can be summarized as causing small changes in the magnitudes of the momentum convergence terms but not in their large scale patterns. These small changes nevertheless are related to rather important differences in the structure of the mean flow.

b. Moderate Rotation Rates

Returning to the flows with  $\mathcal{B}$  absent we consider typical results at moderate rotation rates  $\mathcal{L}^{-1} = 6.67$ ,  $\tau_A^* = 0.05, 0.06, 0.1$  and  $0.3$  all in Fig. 7. Consideration of Fig. 2 in the light of the previous discussion of the local continuity of the results should lead us to anticipate that the  $I_N$  at  $\tau_A^* = 0.10$  and  $I_E$  at  $\tau_A^* = 0.3$  should be similar in form to their counterparts at  $\mathcal{L}^{-1} = 20$ , and indeed examination of Fig. 7 shows this to be so. The similarities are so close moreover that there seems little value in offering any detailed discussion of the momentum and mean velocity configurations; the previous descriptions are adequate for the present cases with one important exception. This relates to the relative changes in magnitude of the eddy convergence and the  $f[\chi]_y$  terms as the rotation rate decreases. In particular comparison of the  $\tau_A^* = 0.1$  cases in Figs. 4 and 7 shows that  $f[\chi]_y$  increases more for decreasing  $\mathcal{L}^{-1}$  than do either eddy convergence terms (the lower level eddy convergence actually decreases) and assumes a more important role in the momentum balance. This may be noted as an example of the inhibition of large scale vertical motions by rotation as described by Starr (Tellus 1959) in that  $[\chi]_y$ , the mean meridional velocity, is by continuity directly a function of the implicit vertical motion required for geostrophic balance.

The increase in the vertical and associated mean meridional motions coupled with the quite marked increase in the zonal flow magnitude bring about also a considerable increase in the ageostrophic convergence terms. This is most clear in the  $\tau_A^* = 0.3$  case when these terms are substantially

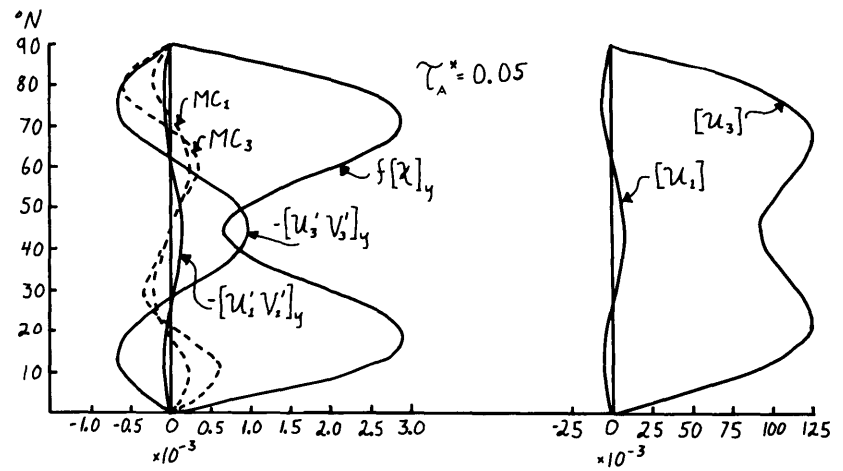
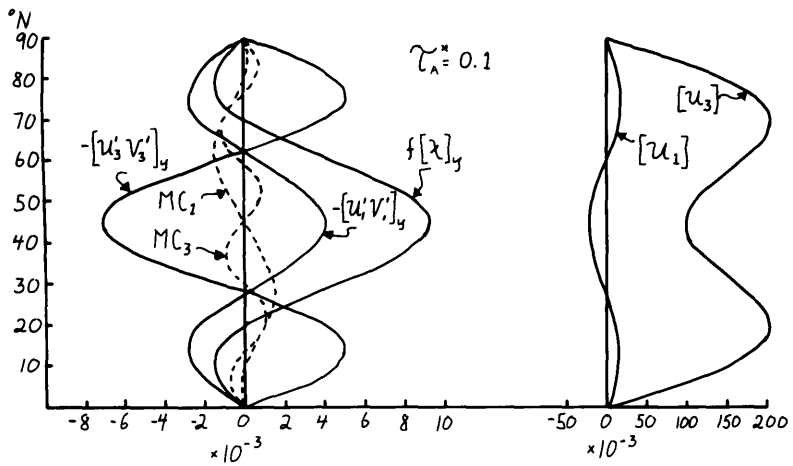
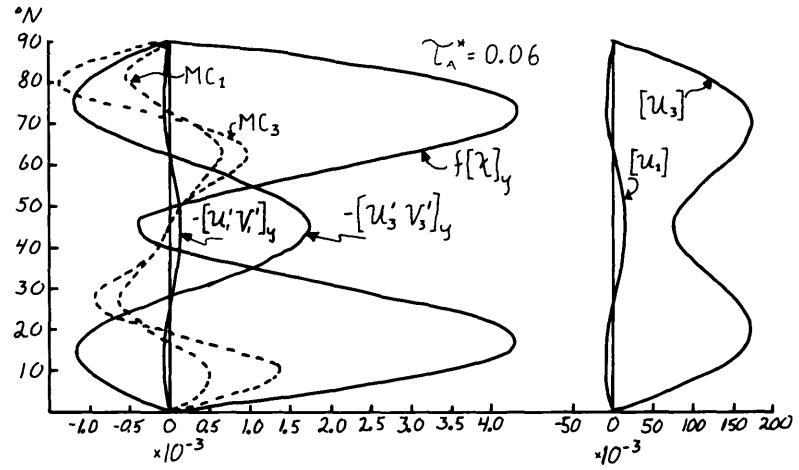
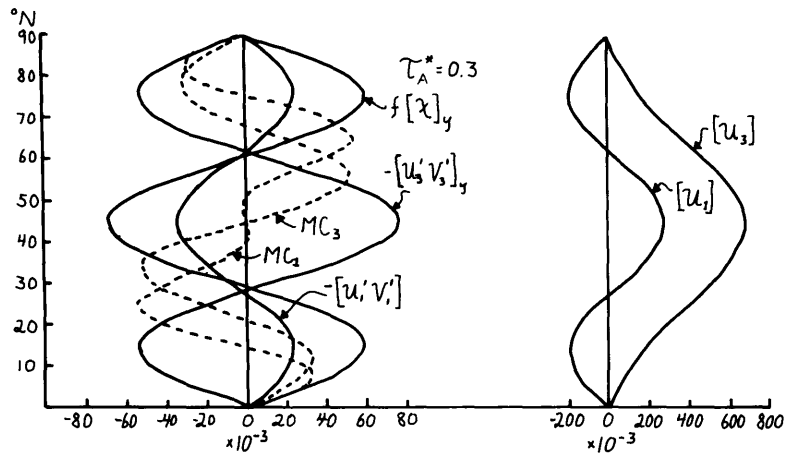


Fig. 7. Same as Fig. 4.  $l^{-1} = 6.67$

$\beta = 0.0$

equal to the geostrophic terms. The maximum of the nondimensional  $[u_3]$  is seen to be in excess of 0.6 and if this is taken as a Rossby number it is quite blatantly in excess of any geostrophic value. Although further discussion of this ageostrophicity is deferred until later it would seem reasonable to assert that modeled flows in which the ageostrophic convergences are as large or larger (as they are for higher  $\tau_A^*$ ) than the geostrophic convergences are of highly questionable validity in the sense that the model is not representing any real hydrodynamic flows. For this reason flows with  $\tau_A^*$  greater than 0.3 have not been described in any detail other than to indicate the gross nature of the numerical solution on Figs. 2 and 3.

Figure 7 does contain for  $\tau_A^* = 0.05$  and  $0.06$  a third variety of flow dissimilar to the ones encountered previously and deserving of closer scrutiny. As with the higher rotation rates and higher  $\tau_A^*$  for the same rotation the zonal flow in the upper level shows a distinct double maximum but in marked contrast the eddy convergence in the upper layer is positive in mid latitudes describing a transfer of momentum out of the maxima of the zonal flow. The double maxima are maintained against the everywhere negative frictional convergence by the earth's angular momentum term which as noted previously has grown considerably in importance over its role in the higher rotation rate cases. In the lower layer the eddy convergence is also positive in mid latitudes in contrast to the previous cases where the upper and lower eddy convergences were of opposite sign. In mid-latitudes this convergence plus

that of the frictional transfer from the upper layer is balanced by the frictional loss to the ground and the earth angular momentum term. At the high and low latitudes the convergent terms are the vertical friction and the ground friction which must be balanced by the others.

The ageostrophic terms are a moderate fraction of the others, even at the low  $\tau_A^*$ , and in particular are larger than the lower layer eddy momentum term. This lack of geostrophicity is also reflected in the magnitude of  $[\nu_3]$  as it exceeds 0.12. The mean cell convergences are still small however relative to the principal geostrophic term,  $f[\chi]_y$ , leaving us with some assurance the geostrophic assumption is not too severely violated.

The reintroduction of  $\beta$  is illustrated in Fig. 8. Again where  $\beta$  does not induce a major change in the character of the flow, i.e. for  $\tau_A^* = 0.05$  where the Hadley circulation is rendered stable and for  $\tau_A^* = 0.15$  where the vacillation is changed to a type I flow, its effect is slight, inducing quantitative changes somewhat greater than at  $\ell^{-1} = 20.0$  but no qualitative differences except, as before, in the lower layer zonal flow. This last effect is itself somewhat limited as it is only to induce earthlike lower layer flows where non-earthlike flows existed previously, not the reverse. In particular for  $\tau_A^* = 0.06$  the only marked quantitative change is a considerable enhancement of the eddy convergence of the lower layer along with a slight reduction in the  $f[\chi]_y$  term and the relative intensity of the double maxima of  $[\nu_3]$ . Essentially the same observations are valid for  $\tau_A^* = 0.1$  with the additional note of the reversal of

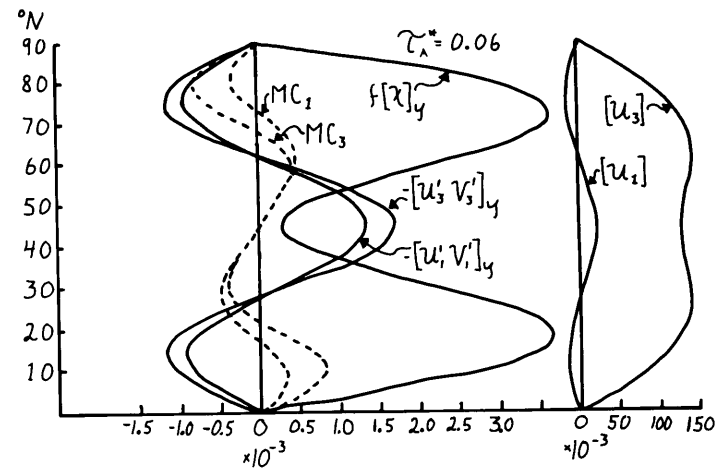
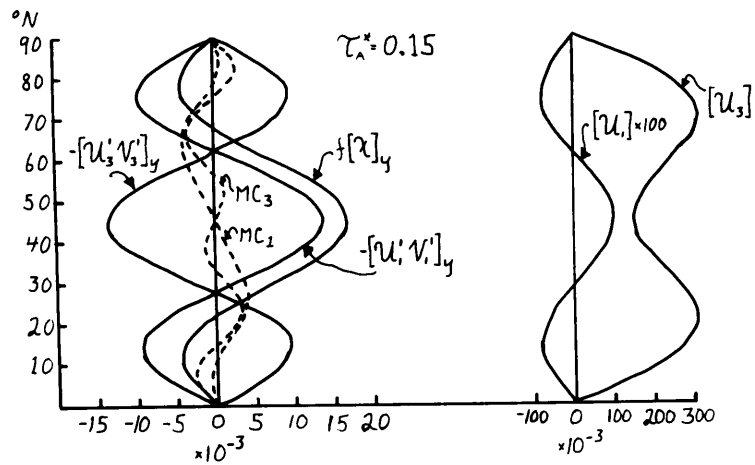
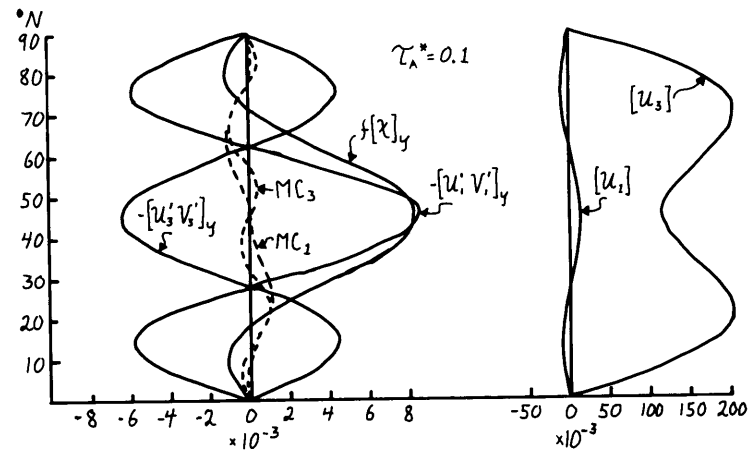
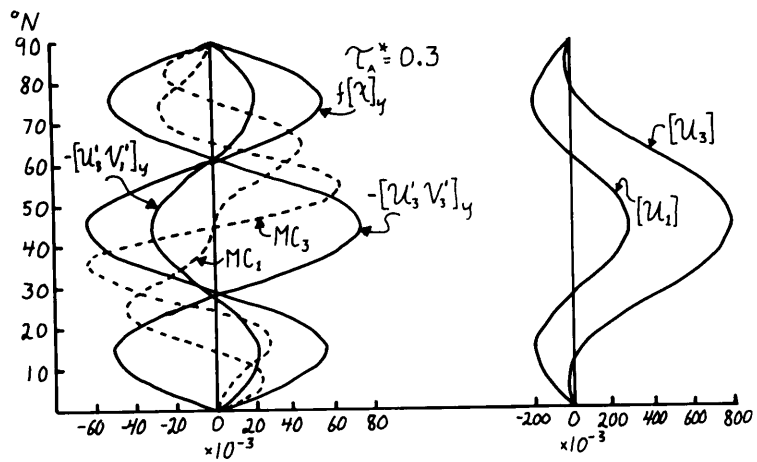


Fig. 8. Same as Fig. 4.  $\ell^{-1} = 6.67$   $\beta = 0.6065$

the  $[u_1]$  flow. The flow at  $\tau_A^* = 0.15$  is just a quantitative modification of those at lower forcing as is that at  $\tau_A^* = 0.17$  (not shown) where  $[u_1]$  has become non-earthlike. The  $\beta$  induced modifications of the  $\tau_A^* = 0.30$  flow are also slight, the only striking change being the small areas of easterly flow in  $[u_3]$ . This is partially a result of the flow's being in the region of  $\tau_c < 0$  as indicated on Fig. 3.

The  $\beta$  effects noted above, in particular the increase of  $-[u_1, v_1]_y$  for the  $\tau_A^* = 0.06$  case, are reassuring with respect to the geostrophicity of the flow. Although the ageostrophic convergences are still an appreciable fraction of the others they are no longer actually larger than any of the geostrophic terms, except as always over limited latitude bands. This increase in the geostrophicity can also be noted in the decrease of the  $[u_3]$  maximum from 0.17 to 0.14 with the introduction of  $\beta$ . The magnitude of the ageostrophic terms themselves diminish also.

### c. Low Rotation Rates

Further decreasing the rotation rate to  $\ell^{-1} = 2.5$  results in the flows portrayed in Figs. 9 and 10 (without and with  $\beta$  respectively) for  $\tau_A^* = 0.15$  and 0.3. Inspection of the figures quickly shows that no marked changes in the geostrophic momentum terms occur other than variations of the magnitudes of the terms. Both with and without  $\beta$  the  $\tau_A^* = 0.3$  momentum structure is almost the same as at the higher rotation rates and the  $\ell^{-1} = 2.5$   $\tau_A^* = 0.15$  flows also resemble very closely the  $\ell^{-1} = 6.67$   $\tau_A^* = 0.06$  flows.

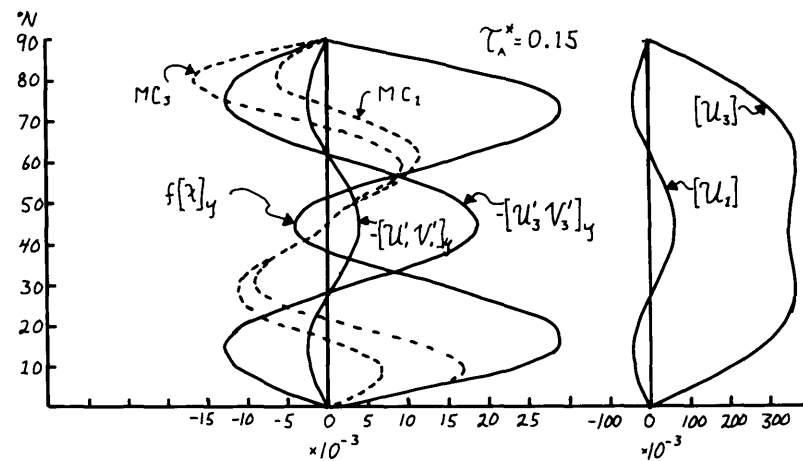
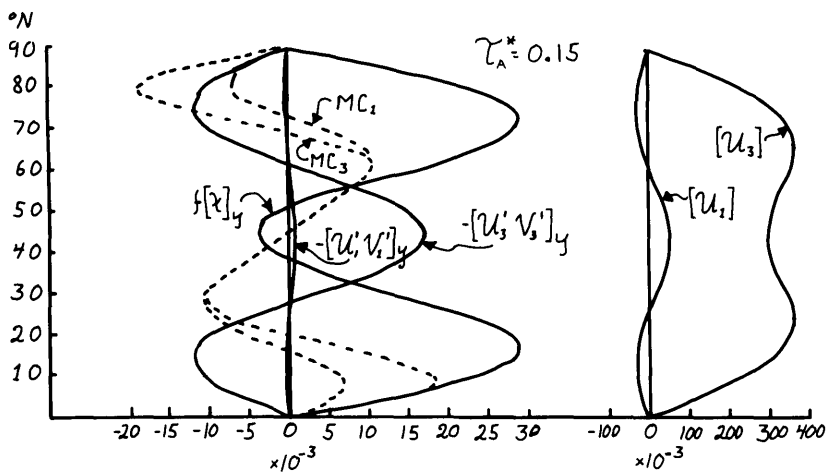
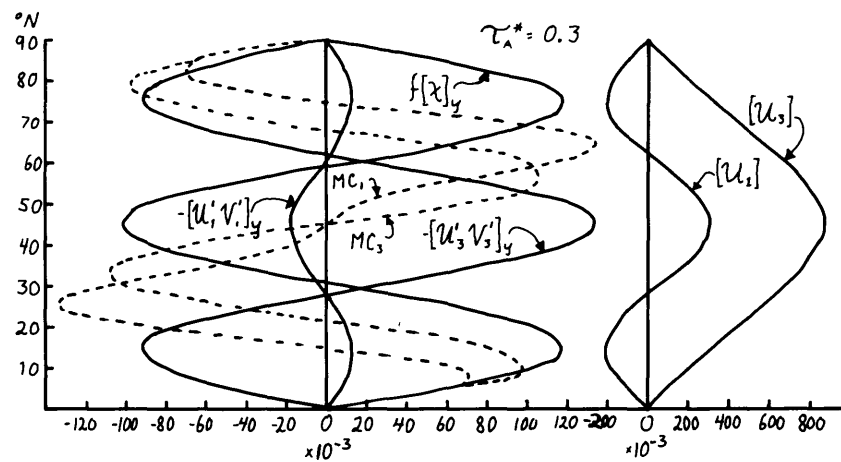
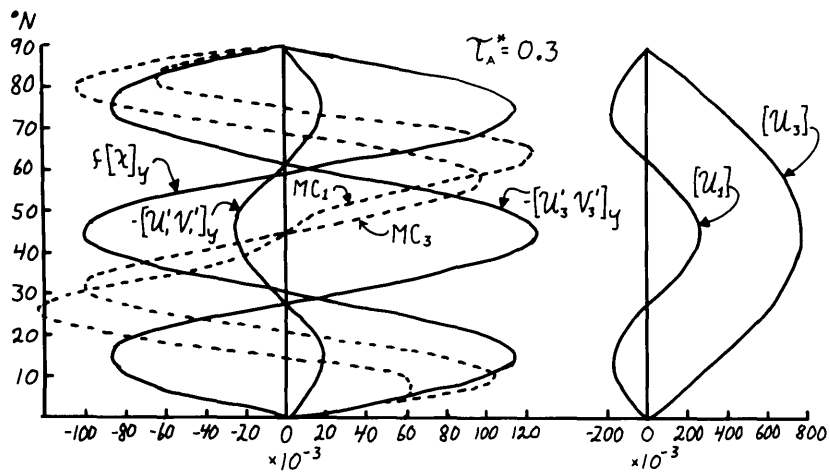


Fig. 9. Same as Fig. 4  $l^{-1} = 2.5$   $\beta = 0.0$

Fig. 10. Same as Fig. 4.  $l^{-1} = 2.5$   $\beta = 0.6065$

Moreover the beginnings of a resemblance of the  $I_E$  flows at  $\tau_A^* = 0.15$  and  $0.3$  may be noted in Figs. 9 and 10. This is seen principally in the  $f[\chi]_y$  term which exhibits an increased dominance of the  $W_C$  portion. Inspection of the results for still lower rotation rates (not reproduced) shows the changes between the illustrated  $\tau_A^* = 0.15$  and  $\tau_A^* = 0.3$  cases to be continuous:  $W_C$  increases in importance in the  $f[\chi]_y$  term and  $-[u_i', v_i']_y$  changes sign smoothly. This observation was the inspiration for the previous statement relating to continuous changes resulting eventually in substantially differing patterns of momentum transport.

As for the ageostrophic transports the figures show them to be quite as large as the geostrophic ones further accentuating the questionable validity of the geostrophic assumption in the low rotation rate region of Figs. 2 and 3 under consideration. Similarly the maxima of  $[u_3]$  are substantially above 0.1.

#### ii. Vacillation

Prior to looking closely at the momentum convergence structure of a typical vacillating flow we shall give brief consideration to a means of partially representing the flow short of presenting "weather" maps synthesized from the computational results. This method, employed by Lorenz (1963), is to consider the thirteen variables of the equations (or twelve variables when the moving coordinate system is employed) as defining a point in phase space, and the solutions to the equations as

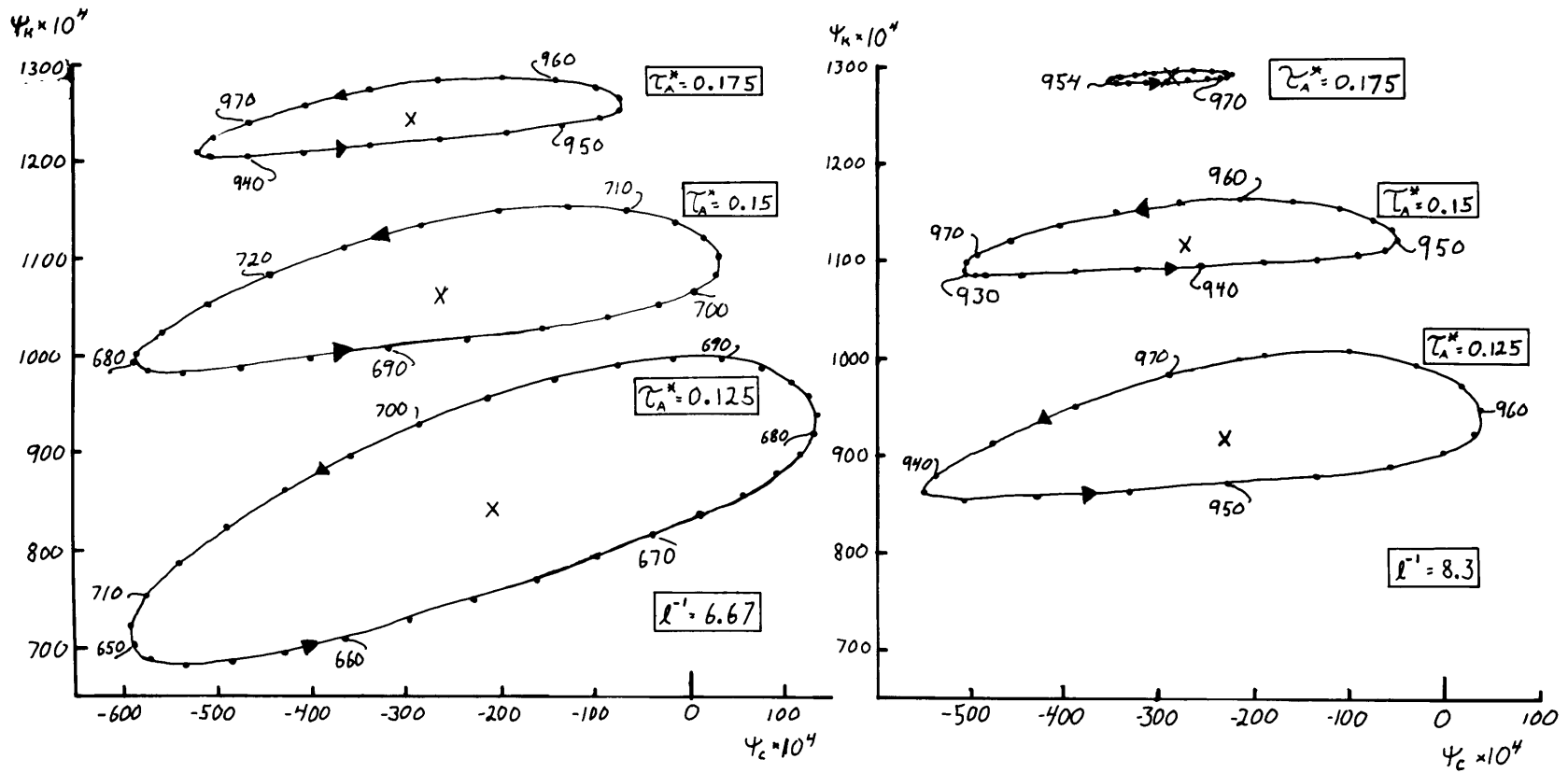


Fig. 11. Two dimensional phase space trajectories ( $\Psi_R$  vs  $\Psi_C$ ) of vacillation cycle.  $l^{-1}$  and  $\tau_A^*$  as indicated,  $\beta = 0.0$

tracing out a 13 (or 12) dimensional trajectory in the phase space. Viewing a two dimensional projection of the trajectory then gives a good picture of the vacillation cycle. Figure 11 presents some quite typical results where  $\Psi_K$  (in the moving coordinate system) and  $\Psi_C$ , both multiplied by  $10^4$  are selected as the coordinates. The relevant forcing parameters are indicated in the figure and the examples illustrated are seen to come from near the center of the lower of the two  $II_E$  regimes of Fig. 2. In the figures the small cross within each trajectory is the position of the average of  $\Psi_K$  and  $\Psi_C$  and the small dots and numbers on the trajectories indicate the iteration step numbers.

The variation in the nature of the flow with variations in the forcing parameters, i.e. a decrease in the size of the ellipsoids with increasing  $\tau_A^*$  and  $\ell^{-1}$ , is typical of the lower  $II_E$  regime for  $\beta = 0$  (Fig. 2) and the left lobe of the same regime with  $\beta = 0.6065$ . The upper  $II_E$  regime trajectories both with and without  $\beta$  behave differently; they exhibit the same shape as those of Fig. 11 but show no marked variation with  $\ell^{-1}$  and tend to increase in dimensions for increasing  $\tau_A^*$ . The right lobe of the lower  $II_E$  region,  $\beta = 0.6065$ , shows more marked differences both in shape and behaviour with changes in the forcing. Figure 12 is a representative sampling of these, and illustrates the crescent shape of the trajectories in this region as well as indicating the tendency for increase in dimensions of the pattern with  $\tau_A^*$  and  $\ell^{-1}$ , in direct contrast to the characteristics of the left lobe flow.

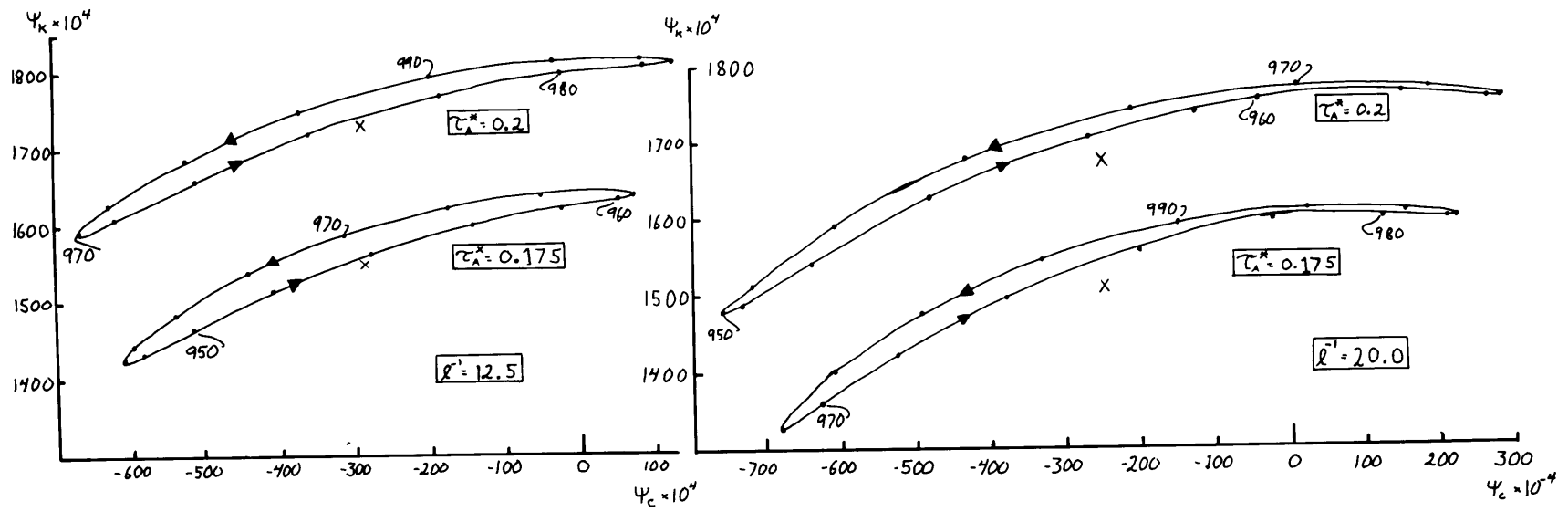


Fig. 12. Two dimensional phase space trajectories ( $\Psi_K$  vs  $\Psi_C$ ) of vacillation cycle.  $l^{-1}$  and  $\tau_A^*$  as indicated,  $\beta = 0.6065$

The sequence of momentum convergences and zonal winds for the lower vacillating regimes are typified by the series for  $\ell^{-1} = 6.67$   $\tau_A^* = 0.15$   $\beta = 0$  in Fig. 13 and  $\ell^{-1} = 20.0$   $\tau_A^* = 0.175$   $\beta = 0.6065$  in Fig. 14. At first glance these figures appear rather formidable in their complexity but much of this is reduced on closer examination. The behaviour of the upper  $II_E$  regimes, both with and without  $\beta$ , is essentially similar in its qualitative characteristics to Fig. 13 except that the ageostrophic terms are as large or larger than the geostrophic momentum terms. Because the net momentum convergences are no longer zero at any given latitude as they were for the type I flows the net of the three geostrophic terms for the upper layer (eq. 47) and the four for the lower (eq. 48) have been added to the figures and indicated by  $NET_3$  and  $NET_1$  respectively. Further because of the over-abundance of lines the convergence figures for the two layers have been plotted on separate abscissas. As before the ageostrophic convergences in the two layers,  $MC_3$  and  $MC_1$ , are included as dashed lines where they are large enough to be discernible and the zonal winds of the layers are found on a third abscissa.

Both the vacillation cycles of Figs. 13 and 14 can be seen to be similar in their overall patterns despite differences in detail. The principal similarity is that both approach a state of flow quite similar to the higher  $\tau_A^*$  regime of  $I_E$  flow on Figs. 2 and 3, e.g. Fig. 5. On Fig. 13 this state occurs more or less between iteration steps 710 and 720 and on Fig. 14 at about step 990. Reference to Figs. 11 and 12

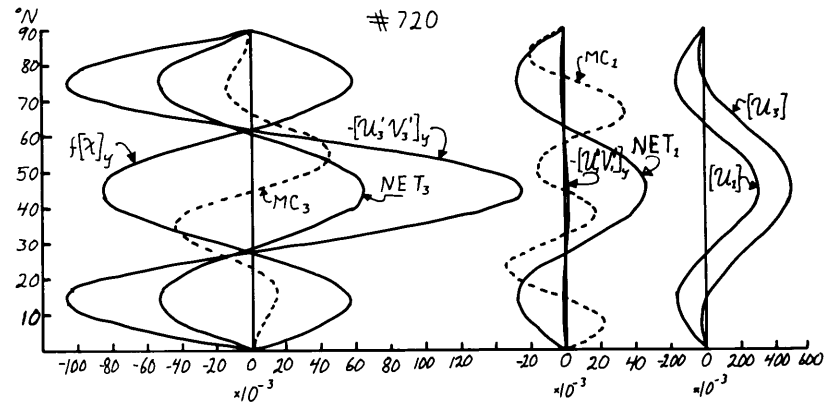
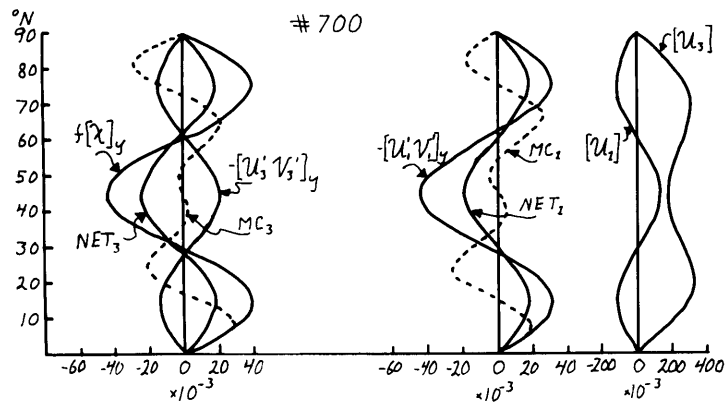
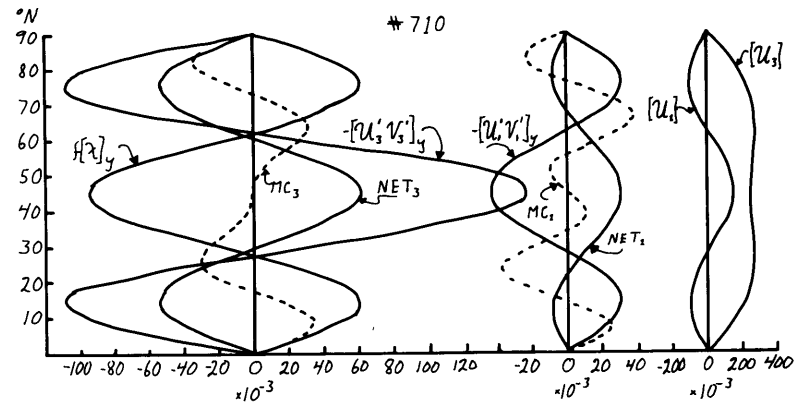
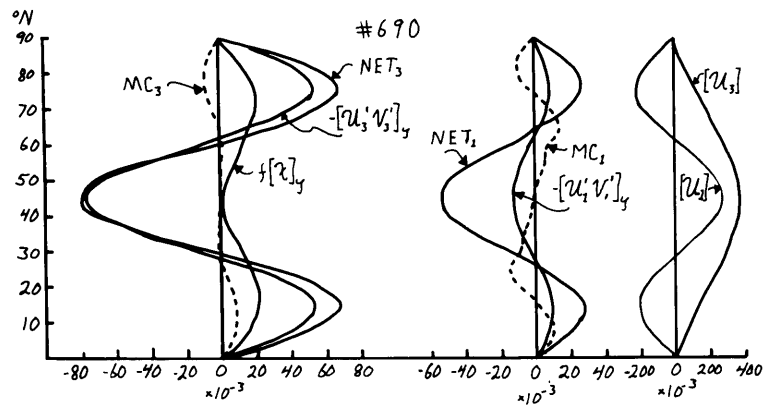


Fig. 13. Momentum Convergences and Zonal Velocities (nondimensional) for vacillation cycle with  $\ell^{-1} = 6.67$ ,  $\tau_A^* = 0.15$ ,  $\beta = 0.0$

shows that this similarity to  $I_E$  flow occurs during the upper portion of the  $\Psi_k - \Psi_c$  trajectory. Elsewhere in the cycles the flows nowhere resemble any of the previously encountered ones. In both cases the complete cycle is easily described with particular reference to the upper level convergence and  $[u_3]$ . Starting with a strong single velocity maximum the eddy convergence tends to spread the momentum out of the center (Fig. 13 step 690, Fig. 14, 976) until a double maxima in  $[u_3]$  is attained. But by this time the eddy convergence has reversed itself so that the momentum is tending to be concentrated in the central latitudes. This process continues (the upper  $I_E$  state) until the strong maximum has occurred but again the convergence changes sign and the process repeats. In the lower layer an essentially similar cycle takes place except that the zonal wind oscillation is between earthlike and non-earthlike states (Fig. 14) or an earthlike regime with varying strength (Fig. 13) rather than an alternation between single and double maxima of a principally westerly flow. Also in the lower layer the  $-f[\chi]_y$  term accounts for the momentum convergence to a greater extent than the eddy term in contrast to the upper layer where the eddy convergence predominates.

The principal differences between the flows are essentially those noted in conjunction with the type I flows. Fig. 13 with the lower rotation rate and no  $\beta$  exhibits a relatively more important  $f[\chi]_y$  term than Fig. 14 throughout and, in conjunction with this, ageostrophic terms of considerably greater magnitude relative to the geostrophic terms than

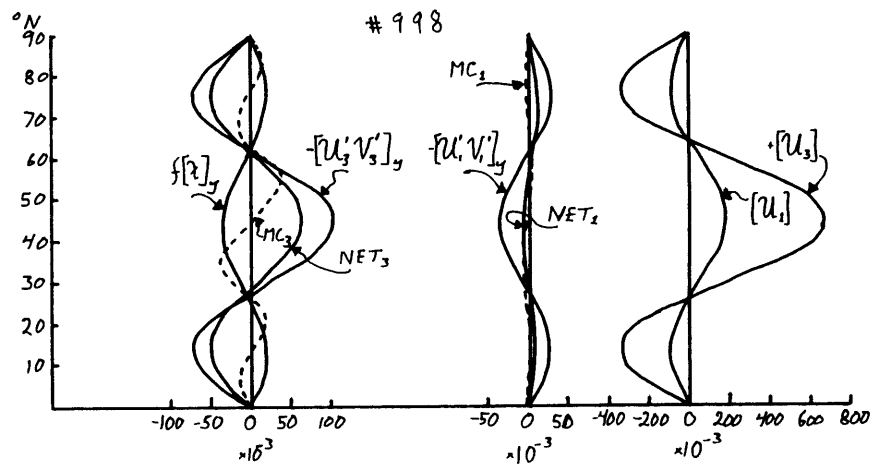
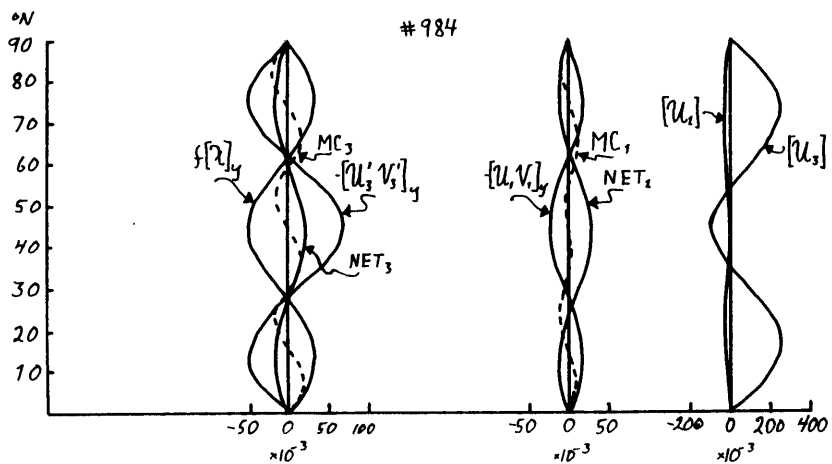
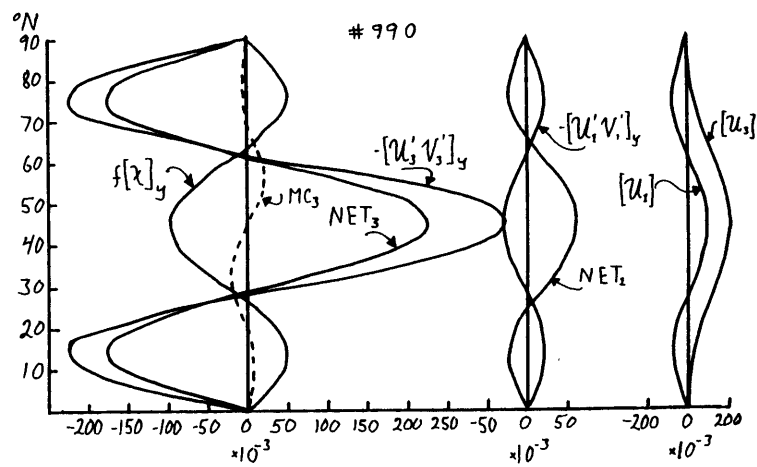
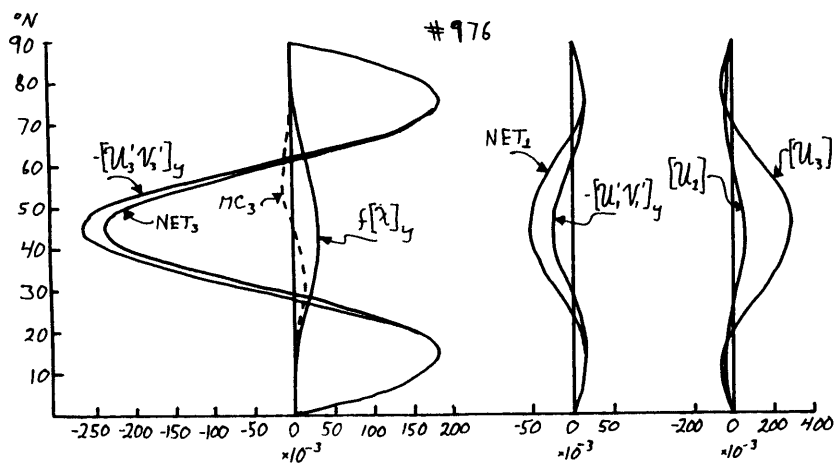


Fig. 14. Momentum Convergences and Zonal Velocities (nondimensional) for vacillation cycle with  $\ell^{-1} = 20.0$ ,  $\tau_A^* = 0.175$ ,  $\beta = 0.6065$ .

in the high rotation  $\beta$  flow. One other major difference not alluded to previously relates to the period of the moving wave with respect to the period of the vacillation. For all of the vacillating cases except those typified by Figs. 12 and 14, the wave and vacillation periods are of the same order of magnitude differing by no more than a factor of two or less. However within the  $\beta$  induced high rotation rate vacillation regime, the wave period is a full order of magnitude or more larger than the vacillation period.

### C. Energetics

Although not as vital to the present study as the momentum convergence and balance, the energetical characteristics of the various types of flows encountered are of interest. As with the momenta all the steady state type I flows are in energetic balance, any particular form of energy is constant in time and the energy interchange terms, Fig. 1, are so arranged that the net transfer to any particular form of energy is zero. For ease in comparison of cases the energetics for the various flows will be presented not in terms of the actual non-dimensional values but as percentages of the total: i.e. each of the four energy storage terms will be given as a percentage of the total energy, the sum of the four, and each of the eight interchange terms will be given as a percentage of  $\{Q \cdot \bar{A}\}$  the only energy source for the system (barring the non physical source of computational instability) thereby indicating the distribution of energy among the available modes and showing how the input energy passes through the system.

The tables which follow give the energetic terms appropriate to the flows for which the momentum convergences have been investigated. In the tables the four energy storage term percentages are given along with the nondimensional value of the total energy and four of the energy interchange percentages along with the nondimensional value of  $\{Q \cdot \bar{A}\}$  are also given. The redundant frictional and thermal energy loss rates  $\{\bar{K} \cdot F\}$ ,  $\{K' \cdot F\}$  and  $\{A' \cdot Q\}$  can be easily deduced.

Table 2. Percentage Energetics Corresponding to Figures 4 and 6.

$\tau_A^* \%$	$l^{-1} = 20.0$								$\frac{\Sigma E}{L^2 F^2}$	$\frac{\{Q \cdot \bar{A}\}}{L^2 F^3}$
	$\bar{A}$	$\bar{K}$	$A'$	$K'$	$\{\bar{A} \cdot A'\}$	$\{\bar{A} \cdot \bar{K}\}$	$\{A' \cdot K'\}$	$\{K' \cdot \bar{K}\}$		
0.30	10.2	3.8	11.6	74.5	98.4	1.5	68.5	1.3	0.187	0.0072
0.125	46.0	8.5	14.0	31.5	85.9	14.1	36.9	-1.2	0.144	0.0041
0.10	16.0	1.0	32.7	50.2	100.2	-0.2	38.4	0.4	0.064	0.0034
0.05	34.1	0.8	44.2	20.9	99.9	0.0	17.2	0.2	0.054	0.0029

$\beta = 0.6065$										
$\tau_A^* \%$	$\bar{A}$	$\bar{K}$	$A'$	$K'$	$\{\bar{A} \cdot A'\}$	$\{\bar{A} \cdot \bar{K}\}$	$\{A' \cdot K'\}$	$\{K' \cdot \bar{K}\}$	$\frac{\Sigma E}{L^2 F^2}$	$\frac{\{Q \cdot \bar{A}\}}{L^2 F^3}$
0.15	12.4	1.2	19.4	67.0	100.0	-0.0	43.1	0.4	0.147	0.0050
0.10	19.6	1.0	32.3	47.2	99.8	0.2	23.2	0.1	0.113	0.0048
0.05	49.0	0.7	36.3	14.0	99.8	0.3	7.1	-0.0	0.116	0.0046

Table 2 contains the energetic terms for the high rotation rate I flows with and without  $\beta$  corresponding to figures 4 and 6. The variation of the energy terms induced by changes in  $\tau_A^*$ ,  $\bar{A}$  decreasing,  $A'$  increasing with increasing  $\tau_A^*$  etc., suggested by the table are indeed those which

are noted in an examination of the energy terms for all the results and the changes appear continuous within any given region of similar type flow. This was to be expected as a consequence of the continuity of the numerical results themselves, noted previously.

The flows are seen to be all baroclinically unstable with amplifying waves, if we may apply the language of stability theory to the finite amplitude waves, in the sense that  $\{A' \cdot K'\}$  is positive, and barotropically damped with two exceptions in that  $\{K' \cdot \bar{K}\}$  is also positive.  $\{K' \cdot \bar{K}\}$  is considerably smaller than  $\{A' \cdot K'\}$  however indicating that most of the energy reaching  $K'$  is lost to friction rather than being changed to zonal kinetic energy. Further, except at the highest  $\tau_A^*$  considered, better than 50% of the energy reaching  $A'$ , which in turn is virtually all the energy entering the system via  $\{Q \cdot \bar{A}\}$  as  $\{\bar{A} \cdot \bar{K}\}$  is very small, is lost by thermal dissipation. Indeed at  $\tau_A^* = 0.03$ ,  $\{\bar{A} \cdot A'\} = 99.6\%$  and  $\{A' \cdot K'\} = 1.1\%$  which is typical of the energy interchanges all along the lower boundary between the type I flow and the Hadley circulation.

There seem to be no striking differences in the energetic terms between the upper and lower I regimes nor any induced in the lower I regime by the inclusion of  $\beta$ . An exception might be made for  $\{\bar{A} \cdot \bar{K}\}$  which seems to be of greater importance in the upper  $I_E$  regime than elsewhere. An additional note should be made relevant to this term measuring the energy transfer due to mean meridional circulations. Even though this term is predominantly positive in the upper  $I_E$  regime

( $\beta = 0$ ) inspection of Fig. 4 does indicate the existence of a strong indirect cell over the mid latitudes. The direct cells at the extremes of latitude coupled with the larger latitudinal temperature gradients there account for the overall positive conversion of mean available potential energy to mean kinetic energy. In the lower I regime, both  $\beta$  cases, the situation is reversed with a mid latitude direct cell being very closely balanced in its energetic effects by indirect cells at the latitudinal extremes.

Table 3 contains the energetics for the moderate rotation rates corresponding to figures 7 and 8. As noted in conjunction

Table 3. Percentage Energetics Corresponding to Figs. 7 and 8.

$$\bar{l}' = 6.67 \quad \beta = 0.0$$

$\tau_A^* / \%$	$\bar{A}$	$\bar{K}$	$A'$	$K'$	$\{\bar{A} \cdot A'\}$	$\{\bar{A} \cdot \bar{K}\}$	$\{A' \cdot K'\}$	$\{K' \cdot \bar{K}\}$	$\frac{\Sigma E}{L^2 f^2}$	$\frac{\{a \cdot \bar{A}\}}{L^2 f^3}$
0.30	35.8	13.5	5.3	45.5	95.6	4.0	72.4	9.1	0.364	0.0250
0.10	60.4	4.4	12.2	22.9	97.4	1.7	42.6	0.8	0.147	0.0098
0.06	93.5	0.9	5.0	0.6	95.4	2.4	5.9	-0.2	0.422	0.0070
0.05	94.9	0.4	4.5	0.2	97.4	1.1	2.0	-0.0	0.628	0.0089

$$\beta = 0.6065$$

0.30	33.2	13.1	8.0	45.7	103.3	-3.3	67.9	14.8	0.404	0.0275
0.15	48.1	6.1	7.4	38.4	96.1	2.6	58.6	1.4	0.217	0.0128
0.10	57.6	3.6	13.9	24.8	98.2	1.6	34.7	0.6	0.167	0.0110
0.06	90.8	0.8	6.9	1.4	98.6	1.4	5.8	0.1	0.394	0.0088

with table 2, the variations of the energetic terms with  $\ell^{-1}$  and  $\tau_A^*$  suggested by the tables is that which is observed in all the results. The discontinuities in the energetics, if indeed there are any, across the boundary between the two types of I flow at the lower values of  $\tau_A^*$  are not very marked; the relatively lower values of  $\{A' \cdot K'\}$  for  $\tau_A^* = 0.05$  and  $0.06$  than for higher  $\tau_A^*$  and higher rotation do seem to be characteristic of this third type of motion without change of shape. Again the only really noticeable effect of  $\beta$  is in the  $\{\bar{A} \cdot \bar{K}\}$  term for  $\tau_A^* = 0.30$  where its addition induces a negative value.

Finally table 4 presents the energetics for the low rotation rates. The main thing to note in conjunction with these data is the generally rather small effect that  $\beta$  has for these low rotation results. Otherwise the comments made relative to the previous tables apply here as well.

Table 4. Percentage Energetics Corresponding to Figs. 9 and 10.

$\ell^{-1} = 2.5 \quad \beta = 0$										
$\tau_A^* \backslash \%$	$\bar{A}$	$\bar{K}$	$A'$	$K'$	$\{\bar{A} \cdot A'\}$	$\{\bar{A} \cdot \bar{K}\}$	$\{A' \cdot K'\}$	$\{K' \cdot \bar{K}\}$	$\frac{\Sigma E}{L^2 f^2}$	$\frac{\{Q \cdot \bar{A}\}}{L^2 f^3}$
0.30	63.6	14.3	4.4	17.7	84.6	12.8	51.1	7.1	0.534	0.0554
0.15	90.6	3.4	4.1	1.9	86.1	8.1	14.4	-0.0	0.641	0.0290
$\beta = 0.6065$										
0.30	66.7	14.2	4.2	14.9	86.1	11.9	48.2	12.1	0.603	0.0535
0.15	91.9	3.0	3.3	1.7	89.6	8.5	14.1	0.7	0.738	0.0260

The energetics of the two vacillating flows of figures 13 and 14 are presented in Fig. 15. In this figure the ordinate is the nondimensional energy or energy transformation rates and the abscissa the iteration step number. The small vertical lines indicate the positions in the cycle of the flows selected for the momentum convergence figures. In both cases the "beginning" of the cycle was the step at which  $\psi_A$  reached a maximum; in that  $\psi_A$  was in general larger than the other zonal terms the beginning was also the step of maximum  $\bar{K}$ .

The differing nature of the two types of vacillating flow is quite clearly brought out by figure 15 where Figs. 13 and 14 tended not to show any very great differences in the momentum structure. Among the most noticeable of differences is the complete reversal of phase between  $\bar{A}$  and  $\bar{K}$  from the high rotation case where they are very closely in phase to the moderate rotation where they are almost  $180^\circ$  out of phase. No such change takes place between the eddy energy components. Similar phase shifts can be noted in the energy interchange rate terms although these are somewhat hidden by the appearance of double periodicities in these terms for the high rotation case when only single periodicities were found at the moderate rotation rates. Most noticeable of these is the  $\{\bar{A} \cdot A'\}$ ,  $\{K' \cdot \bar{K}\}$  pair which are strongly doubly periodic and clearly out of phase for the high rotation while for the lower rotation the shorter period variation has vanished for  $\{\bar{A} \cdot A'\}$ , has been considerably reduced in  $\{K' \cdot \bar{K}\}$  and the two appear more or less in phase.

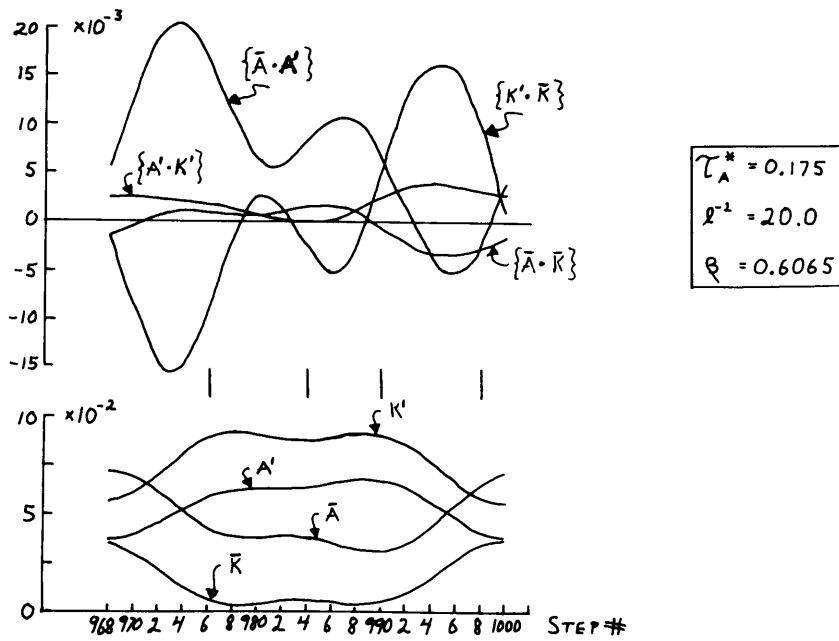
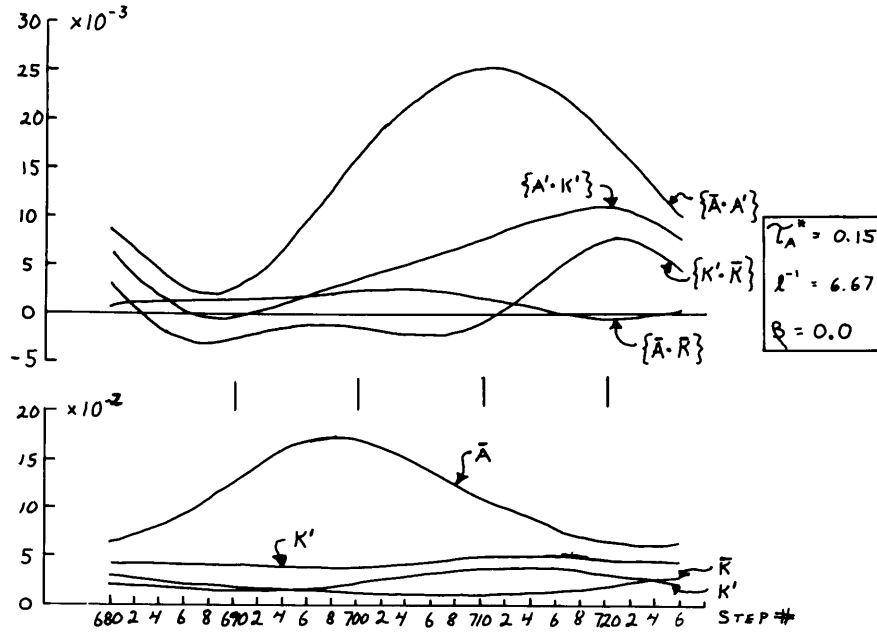


Fig. 15. Energy storages and conversions (nondimensional) for vacillation cycles with parameters as indicated.

The gross character of the two vacillating energy cycles can best be described with reference to the previous description of the momentum convergence structure. During the spreading of momentum from the single  $[u_3]$  maximum ( $\beta = 0.0$  step 690;  $\beta = 0.6065$ , step 976) both flows show barotropically amplifying waves,  $\{K' \cdot \bar{K}\} < 0$ , while the high rotation  $\beta = 0.6065$  flow show baroclinically amplifying waves as well  $\{A' \cdot K'\} > 0$ . The low rotation case shows a brief period of baroclinic damping but during most of the time of the extraction of momentum from the zonal maximum it too shows baroclinic amplification of the waves at the expense of the eddy available potential energy. During the period of momentum concentration into a single zonal maximum, analogous to the higher  $\tau_A^* I_E$  flows, both flows exhibit baroclinic amplification and barotropic damping of sufficient magnitude that the net effect is seen to be an increase in  $\bar{K}$  and a decrease in  $K'$ . It is also during this time, particularly for the high rotation  $\beta = 0.6065$  case, that  $\{\bar{A} \cdot \bar{K}\} < 0$  showing the thermally indirect mid-latitude cell predominating over the direct cells at the extremes of latitude. Indeed the magnitude of this term is sufficiently large during this portion of the cycle that the average over the complete vacillation cycle is also negative. This is true for all the  $II_E$  flows in the right lobe of Fig. 3 as well as the  $I_E$  flows immediately to the left of this region ( $\lambda^{-1} = 8.33$ ,  $\tau_A^* = 0.20, 0.25, 0.30$ ) as well as the  $I_E$  flow for  $\tau_A^* = 0.30$  noted in table 3.

The inclusion of  $\beta$  into the equations can be seen then to have a marked effect upon the energetics of the higher rotation rate computations

particularly in the  $\{\bar{A} \cdot \bar{R}\}$  term, much as it had a profound effect upon the surface flow character at lower  $\tau_A^*$ .

#### D. Other Features

A number of other not uninteresting phenomena observed in the numerical solutions could be studied in some detail but it would seem that by their nature they are of greater interest from the point of view of investigating the behaviour of the set of equations rather than investigating various aspects of the general circulation with a simplified model. We shall note a few of these other features here as a matter of general interest but not concern ourselves with the details since they would seem to be of less immediate relevancy to the problem at hand.

One of these is the problem of the nature and cause of the discontinuous changes in flow character between the various regimes portrayed in Figs. 2 and 3. This general problem has been investigated by Lorenz (1963) for a similar but somewhat simpler set of equations in terms of instabilities of preexisting regimes of flow. No attempt was made to do that here but some similar observations can be made empirically on the basis of Fig. 11. As was noted previously the vacillation decreases in magnitude as the upper boundary of the lower  $II_E$  region (left lobe only in Fig. 3) is approached. Also consideration of the averages over the vacillation cycle of the  $\Psi$ 's and  $\tau$ 's shows them to be essentially continuous with their counterparts in the  $I_E$  region above. The same continuity is noted across the lower boundary of the upper  $II_E$  regime,

and the dimensions of the vacillation trajectories increase with increasing  $\tau_A^*$  in that area. This is not so much suggestive of instability of one mode of flow with respect to perturbations which induce the other mode but more that one type of solution simply doesn't exist when the other is found for particular values of the forcing parameters. This suggestion was partially confirmed by making an integration with the forcing parameters  $\ell^{-1}$  and  $\tau_A^*$  set at values which previously resulted in a  $II_E$  solution near the upper boundary of the lower  $II_E$  region but with initial conditions not the perturbed Hadley flow but the average of the  $II_E$  flow which was clearly continuous with the  $I_E$  results at slightly higher  $\tau_A^*$ . The solution quite quickly departed from the initial conditions and returned to the previous  $II_E$  flow.

On the other hand the entire lower boundary of the lower  $II_E$  regimes, and the  $I_E$   $I_N$  boundary for high rotation  $\beta = 0$ , very definitely suggested instability characteristics both by the increasing dimensions of the  $II_E$  trajectories for decreasing  $\tau_A^*$  and the marked discontinuity of the I solutions with respect to the average of the II solutions. Experimental investigation of the lower boundary discontinuities gave indications of the nature of the instability of one type of flow with respect to the other. By using the type I steady state solutions as initial conditions for integrations with slightly higher  $\tau_A^*$ , for the same  $\ell^{-1}$ , it was possible to obtain type I solutions for  $\tau_A^*$  as high as 0.2 both with and without  $\beta$  for  $\ell^{-1}$  greater than 4.0. It seems worth noting that  $\ell^{-1} = 4.0$  is the approximate rotation rate at which the division between the two types of I flow for  $\tau_A^*$  less than

0.15 or 0.1, depending upon  $\beta$ , intersects the  $II_E - I$  boundary. It was the type  $I_E$  flows to the left of this division which was noted to have resemblance to the  $I_E$  flows at higher  $\tau_A^*$  which in turn could not be extrapolated down into the II region just as the lower  $\tau_A^*$   $I_E$  flows at  $\ell^{-1} < 4.0$  could not be extrapolated up into the II region.

Similarly a limited number of computations indicated the possibility that the  $II_E$  regime could be extended downward somewhat, to  $\tau_A^* = 0.08$  for  $\beta = 0.0$  and  $\tau_A^* = 0.15$  for  $\beta = 0.6065$ , by a similar extrapolation procedure.

In effect then the region of Figs. 2 and 3 between  $\tau_A^* = 0.2$  and 0.15 or 0.08 (depending upon  $\beta$ ) for  $\ell^{-1} > 4.0$  is an area in which the equations are capable of producing two quite different solutions. At high enough  $\tau_A^*$  small departures from a possible I solution grow and generate a II solution and vice versa for low  $\tau_A^*$ . Another way of viewing the matter would be to say that there exists a 12 (or 13) dimensional volume of phase space, for a given  $\ell^{-1}$  and  $\tau_A^*$ , such that initial conditions within this volume lead to type I solutions and outside to II solutions. This volume seems to shrink for increasing  $\tau_A^*$  such that eventually there can be no type I solutions of the type under consideration. The determination of the limits of this volume would be a formidable task, seemingly of limited value. Finally this implies that the lower boundary of the lower  $II_E$  regime as drawn on Figs. 2 and 3 is somewhat arbitrary dependent as it is upon the perturbed Hadley flow initial conditions being within the volume leading to a type I solution or not.

Another matter is the performance of the equations in the type III irregular flow at rather high values of  $\tau_A^*$ . These flows have not been

considered in any detail because the ageostrophic momentum transports are very large, at times substantially exceeding the geostrophic terms; or looking at the same thing in a different way the Rossby number defined by equation (81) frequently exceeds 1.0 and the nondimensional  $[\mathcal{U}_3]$  often is greater than 2.0. All this clearly indicates that using the quasi-geostrophic model with these large values has relevancy only to simply seeing how the equations behave and not to modeling any physically realizable flow. The typical performance of the type III solutions in the phase space projection is an expanding spiral with the speed of the solution point increasing until the point is thrown out of the spiraling mode, wanders about rather aimlessly and then slowly returns to the center of the spiral. The pattern then repeats, but not exactly, with perhaps a different number of spiral loops and a differing "aimless" pattern, still in the same general area of phase space. The number of spiral loops and overall dimensions are, as would be expected, effected by the value of  $\ell^{-1}$ ,  $\tau_A^*$ , and  $\beta$ . In terms of the behaviour of the equations it is good to see that at least some degree of irregularity can be produced by the equations if only for rather high  $\tau_A^*$  forcing.

#### 4. The Atmosphere and the Equations

##### I. Meteorology or Merely Mathematics?

The major portion of the preceding chapter has, quite naturally, dealt with the nature and various properties of the solutions to the highly simplified set of atmospheric modeling equations. In spite of the amount of simplification the equations are capable of producing a quite startling variety of solutions, almost an embarrassment of riches. But in all of the solutions there are none which show the highly irregular time dependence so characteristic of the atmosphere, except possibly for limited portions of some of the III flows. It can be reasonably argued that the extreme simplification causes such a reduction in the number of degrees of freedom that highly irregular flows should not be expected. But this leads to a rather crucial question: have the simplifications been too drastic? Is it saying too much to claim that the solutions to the set of nonlinear equations discussed here have any real relationship to the atmosphere, as we have done implicitly by describing the solutions with terms like "momentum convergence," "energy interchange," "zonal wind" etc? Or are they just a set of figures and diagrams of interest in and of themselves, possibly of value to a mathematician concerned with the behaviour of this sort of equation set, and more appropriately described in terms of phase space trajectories, multiple solutions, etc.?

In order to answer these and related questions and in so doing draw conclusions about the significance of the numerical experiments performed we must reconsider what we set out to do in the light of some of the results achieved. It goes without saying that at no time was anything approaching a complete representation of the atmosphere contemplated in the style for example of the recent study by Smagorinsky (1963). Indeed virtually the opposite is intended. Here we wished to start with a complete, or nearly so, representation capable of reproducing many of the features of the atmosphere and then extract from the representation that part of it which is considered, à priori, to be sufficient to represent the particular features of the atmosphere of interest and discard the rest. In the present case the features of interest are the meridional distribution of zonally averaged surface and upper level winds including the formation of a single maximum, the associated convergences of momentum, and to a lesser degree the energetics of the atmosphere. The question to be answered then, by experiment, is, once the elements of the representation are selected, whether the desired features of the complete representation, or of the atmosphere itself, will be correctly generated when the selected elements are incorporated into the dynamic equations. It is by no means obvious at the start that this will happen; some discarded element may have a compelling and unsuspected implicit dynamic effect necessary to rule out a dynamically possible but non-atmospheric phenomenon.

It is in the process of extracting the presumably relevant elements or discarding the undesired ones that such damage may be done to the retained elements that the criticism could be made that the end result, viewed as a set of modeling elements, is not truly a subset of the original representation. The elements selected may be so distorted by the selection process as to suppress their ability to represent the physical phenomena that they were originally designed to do. As a first step, then, in responding to the question of the relevancy of the numerical results to atmospheric circulations we should consider in some detail the damage to representational ability done in making the succession of simplifications of chapter 2.

The first step of the selection of relevant matter from an (assumed) complete representation of the atmosphere was the selection of a two layer model. It would seem that the best argument that this is not a damaging simplification is in the accumulation of experience using such two layer models. There seems no need to detail the successes of these models in representing the atmospheric flow and in particular in reproducing the gross features under consideration. Some of these were noted on the introductory chapter. It seems worth noting however, that the present model is less restrictive in one particular than many used previously: the spatially averaged static stability is no longer constrained to be a constant in time. It seemed to be too drastic to discard completely the variability of the stability in the light of the simplifications to come; on the other hand neglect of spacial variations would seem consistent with a planned representation of only large scale features.

The next step, taken concurrently with the previous one, was assuming the flow could be described adequately as quasi-geostrophic. Again experience would seem to indicate that this simplification is not a damaging one in general, but in the present experiments there is considerable reason for caution under some conditions. These, of course, are when the Rossby number or the maximum of  $[\mathcal{U}_3]$  (nondimensional) exceed 0.1 by any appreciable amount or, somewhat equivalently, the mean cell ageostrophic momentum convergences become an appreciable fraction of the geostrophic convergences included in the model. These conditions are realized in the experiments generally either when the rotation rates are low or  $\tau_A^*$  high, or both at once. There would seem to be two ways of considering and dealing with the fact of appreciable ageostrophicity. For one since the atmosphere behaves quasi-geostrophically in the large scale it is certainly of interest to see how a quasi-geostrophic model performs for forcing conditions beyond the range of conditions encountered in the real atmosphere. But in so doing the likelihood must be born in mind that the real atmosphere, if subjected to the extremes of forcing, could no longer be described in quasi-geostrophic terms, and hence the model would have little relevancy to any physical flows. Thus we can use the appearance of substantial ageostrophicity to delineate regions of good or poor representation by the model. This consideration was the rational for presenting all of the flows encountered on Figs. 2 and 3 but only looking closely at those for which the ageostrophic terms were not excessively large. A second way of somewhat alleviating concern over

ageostrophicity is by considering that after all we do have a highly simplified model which neglects a considerable number of phenomena, so to express concern over the neglect of one effect with so many others neglected as well may be a little inconsistent. It would seem rather extreme to use this observation as a basis for accepting the high  $\tau_A^*$  flows as particularly relevant to any real flows but reasonable to use it as a justification for not ruling out the relevancy of the lower  $\tau_A^*$  flows studied in detail simply because they show ageostrophic terms which are an appreciable fraction of the terms included in the model. In summary then the geostrophic approximation could be damaging but if used with discretion the harm can be minimized.

Also included in the dynamic model was the parameterization of the heating and friction into rather simple terms. Again it would seem that previous experience with this sort of simplification would be adequate justification for its inclusion here. Furthermore in the light of the simplifications yet to come there would seem to be no alternative to the present method.

The major simplification or selection of relevant matter from a complete description of the flow is, of course, the expression of the field of flow as a truncated series of orthogonal functions. The use of orthogonal functions is in itself not really any simplification nor does it involve any loss of generality in the description of the flow;

the violence to the description is done in the interrelated process of selecting the particular functions (the choice of geometry) and in the actual truncation.

We have already described what the particular choice of functions and retained terms can represent: it is in order to consider the distortions inherent in the representation and the possible significance of the modes of motion that are suppressed in the model. The geometric distortions are obvious but not too grievous if they are recognized. The choice of the double Fourier expansion for the infinite channel has eliminated all effects related to the sphericity of the earth. However the inclusion of the  $\beta$  effect in the motion of the waves would seem to have approximately reinstated the most important of these eliminated effects. Further the distortion of the pole and considerable enlargement of the surface area of the northern regions with consequent large (relative to the earth) surface frictional momentum convergences makes direct comparison with atmospheric flow patterns in those regions also somewhat less meaningful.

Another distortion quite noticeable on any "weather maps" synthesized from the Fourier amplitudes is the symmetry between high and low "pressure" regions. This is to be expected in view of the nature of the simplifications introduced. And in spite of this the qualitative resemblance to major aspects of real weather maps is still quite apparent, so much so that one cannot feel too disturbed about the symmetry. The symmetry in the momentum convergence is equally

apparent, and arises, in a physical sense, from the geometric distortion of substituting the channel for a sphere. This symmetry leads to momentum transports across, say,  $60^{\circ}\text{N}$  that will be unrealistically large in comparison with observations in the atmosphere. Again if we take this in stride recognizing it as a limitation of the model it would seem that this is a not overly serious departure from reality. The damage done by the geometric simplifications would seem, then to be ones of detail rather than altering or ignoring any important physical phenomenon when  $\beta$  is incorporated.

The most extreme step in the selection of physical phenomena is finally the restriction placed upon allowable scales of motion and in particular the elimination of all but one wave disturbance in the zonal flow. Completely ruled out by this is the interaction between different scales of wave motion of the sort studied by Saltman and Fleisher (1960). This is obviously important in the dynamics of the atmosphere but would seem of greater importance in the study of the "fine structure" than the present study of large scale phenomena. The single wave that is retained is capable of doing, dynamically, all that the collection of waves observed in the atmosphere can do as a group as far as momentum and energy convergences and transformations are concerned so all that is lost as far as dynamic capability is concerned is the interactions of the waves with each other. This may be a significant loss for a proper representation, even simplified, of the atmosphere; it is part of the experiment to see if this is so.

To reply to the question initially proposed, it would seem that we can reasonably conclude that the set of equations we are working with do indeed have a relationship to the atmosphere they purport to model. There are limitations and restrictions, there always will be in any model, but they do not seem so severe that they invalidate the model completely. The preceding discussion delimits the range of validity of the model and leaves us with what appears to be a satisfactory piece of experimental equipment, so to speak, for the investigation of the grossest aspects of the general circulation.

## II. The Model Atmospheres

### A. Qualitative Comparisons

The preceding section argues that the model is capable of representing the gross general circulation; the burden of this section is to see how good a job it does. It is immediately obvious from the discussions in the previous chapter that, qualitatively, the results are something of a mixed bag. All of the atmospheric phenomena of principal interest have been captured by the atmosphere for various sets of forcing conditions but at no time have they all been caught simultaneously.

From the types of flows considered in detail it can be seen that two of them capture at least a majority of the phenomena of principal interest, the lowest  $\tau_A^*$  ( $= 0.05$ ) flows of the moderate rotation ( $\ell^{-1} = 6.67$ ) and those of the same type at lower rotations both with and without  $\mathcal{B}$ , and the higher  $\tau_A^*$  ( $= 0.125$ ) flows at the high rotation rates ( $\ell^{-1} = 20.0$ )

with  $\beta = 0$ . The high  $\tau_A^*$  flows at lower rotation rates also capture a majority but the magnitude of the ageostrophicity in those flows renders them less desirable for direct comparison with the atmosphere

Starting with the high  $\tau_A^*$  we see the flow, earthlike at the surface, increasing with height but not tending to be concentrated into a single relatively narrow maximum. However the tendency for spreading is sufficiently weak that a double maximum is not formed. The eddy momentum transport is "uphill" into the maximum of  $[\mathcal{U}_3]$  and as noted previously is almost balanced by the momentum transport of the forced thermally indirect mean meridional cell in mid latitudes. The zonal wind maximum then, as seems to be the case in the atmosphere, is maintained quasi-geostrophically against friction by the eddy momentum convergence. The lower layer convergences are distinctly non-atmospheric in form with mid latitude divergences almost as large as the upper layer convergences. In spite of this the earthlike lower layer flow is maintained against the frictional and eddy divergences by the meridional cell. The ageostrophic momentum terms are seen as suggesting a tendency to move the upper layer wind maximum somewhat northward of  $45^\circ$ , and in the lower layer to strengthen the tropical easterlies at  $20^\circ$  and diminish the polar easterlies at  $70^\circ$ . Their effect in the upper layer, if these tendencies did actually result from inclusion of the balance terms in the model, would be somewhat contrary to atmospheric experience where the zonal wind maximum is generally found south of  $45^\circ$ , while their lower layer effect is one more in agreement with atmospheric circulations.

With respect to the energetics comparison can be made with other numerical experiments, principally those of Phillips (1954) and Smagorinsky (1963). Table 5 presents the average percentage energetics for those experiments including the energy interchange rates. It seems worth noting that although Phillips' and Smagorinsky's results here show

Table 5. Percentage Energetics: Other Numerical Experiments

%	$\bar{A}$	$\bar{K}$	$A'$	$K'$	$\{\bar{A} \cdot A'\}$	$\{\bar{A} \cdot \bar{K}\}$	$\{A' \cdot K'\}$	$\{K' \cdot \bar{K}\}$
Phillips	76.5	17.5	1.6	4.4	152.7	-16.1	143.3	60.9
Smagorinsky	74.3	21.6	1.4	2.7	129.8	-4.7	110.5	54.4

rather nice agreement neither is in energetic balance. Presumably this could be attributed to the computational introduction of spurious energy of the sort that brought Phillips' experiment to a close; Smagorinsky noted this to occur as well, although not so violently. Comparison with the high  $\tau_A^*$  values in table 2 shows the present results to contain substantially more energy in  $K'$  and  $A'$  than in the above table with the mean terms reduced accordingly. The interchange terms vary considerably from the values of table 5 principally in considerably smaller  $\{K' \cdot \bar{K}\}$  and  $\{A' \cdot K'\}$  terms relative to the others. Also  $\{\bar{A} \cdot \bar{K}\}$  is seen to be positive in table 2, while table 5 gives it as negative as has come to be accepted for the atmosphere. It would seem safe to conclude that the positive value is explained by the disproportionately large direct cell in the polar regions in the simple model.

For atmospheric comparisons, table 6 has been prepared from data collected by Oort (1964) and gives approximate values (adjusted to be in balance) of the percentage energetics for the atmosphere. Except for the negative value of  $\{\bar{A} \cdot \bar{K}\}$  these numbers are somewhat closer to the

Table 6. Percentage Energetics: Approximate Atmospheric Measurements (Oort (1964))

%	$\bar{A}$	$\bar{K}$	$A'$	$K'$	$\{\bar{A} \cdot A'\}$	$\{\bar{A} \cdot \bar{K}\}$	$\{A' \cdot K'\}$	$\{K' \cdot \bar{K}\}$
	54	6	24	16	106	-6	85	17

values obtained in the simplified model than the other numerical experiments. This is not to claim that the present model is better than the others, but only to point out that its gross characteristics do not depart violently (in the energy terms) from the real atmosphere.

The other flow type that seems to capture a majority of the phenomena of principal interest is the lowest  $\tau_A^*$  (0.06, 0.05) flows of the moderate rotation rate case ( $\ell^{-1} = 6.67$ ), Figs. 7 and 8. As before the flow, earthlike at the surface, increases with height, here actually forming a double maximum, which is less pronounced when  $\beta$  is included in the equations. The eddy momentum transport is into the center this time in both layers but it appears that the zonal flow is principally maintained against friction by the mean meridional circulation, again thermally indirect in mid latitudes. The eddy convergence and mean cell are quite obviously not in balance, the friction making up the difference.

Also the central indirect cell is not strong enough to induce a mid-latitude southerly mean velocity, except for a small region in one of the cases. The ageostrophic momentum convergences are similar to those of the high  $\tau_A^*$  flows described above.

Energetically comparison of the relevant portions of table 3 with tables 5 and 6 shows these flows under consideration to be considerably at variance with both the other models and the atmosphere. Almost all of the energy of the system is contained in  $\bar{A}$  and almost all of the energy entering the system passes through  $A'$  and is then lost by the  $\{A' \cdot Q\}$  process.

In sharp contrast to the others the low  $\tau_A^*$ , high rotation case is the least atmospheric of the flow types encountered. The upper level shows a double maximum in the zonal wind with the eddy momentum transport out of the center slightly over compensated for by the convergence from a thermally direct mid-latitude meridional cell. Indirect meridional cells at the extremes of latitude serve to balance the eddy momentum convergence there. The overall impression obtained from this particular type of flow is that it is in many ways a reversal of the higher  $\tau_A^*$  flow.

In spite of the dissimilarity to the atmosphere this flow would seem to have importance in the present context because of the previously noted effect of  $\beta$  upon the surface flow, and to a lesser extent upon the upper flow as well. In this particular case it seems reasonable to

assert that the  $\beta$  effect is a major element of the representation necessary to obtain an earthlike surface wind distribution. The inclusion of  $\beta$  may also be seen to increase the strength (moderately) of the earthlike surface flows found for lower rotations relative to what they are when  $\beta$  is left out of the equations.

The atmospheric effect most conspicuous by its absence in all of the type I flows discussed here is of course the variability of the flow. This is partially captured by the vacillating flows detailed in Figs. 13 and 14 although their periodic character is scarcely representative of the randomness of the atmosphere. The sequence of dynamic configurations of Figs. 13 and 14 do not seem to be analogous to any phenomenon of the atmosphere; however the averages of the various convergence terms and zonal velocities of the figures are qualitatively and, within a factor of two or so, quantitatively identical to the higher  $\tau_A^*$  type I<sub>E</sub> flows found in the neighboring regions of the  $l^{-1}$ ,  $\tau_A^*$  plane. The type II flows do resemble, of course, the vacillating flows studied by Hide (1958) and Fultz et al. (1959) in their rotating annulus experiments although exact comparisons are not possible because of the inability to measure, in the fluid experiments, momentum convergences and zonal velocities in the lower portions of the fluids.

One of Fultz's results seems worth noting in conjunction with the present results. He measures the average zonal velocity and the momentum convergences at the upper surface of the flow for a vacillating wave, finding a distinct double maxima in the zonal flow and what appears

to be a maximum eddy momentum convergence about midway between the maxima. The qualitative comparison between this observation and the present results for the moderate and low rotation lower  $\tau_A^*$  results is immediate and quite striking. It would seem then that momentum balance considerations would require a meridional circulation in the annulus, in the mean, similar to that seen in the low  $\tau_A^*$  flows of Figs. 7 and 8, although the difference in geometry would alter the qualitative appearance.

#### B. Quantitative Comparisons

Introduction of quantitative comparisons between the model and observed atmospheric quantities furthers the impression gained previously that the results are somewhat mixed although by no means unrepresentative of major atmospheric phenomena. Table 7 gives values of the various non-dimensionalizing quantities and the factors which when multiplied by the nondimensional quantities give the dimensional values in familiar units. The basic nondimensionalizing length quantity  $L$  was defined, it will be recalled, as  $\frac{\omega}{\pi}$  with  $\omega$  the width of the cartesian strip. The time quantity is the coriolis parameter. If we take  $\omega$  as the pole to equator distance,  $10^9$  cm, and  $f$  as its value at  $40^\circ N$  latitude the values in table 7 follow directly. We must make note of a slight shift of emphasis implied by the fixing of  $f$  at a particular value. In the previous discussion we have been describing flow variations as a function of the nondimensional rotation rate,  $\ell^{-1}$ , nondimensionalized in effect by the

Table 7. Atmospheric Dimensionalizing Factors

$$L = 3.185 \times 10^8 \text{ cm}; \quad f = 0.926 \times 10^{-4} \text{ sec}^{-1}; \quad C_p = 1.004 \times 10^7 \text{ cm}^2 \text{ sec}^{-2} \text{ deg}^{-1}; \\ b = 0.124$$

<u>Dimensional Quantity</u>	= <u>Factor</u>	x	<u>Nondimensional</u>
Temperature °C	= $6.98 \times 10^2$	x	$\tau_A^* / L^2 f^2 C_p^{-1} b^{-1}$
Zonal Velocity cm sec <sup>-1</sup>	= $2.95 \times 10^4$	x	$[u] / Lf$
Momentum Convergence cm sec <sup>-2</sup>	= 2.73	x	$-[u'v']_y / Lf^2$
" " m sec <sup>-1</sup> day <sup>-1</sup>	= $2.36 \times 10^3$	x	"
Energy per unit mass cm <sup>2</sup> sec <sup>-2</sup>	= $8.70 \times 10^8$	x	$K / L^2 f^2$
Energy transfer per unit mass cm <sup>2</sup> sec <sup>-3</sup>	= $8.06 \times 10^4$	x	$\{K', R'\} / L^2 f^3$

friction coefficient  $\ell''$ , in which  $f$  of course would not be a constant. For purposes of quantitative comparison however we specify the rotation rate at a value appropriate for the earth and seek flows bearing a quantitative similarity to the atmosphere. The discovery of such will effectively determine the value of the friction and heating coefficients appropriate to the model, quantities about which a priori guesses would be quite inexact anyway.

From table 5 then a nondimensional  $\tau_A^*$  of 0.15 implies a nondimensional pole to equator difference of twice that, or a difference of about 210°C as that which would exist in the absence of any circulation. Virtually all of the flow types investigated in detail are found at forced temperatures within a factor of 2 or so of this value and in particular the flows with many earthlike qualities were found near this temperature with  $\ell^{-1} = 20.0$ .

210°C may be somewhat in excess of the correct value for the earth; Charney (1959) for example computes the equilibrium temperature difference for the earth at about 100°C; in the light of the drastic simplifications made in the model a factor of two does not seem too serious a discrepancy. Furthermore in the flows in the neighborhood of  $\lambda^{-1} = 20.0$   $\tau_A^* = 0.15$  the actual temperature difference is on the order of 85°C, a large value but not outrageously so.

Looking then at the higher  $\tau_A^*$  large  $\lambda^{-1}$  type I flows, Figs. 4 and 5, the 45°N upper layer eddy momentum convergence value is about 0.03 or so, as is the balancing meridional circulation term and the negative lower layer eddy term. This corresponds to  $8.2 \times 10^{-2}$  cm sec<sup>-2</sup> or 71 m sec<sup>-1</sup> day<sup>-1</sup>. The zonal velocity maxima in the upper and lower layers are 0.2 and 0.125 nondimensionally or about 59.0 meters per second and 37.5 meters per second, respectively. Calculations of the mean meridional velocity,  $[\bar{v}]$ , by Gillman (1963) (for the southern hemisphere using IGY data) give maximum values in the upper portions of the atmosphere at mid latitudes of 23 cm sec<sup>-1</sup> which corresponds to a momentum divergence there of approximately 2 meters sec<sup>-1</sup> day<sup>-1</sup>. Wiin-Nielsen et al. (1963) compute eddy momentum convergences of 8 meters sec<sup>-1</sup> day in the same region for one month (January) of northern hemisphere wind data. The experiments of Phillips and Smagorinsky give convergences of about the same order of magnitude or smaller, the latter being particularly true in the lower layer of their two layer models. The conclusion is quite obvious that the present model while representing the zonal wind magnitudes

reasonably well, grossly over estimates, by an order of magnitude or more, the momentum convergences. At lower values of  $\ell^{-1}$ , for the same higher  $\tau_A^*$ , both the zonal velocities and momentum convergences are larger still, both being approximately doubled for  $\ell^{-1} = 6.67$  and quadrupled for  $\ell^{-1} = 2.5$ .

The energetics for the flow under consideration do not fare much better when cast into dimensional values. The data in Oort (1964) (used in drawing up table 6) suggest a reasonable value for  $\{\bar{A} \cdot A'\}$ , for example, to be  $1.9 \text{ cm}^2 \text{ sec}^{-3}$  while the nondimensional values, for the higher  $\tau_A^*$ , in table 2 give  $\{\bar{A} \cdot A'\} \approx 400 \text{ cm}^2 \text{ sec}^{-3}$ , very substantially in excess of the observed values. The other conversion terms are similarly excessive. Table 8 gives values for the energy storage terms from Oort (1964) along with the values from table 2 with  $\tau_A^* = 0.125$  and  $0.3$ .

Table 8. Energy Storage Terms - Units:  $10^6 \text{ cm}^2 \text{ sec}^{-2}$

	$\bar{A}$	$\bar{K}$	$A'$	$K'$
Oort (1964)	2.7	0.3	1.2	0.8
Model: $\tau_A^* = 0.125$ :	57.5	10.5	17.5	40.5
Model: $\tau_A^* = 0.3$	16.50	6.2	19.0	122.0

Again the model energies appear an order of magnitude or more larger than observed estimates, particularly the  $K'$  term.

The other reasonably earthlike flow:  $\ell^{-1} = 6.67$   $\tau_A^* = 0.06$  and 0.05 (equivalent to about  $75^\circ$  Pole-Equator) with and without  $\beta$  (Figs. 7 and 8), show considerably more reasonable maximum eddy convergence values, about  $3.5 \text{ m sec}^{-1} \text{ day}^{-1}$  in the upper layer (and lower layer as well when  $\beta$  is included) and values about one tenth as large in the lower layer without  $\beta$ . Except for the double maximum formation the mean zonal velocities seem also quite similar to atmospheric observations approximating  $37 \text{ m sec}^{-1}$  in the upper layer and on the order of 7 or 8  $\text{m sec}^{-1}$  in the lower layer. The mean cell convergences, although not excessive, approaching  $9 \text{ m sec}^{-1} \text{ day}^{-1}$  at their largest, are as was noted previously, simply not arranged in a manner familiar from atmospheric examinations.

The magnitudes of the energy terms for this particular region of the  $\ell^{-1}$ ,  $\tau_A^*$  plane are also somewhat mixed.  $\{\bar{A} \cdot A'\}$  is approximately  $645 \text{ cm}^2 \text{ sec}^{-3}$  again a clearly excessive value, although for this flow, unlike the previous one,  $\{A' \cdot Q\}$  is so large that the other energy transfer terms seem to be of a reasonable magnitude. The energy storage terms for  $\beta = 0.6065$ ,  $\tau_A^* = 0.06$  are in table 9 and can be seen to be generally too large.

Table 9. Energy Storage terms - Units:  $10^6 \text{ cm}^2 \text{ sec}^{-2}$

$\beta = 0.6065$				$\ell^{-1} = 6.67$				$\tau_A^* = 0.06$						
$\bar{A}$		$\bar{K}$		$A'$		$K'$		$\bar{A}$		$\bar{K}$		$A'$		$K'$
310.0		2.75		23.7		4.8		310.0		2.75		23.7		4.8

The dimensional values of the various dynamic quantities for the two vacillation cycles considered are easily seen to be quite generally in excess, by an order of magnitude or more, of the atmospheric values cited above. Also comparison with such measurements as are available from Fultz's experiments (principally the eddy momentum convergences) shows the present values to be considerably too large both for the type II flows and the low  $\tau_A^*$  moderate rotation rate type I case that bore a close qualitative resemblance to the average of the vacillating flow in Fultz's tank experiments.

It seems reasonable to rationalize the excessive energy values encountered in the solutions in terms of the geometry of the model, in particular by noting that the single allowed wave stretches from the equator to the greatly enlarged polar regions in contradistinction to the more limited waves in the atmosphere. Hence one might anticipate that integral properties of the wave, namely the energy and energy interchanges, could be larger than their atmospheric counterparts.

### III. Summary, Conclusions and Lines of Further Investigation

In brief compass we can summarize the principal results of the experiments relating to the representation of the general circulation by the highly simplified model. This model, it will be recalled, represents the atmosphere by a two level quasi-geostrophic energetically consistent scheme which allows variation in the horizontally averaged static stability, constrains the zonally averaged wind to have the form

$\sqrt{2} \psi_A \sin y + 3\sqrt{2} \psi_C \sin 3y$  in a zonally infinite channel with sides at  $y = 0$  and  $y = \pi$  ( $\psi_A$  and  $\psi_C$  are essentially the nondimensionalized magnitudes of the two modes of zonal flow), and constrains departures from the zonal mean to be in the form of a single baroclinic wave in the  $x$  direction capable of interacting with both modes of the zonal flow and, at the option of the experimenter, with the latitudinal variation of the coriolis parameter, the  $\beta$  effect. Also in the model is an impressed equator to pole temperature difference and frictional dissipation of the motion, both of which are controllable parameters. Because of the nondimensionalization of the equations it is possible and indeed more logical to interpret variations in the frictional parameter as variations in the rotation rate (they are inverses of one another) and this is done throughout.

For values of the temperature forcing somewhat in excess of a value appropriate to the earth and relatively high values of the rotation (with  $\beta = 0$ ) we obtain a zonal wind structure of a correct form: mid-latitude westerlies flanked by easterlies in the frictionally influenced lower layer and a single mid-latitude maximum of westerlies in the upper layer. The magnitude of these winds appear to be somewhat larger than their atmospheric counterparts but not excessively so. The momentum convergence in the upper layer is also of the correct form with eddy convergence into the center balanced by divergence from an indirect mean meridional cell there; however the magnitudes of these terms are substantially in excess of atmospheric values. In the lower layer the

momentum convergences depart markedly from atmospheric conditions exhibiting there virtually a mirror image of the upper layer conditions. The energetics of the flow seem reasonably well distributed in the sense that their relative magnitudes do not differ too greatly from the relative magnitudes of atmospheric values but their absolute magnitudes are substantially too large.

When  $\beta$  is introduced with the same forcing conditions the flow takes on a vacillating character the details of which do not appear to have any atmospheric parallels although their similarity to the vacillating flows of the rotating tank experiments is immediately obvious. The average of the vacillating case is very similar in form and magnitudes to the steady flow found when  $\beta$  is absent.

For lower temperature forcing, well within a range of estimates appropriate for the earth, and moderate values of the rotation (both with and without  $\beta$ ) the frictionally influenced surface flow has the correct form and quite reasonable magnitudes as well, while the upper level flow, still of reasonable magnitude, shows a double maximum in the westerlies. The eddy momentum convergences of both layers are in excellent agreement, both in magnitude and shape, with atmospheric values, while the meridional cell convergences appear to be less so as far as structure is concerned; their magnitudes are in good agreement. A mid-latitude indirect cell does exist but of insufficient strength to induce momentum divergences to balance the eddy convergences in the upper layer. It is dominated by the overall direct cell component of the meridional flow. The energetic terms show

generally rather poor distribution relative to each other and also rather poor agreement in magnitude in comparison to the atmosphere.

One would be hard pressed to have to make a final decision as to which of these two flows better represented the atmosphere; there are certainly desirable features in both as well as features that are not so welcome. On the basis of the general quantitative agreement between the model and the atmosphere however and noting that the main discrepancies of the lower temperature moderate rotation flow case seem only two: the excessive strength of the direct cell component of the mean meridional motion which overrides the divergent effect of the center cell, and the structure of the upper level westerlies, one feels that the better case could be made for this one as being the more similar to the atmosphere of the two.

The inclusion of  $\mathcal{B}$  into the wave dynamics, although having considerable effect upon the overall patterns of performance of the equations (vide Figs. 2 and 3), influences the ability of the model to represent atmospheric circulations only in some of the details rather than in any overriding manner. The main effect is to increase the mid-latitude westerlies in both layers of the model over that which was present without  $\mathcal{B}$  in the equations. This increase can take the form of a reduction of the relative intensity of a double maximum in the westerlies in the upper layer and a change of easterlies to westerlies in the lower layer as well as a simple increase of the central westerlies in both layers. This phenomenon seems certainly analogous to the results of theoretical work of Kuo cited previously dealing with the effect of  $\mathcal{B}$  upon the momentum transport tendencies of finite amplitude waves on the earth.

With this summary in mind we can return to the basic point of the essay and inquire into what we have learned about the general circulation in the course of the study, and in particular what insight we have gained for purposes of explaining, physically, why the surface zonal winds are distributed as they are and not the other way around. As in all such matters, explanations of a poorly understood phenomenon are given in terms of more fully understood ones. In this sense Kuo's (1951, 1952) studies explained the momentum transports (and by implication the necessarily associated surface winds) of the atmosphere in terms of the physical nature of barotropically and baroclinically unstable (or stable) waves. Similarly Platzman's (1952), Kuo's (1953) and Lorenz's (1953) studies did the same with terms taken from the study of nonlinear tendencies of various flow configurations. Again Charney (1959) used terms arising from a study of steady state finite amplitude motion to explain the existence of the observed wind configuration.

The nature of the explanation given by numerical studies such as Phillips (1956) and the present one is somewhat different than that of the analytic studies. It is no longer possible to cite specific properties of the dynamic systems considered and show how they can account for the particular phenomena of interest; rather the best that can be done is to assert that the sundry physical properties incorporated in the model acting in concert do (or do not) cause the sought after effect.

From the results of the present study, then, we may conclude that what would seem to be the absolute minimum of the physical properties

which allow of the possibility of an atmospheric surface wind structure, as well as a non-atmospheric structure, that can be incorporated into a dynamically self consistent model, will produce a surface wind structure corresponding to that of the atmosphere and associated momentum convergences with a pattern more or less like that of the atmosphere. The additional property of the  $\beta$  effect improves the resemblance of the model and the atmosphere but cannot be said to have an overriding importance in the model. In effect, then, a single baroclinic wave capable of non-linear interactions with the zonal flow, by its very nature, can be taken as the cause of the zonal wind distribution seen on the earth.

Since non-earthlike surface flows were obtained even when the  $\beta$  effect was incorporated (although over rather limited regions) it would seem too strong a statement to assert that a non-earthlike zonal wind structure is physically inconsistent with the existence of a single baroclinic wave. It would seem definitely worth while to investigate whether two, or more, waves capable of interacting with the zonal flow, and possibly with each other, would eliminate the possibility of non-earthlike surface flows and give some foundation to such an assertion for the case of more than one wave.

An explanation such as this and the others outlined above can never be completely satisfactory. In all cases the reasoning is based upon abstractions from reality and the conclusions strictly, of course, apply to the abstraction, the model, only. One can only argue that the level of abstraction is sufficiently close to the reality that the conclusions have

some connection with the real world. The level of abstraction in the present study seems somewhat more removed from reality than, say, that of the others cited above -- that this distance is not so great as to vitiate the present conclusions is the argument of the first section of this chapter.

That this highly simplified model does, with reasonable success, represent many of the salient features of the circulation of the atmosphere allows us to draw some further implications, somewhat tentatively, about the physics of the general circulation. To state the obvious, detail in a model is necessary to represent details in the flow being modeled, but, seemingly, detail in the model is not necessary to induce the gross features of the flow being modeled. In suppressing the smaller scale details of the flow while still obtaining, fairly well, the large scale structure experimentally, we are led to an hypothesis that the organization of the atmosphere is in a sense separable -- the large scale features are self contained, driven by the large scale forcings and do not depend for their existence upon the details of the smaller features whether the latter be transient or steady with particular geographic locations. Another way of stating this is to conclude that the effect of the many waves of the atmosphere upon the large scale zonal structure is qualitatively similar to the effect of a single wave. The zonal structure with no waves present, the Hadley circulation, is of course markedly different from the structure with one, or many, waves present. If a planetary atmosphere existed somewhere whose characteristics were much like the

earth's except that all but a very few of the long waves were somehow suppressed the present results would indicate that the gross zonal features of this atmosphere would not be excessively different from those of the earth's atmosphere; differences in detail would be quite obvious, of course.

These statements should be modified somewhat -- the smaller scales of motion are not ignored completely; some sort of motion is implied in the frictional linking of the two layers and of the lower with the ground. All other dynamic consequences of this motion are suppressed and it is in this sense that the hypothesis of the large scale flow and forcing being sufficient unto themselves is to be taken.

The question of the necessity of the large scale forcing for a good representation is left uninvestigated by the present study but could be looked into by means similar to the present methods. More, smaller, scales of flow could be allowed in the model both in the zonal and meridional directions and temperature forcings could be applied to the smaller scales only, then whether the larger scale motion took on atmospheric patterns or not would be of considerable interest.

Such a line of investigation, by increasing the number of degrees of freedom, might also serve to introduce a greater degree of irregularity into the flow thereby increasing the verisimilitude of the model in an area where it seems to be quite lacking. Such randomness apparently is not necessary for adequate representation of the flow features sought after. Indeed an investigation of the number of degrees of freedom necessary

to achieve statistically stationary irregular behaviour in an earthlike model with thermal forcing in a reasonable range could be of considerable value. It would seem to be the next step beyond reproducing the mean state of the atmosphere as was attempted here.

A different means of introducing more degrees of freedom without adding smaller scales of motion and one which would have a strong physical rationale behind it would be to subdivide the vertical structure into more than two layers. The study by Gillman (1963) cited previously indicates that the forced meridional circulations are not symmetric about the 500 mb surface as they are required to be in the present model but that the lower portion of the cells (the poleward return flow for the mid-latitude cell) is concentrated in the lowest 200 mb of the atmosphere while the equatorward flow extends from 800 to perhaps 100 mb. This asymmetry could perhaps be captured by replacing the two level by a four level model. Again such a process should be viewed as a means of increasing the ability of the model to represent greater detail of the atmospheric flow.

Both another benefit might accrue from either of these means of increasing the number of degrees of freedom as well as an assured problem. The benefit might be that by increasing the physical representativeness of the model the rather distinctly non-earthlike modes of flow, e.g. those for low thermal forcing and relatively high rotation, would not occur in the model as they do not seem to be encountered in more complex general circulation models. The problem is that the addition of only a small number of modes

of flow will require a substantial increase in the number of terms in the spectral equations and therefore in the amount of computation required. The possible benefits to be gained must be balanced off against the difficulties sure to be encountered and the question of whether a more complicated spectral model has worthwhile advantages for purposes of understanding the physics of hydrodynamic flows over the more customary grid point models.

References

- Bryan, K., 1959: A Numerical Investigation of Certain Features of the General Circulation. Tellus, 11, 163-174.
- Charney, J.G., 1948: On the Scale of Atmospheric Motions. Geofis. Publ., (Oslo), 17, 1-17.
- \_\_\_\_\_, 1959: On the Theory of the General Circulation of the Atmosphere, in The Rossby Memorial Volume, New York, Rockefeller Institute Press, pp. 178-193.
- \_\_\_\_\_, and N.A. Phillips 1952: Numerical Integration of the Quasi-geostrophic Equations for Barotropic and Simple Baroclinic Flows. J. Meteor., 10, 71-99.
- Fulz, D., et al., 1959: Studies of Thermal Convection in a Rotating Cylinder with some Implications for Large Scale Atmospheric Motions. Meteor. Monographs, 4, No. 21, Boston, Amer. Meteor. Soc., 104 pp.
- Gillman, P. 1963: Indirect Measurements of the Mean Meridional Circulation in the Southern Hemisphere. Scientific Report No. 3. Contract No. AF 19(628)-2408. Planetary Circulations Project, Dept. of Meteor., Mass. Inst. Tech., pp. 1-49.
- Haltner, G.J., and R.T. Song, 1962: Dynamic Instability in Barotropic Flow. Tellus, 14, 383-393.
- Haurwitz, B., 1940: The Motion of Atmospheric Disturbances. J. Mar. Res., 3, 35-48.
- Hide, R., 1958: An Experimental Study of Thermal Convection in a Rotating Liquid. Phil. Trans. Royal Soc. London. Ser. A., 250, 441-478.
- Kuo, H.-L., 1951: Dynamical Aspects of the General Circulation and the stability of Zonal Flow. Tellus, 3, 268-284.

- Kuo, H.-L., 1952: Three Dimensional Disturbances in a Baroclinic Zonal Current. J. Meteor., 9, 260-278.
- Kuo, H.-L., 1953: On the Production of Mean Zonal Currents in the Atmosphere by Large Disturbances. Tellus, 5, 475-493.
- Kuo, H.-L., 1956: Forced and Free Meridional Circulations in the Atmosphere. J. Meteor., 13, 521-527.
- Lorenz, E.N., 1953: The Interaction Between a Mean Flow and Random Disturbances, Tellus, 5, 238-250.
- \_\_\_\_\_, 1960a: Maximum Simplification of the Dynamic Equations. Tellus, 12, 243-254.
- \_\_\_\_\_, 1960b: Energy and Numerical Weather Prediction. Tellus, 12, 364-373.
- \_\_\_\_\_, 1962: Simplified Dynamic Equations Applied to the Rotating-Basin Experiments. J. Atmos. Sci., 19, 39-51.
- \_\_\_\_\_, 1963a: Deterministic Nonperiodic Flow, J. Atmos. Sci., 20, 130-141.
- \_\_\_\_\_, 1963b: The Mechanics of Vacillation. J. Atmos. Sci., 20, 448-464.
- Obasi, G.O.P., 1963: Poleward Flux of Atmospheric Angular Momentum in the Southern Hemisphere. J. Atmos. Sci., 20, 516-528.
- Oort, A.H., 1964: On Estimates of the Atmospheric Energy Cycle. Mon. Wea. Rev., 92, (in press).

- Phillips, N.A., 1954: Energy Transformations and Meridional Circulations Associated with Simple Baroclinic Waves in a Two-level, Quasi-geostrophic Model. Tellus, 6, 273-286.
- Phillips, N.A., 1956: The General Circulation of the Atmosphere: A Numerical Experiment. Quart. J. R. Meteor. Soc., 82, 123-164.
- Platzman, G.W., 1952: The Increase or Decrease of Mean-Flow Energy in Large-Scale Horizontal Flow in the Atmosphere. J. Meteor., 9, 347-358.
- Saltzman, B., and A. Fleisher, 1960: The Exchange of Kinetic Energy between Larger Scales of Atmospheric Motion. Tellus, 12, 374-377.
- Smagorinsky, J., 1963: General Circulation Experiments with the Primitive Equations. Monthly Weather Rev., 91, 99-164.
- Starr, V.P., 1959: Note Concerning the Influence of Rotation on Convection. Tellus, 11, 360-363.
- Starr, V.P., and R.M. White, 1954: Balance Requirements of the General Circulation. In Final Report Part 1, Contract No. AF 19-122-153, General Circulation Project, Dept. of Meteor., Mass. Inst. of Tech. pp. 186-242.
- Wiin-Nielsen, A. et al., 1963: On Atmospheric Energy Conversions Between the Zonal Flow and the Eddies. Tellus, 15, 261-279.

Biographical Note

The author, having been born December 28, 1935, attended Milton Academy graduating in 1953, graduated from Amherst College class of 1957 with a BA degree cum laude, and received an MS degree from MIT in 1959.

He is a member of the American Meteorological Society and an associate member of Sigma Xi.

He is married to the former Laurie Eveleth and has two children, so far.